

**IDENTIFICATION OF ACTIVE AGENTS FOR TETRACHLOROETHYLENE
DEGRADATION IN PORTLAND CEMENT SLURRY CONTAINING
FERROUS IRON**

A Dissertation

by

SAE BOM KO

Submitted to the Office of Graduate Studies of
Texas A&M University
in partial fulfillment of the requirements for the degree of

DOCTOR OF PHILOSOPHY

May 2005

Major Subject: Civil Engineering

**IDENTIFICATION OF ACTIVE AGENTS FOR TETRACHLOROETHYLENE
DEGRADATION IN PORTLAND CEMENT SLURRY CONTAINING
FERROUS IRON**

A Dissertation

by

SAE BOM KO

Submitted to Texas A&M University
in partial fulfillment of the requirements
for the degree of

DOCTOR OF PHILOSOPHY

Approved as to style and content by:

Bill Batchelor
(Chair of Committee)

Timothy Kramer
(Member)

Jennifer T. McGuire
(Member)

Bruce E. Herbert
(Member)

David V. Rosowsky
(Head of Department)

May 2005

Major Subject: Civil Engineering

ABSTRACT

Identification of Active Agents for Tetrachloroethylene Degradation in Portland Cement

Slurry Containing Ferrous Iron. (May 2005)

Sae Bom Ko, B.S., Dongguk University;

M.S., Texas A&M University

Chair of Advisory Committee: Dr. Bill Batchelor

Fe(II)-based degradative solidification/stabilization (Fe(II)-DS/S) technology is the modification of conventional solidification/stabilization (S/S). Inorganic pollutants are immobilized by Fe(II)-DS/S while organic pollutants are destroyed. Experimental studies were conducted to identify the active agents for Tetrachloroethylene (PCE) degradation as well as the conditions that enhance the formation of the active agents in the Fe(II)-DS/S system. PCE was chosen as a model chlorinated aliphatic hydrocarbon in this study.

First, the conditions that lead to maximizing production of the active agents were identified by measuring the ability of various chemical mixtures to degrade PCE. Results showed that Fe(II), Fe(III), Ca, and Cl were the the important elements that affect degradation activity. Elemental compositions of the mixtures and the conditions affecting solid formation might be the important factors in determining how active solids are formed.

Second, instrumental analyses (XRD, SEM, SEM-EDS) were used to identify minerals in chemical mixtures that have high activities. Results indicate that active agents for PCE degradation in Portland cement slurries and in cement extracts might be one of several AFm phases. However, systems without cement did not form the same solids as those with cement or cement extract. Ferrous hydroxide was identified as a major solid phase formed in systems without cement.

Finally, the effect of using different types of ordinary Portland cement (OPC) on PCE degradation rate during Fe(II)-DS/S was examined and the solids were examined by instrumental analyses (XRD, SEM, SEM-EDS). Four different OPC (Txi, Lehigh, Quikrete, and Capitol) showed different PCE degradation behaviors. Pseudo first-order kinetics was observed for Capitol and Txi OPC and second-order kinetics was observed for Quikrete. In the case of Lehigh cement, pseudo first-order kinetics was observed in cement slurry and second-order kinetics in cement extract. Calcium aluminum hydroxide hydrates dominated solids made with Txi, Quikrete, and Lehigh cements and Friedel's salt was the major phase found in solids made with Capitol cements. Fe tended to be associated with hexagonal thin plate particles, which were supposed to be a LDH.

To the memory of
my grandfather
(1921-2002)

ACKNOWLEDGEMENTS

I am deeply indebted to my committee chair, Dr. Batchelor, for his support and encouragement for the past 7 years. His ability to approach the problem and develop the solution is truly my inspiration. I can not imagine how I became myself today without him. He always showed me a much wider vision on research and guided me in the right direction whenever I struggled and was lost. I can explore the ideas and deepen the works because of him. He also led me to be a true scientist. Thanks also to Dr. Herbert who has been very kind and generous to me. He always opened the door and listened to all my questions, even stupid and nonsense ones. His advice helped me a lot from the beginning stage of this research. I want to give an appreciation to Dr. Kramer and Dr. McGuire from the bottom of my heart. They encouraged me all the time and provided constructive suggestions and guidance.

Thanks to the Texas Transportation Institute and Geology Department at Texas A&M University for the use of the Rigü automatic X-ray diffract meter and Microscopy and Image center at Texas A&M University for the use of JEOL 6400 Scanning Microscope.

Besides all my committee members, I also really appreciate my lab colleagues, Jungyeon Choi, Bangmi Jung, Jinkun Song, Sihyun Doh, Eunjung Kim, and Ahmed Abdel-Wahab, for their opinions on the research as well as for their friendship.

Special thanks go to my grandparents and parents for their endless prayers and love. I would be unable to finish the Ph.D program successfully unless they supported me. I

won't forget their consistent devotion. Even though my grandfather can not share this pleasant moment right now, I believe that he would be proud of me and be happy in heaven.

TABLE OF CONTENTS

	Page
ABSTRACT.....	iii
DEDICATION.....	v
ACKNOWLEDGEMENTS.....	vi
TABLE OF CONTENTS.....	viii
LIST OF FIGURES.....	xi
LIST OF TABLES.....	xv
 CHAPTER	
I INTRODUCTION.....	1
II BACKGROUND.....	5
2.1 Cement hydration products and layered double hydroxides (LDHs)	5
2.1.1 Portland cement: General.....	5
2.1.2 Cement hydration products and layered double hydroxides.....	6
2.1.3 Morphology of cement hydration products and LDHs.....	12
2.2 Reductive dechlorination.....	17
2.2.1 Biotic reductive dechlorination.....	17
2.2.2 Abiotic reductive dechlorination.....	23
2.2.2.1 Fe(II)-based degradative solidification and stabilization.....	25
2.2.2.2 Iron and sulfide minerals.....	28
2.2.2.3 Zero-valent metals and permeable reactive barriers.....	30
2.3 X-ray diffraction.....	34
2.4 Electron microscopy.....	37
III METHODOLOGY.....	42
3.1 Materials.....	42
3.2 Analytical procedures.....	43
3.3 Experiment procedures.....	44

CHAPTER	Page
3.3.1 Reactor system.....	44
3.3.2 Preparation of 10% (w/v) PCX	44
3.3.3 Identification of conditions that promote formation of the active agents.....	45
3.3.3.1 Ca effect.....	45
3.3.3.2 Effect of cement hydration product.....	47
3.3.3.3 Effect of synthetic cement extract (SCX).....	48
3.3.3.4 Effect of major cement extract element.....	50
3.3.4 Identification of the active agents through instrumental analyses(XRD, SEM and SEM-EDS).....	53
3.3.5 Examination of variability of Ordinary Portland Cement (OPC).....	57
 IV RESULTS AND DISCUSSION.....	 58
4.1 Identification of conditions that promote formation of the active agents through solid activity tests.....	58
4.1.1 Evaluation of kinetic constants.....	58
4.1.2 Effect of Ca.....	59
4.1.3 Effect of cement hydration products.....	67
4.1.4 Effect of synthetic cement extract.....	71
4.1.5 Effect of major element of cement extract.....	73
4.1.5.1 Simple mixing method.....	73
4.1.5.2 Adaptation of GR synthesis method.....	79
4.2 Identification of the active agents through instrumental analyses.	90
4.2.1 10% Portland cement slurry (10% PCS).....	90
4.2.2 10% Portland cement extract (10% PCX).....	99
4.2.3 Synthetic cement extract (SCX).....	106
4.2.3.1 Full synthetic cement extract (FSCX).....	106
4.2.3.2 Minor synthetic cement extract (MSCX).....	108
4.2.3.3 Fe(II)(III)Cl.....	111
4.3 Examination of variability of ordinary Portland cement (OPC)...	120
4.3.1 PCE degradation kinetic tests.....	120
4.3.1.1 10% cement slurry solids with Fe(II).....	120
4.3.1.2 10% cement extract solids with Fe(II).....	125
4.3.2 Instrumental analyses: XRD, SEM, and EDS.....	131
4.3.2.1 10% cement slurry solids.....	131
4.3.2.2 10% cement extract solids.....	139
 V SUMMARY AND CONCLUSION.....	 151

	Page
LITERATURE CITED.....	156
APPENDIX A.....	167
APPENDIX B.....	179
APPENDIX C.....	180
VITA.....	181

LIST OF FIGURES

		Page
FIGURE 2-1	Schematic X-ray diffractogram of Portland cement paste.....	9
FIGURE 2-2	Schematic representation of a LDH structure.....	10
FIGURE 2-3	SEM image shows hexagonal shape of calcium hydroxide, needle-like Ettringite, and sheet-like calcium silicate hydrates....	13
FIGURE 2-4	SEM image of hexagonal Friedel's salt and Ettringite needles.....	14
FIGURE 2-5	SEM images and EDS spectra of electrodeposited GR.....	15
FIGURE 2-6	SEM micrographs of CuLDH.....	16
FIGURE 2-7	Reductive dechlorination pathway of PCE.....	17
FIGURE 2-8	Schematic sequential bioremediation processes.....	20
FIGURE 2-9	Schematic diagrams of (A) biobarrier and (B) the trench system	22
FIGURE 2-10	Hypothesized reaction pathways for the chlorinated ethylenes and other intermediates during reduction by Fe(0).....	24
FIGURE 2-11	Dependence of initial degradation rates on initial substrate concentration.....	27
FIGURE 2-12	The reaction and schematic diagrams of pyrite formation.....	28
FIGURE 2-13	Scheme showing proposed pathways for reductive dehalogenation in anoxic Fe ⁰ -H ₂ O systems.....	32
FIGURE 2-14	X-ray spectra.....	36
FIGURE 2-15	Types of signals resulting from the interaction of an electron beam with a sample.....	39
FIGURE 2-16	Schematic of SEM showing the electron column, the deflection system and the electron detectors.....	40

	Page
FIGURE 3-1 Schematic diagram of method of synthesizing solids to examine effect of calcium.....	46
FIGURE 3-2 Two layers of solids after centrifugation of Fe(II) containing PCS solids.....	56
FIGURE 4-1 The variation of normalized pseudo first-order rate constants with respect to CPCX contents.....	64
FIGURE 4-2 The variation of normalized pseudo first-order rate constants with respect to PCX contents.....	65
FIGURE 4-3 The effect of pH on pseudo first-order rate constants normalized with Fe(II) concentration ($k_{Fe(II)}$).....	66
FIGURE 4-4 X-ray patterns of 10% Capitol cement slurry.....	92
FIGURE 4-5 The first SEM image and EDS of Capitol cement slurry without Fe(II).....	96
FIGURE 4-6 The second SEM image and EDS of Capitol cement slurry without Fe(II)....	97
FIGURE 4-7 SEM image and EDS of Capitol cement slurry with Fe(II).....	98
FIGURE 4-8 X-ray patterns of 10% Capitol cement extract.....	101
FIGURE 4-9 SEM image and EDS of Capitol cement extract without Fe(II)...	104
FIGURE 4-10 SEM image and EDS of Capitol cement extract with Fe(II).....	105
FIGURE 4-11 XRD patterns of FSCXFe solids.....	106
FIGURE 4-12 SEM image and EDS of full synthetic cement extract with Fe(II).....	107
FIGURE 4-13 XRD pattern and mineral identification using software program, JADE, of MSCXFe solids.....	109
FIGURE 4-14 SEM image and EDS of minor elements synthetic cement extract with Fe(II).....	110

	Page
FIGURE 4-15 XRD pattern and mineral identification using software program, JADE, of Fe(II)(III)Cl solids.....	113
FIGURE 4-16 SEM image and EDS of Fe(II)(III)Cl_Simple Mixing.....	117
FIGURE 4-17 SEM image and EDS of Fe(II)(III)Cl_GR12.....	118
FIGURE 4-18 SEM image and EDS of Fe(II)(III)Cl_GRN.....	119
FIGURE 4-19 Kinetics of PCE reduction by slurries prepared with Fe(II) and 10% Quikrete cement, QPCSF _e	123
FIGURE 4-20 Kinetics of PCE reduction by slurries prepared with Fe(II) and 10% Lehigh and Txi cement, LPCSF _e and TPCSF _e , respectively.....	124
FIGURE 4-21 Kinetics of PCE reduction by extracts prepared with Fe(II) and 10% Txi cement, TPCXF _e	129
FIGURE 4-22 Kinetics of PCE reduction by extracts prepared with Fe(II) and 10% Lehigh and Quikrete cement, LPCXF _e and QPCXF _e , respectively.....	130
FIGURE 4-23 XRD patterns of solids prepared with Fe(II) and 10% Portland cement	132
FIGURE 4-24 SEM image and EDS of solids prepared with Fe(II) and 10% Txi cement.....	136
FIGURE 4-25 SEM image and EDS of solids prepared with Fe(II) and 10% Quikrete cement	137
FIGURE 4-26 SEM image and EDS of solids prepared with Fe(II) and 10% Lehigh cement	138
FIGURE 4-27 X-ray diffractograms of solids prepared with 10% Portland cement extracts without Fe(II).....	140
FIGURE 4-28 X-ray diffractograms of solids prepared with Fe(II) and 10% Portland cement extracts prepared from cements made by Txi (TPCXF _e), Quikrete (QPCXF _e), and Lehigh (LPCXF _e).....	142

	Page
FIGURE 4-29 SEM image and EDS of solids prepared with Fe(II) and 10% Txi cement extract.....	145
FIGURE 4-30 The first SEM image and EDS of solids prepared with Fe(II) and 10% Quikrete cement extract.....	146
FIGURE 4-31 The second SEM image and EDS of solids prepared with Fe(II) and 10% Quikrete cement extract.....	147
FIGURE 4-32 The first SEM image and EDS of solids prepared with Fe(II) and 10% Lehigh cement extract.....	148
FIGURE 4-33 The second SEM image and EDS of solids prepared with Fe(II) and 10% Lehigh cement extract.....	149

LIST OF TABLES

		Page
TABLE 2-1	Hydration reactions for Portland cement mineral phases.....	8
TABLE 2-2	Catabolic H ₂ -releasing reactions of biotic reductive dechlorination	19
TABLE 2-3	X-ray wavelengths and suitable filters to give $K_{\beta 1}/K_{\alpha 1} = 1/100$...	36
TABLE 3-1	The procedure to examine the effect of cement hydration product.....	48
TABLE 3-2	Stock solution of each element consisting in SCX and element composition of SCX in each experiment.....	49
TABLE 3-3	Different element compositions for the simple mixing method in which solids were synthesized from major element of PCX...	51
TABLE 3-4	Different element compositions and element addition orders for the GR synthesis method in which solids were synthesized from major element of PCX.....	51
TABLE 3-5	Solids to be analyzed by XRD and SEM with EDS.....	56
TABLE 4-1	Pseudo first-order rate constants for PCE reduction by Fe(II)-PCX solids with and without Ca.....	62
TABLE 4-2	Iron and solid concentrations in different cement extract contents of 24 hour-mixed CPCX solid II and Fe(II)-PCX solid	63
TABLE 4-3	Pseudo first-order rate constants for PCE reduction by cement hydration products (tetracalcium aluminate, Friedel's salt, and Kuzel's salt) by themselves, with Fe(II) and with both Fe(II) and Fe(III).....	69
TABLE 4-4	Pseudo first-order rate constants of PCE reduction by various kind of synthetic cement extracts.....	72
TABLE 4-5	Pseudo first-order rate constants of PCE reduction by solids composed of major elements of cement extract.....	74

	Page
TABLE 4-6	Iron and solid concentrations of solids containing Fe(II), Fe(III), and Cl with different initial Fe(III) concentration..... 76
TABLE 4-7	Pseudo first-order rate constants of PCE reduction by solids Fe(II), Fe(III), and Cl with different initial Fe(III) concentrations..... 77
TABLE 4-8	Pseudo first-order rate constants of PCE reduction by solids containing Fe(II), Fe(III), and Cl with different solid synthesis mixing time..... 78
TABLE 4-9	Pseudo first-order rate constants of PCE reduction by solids containing Fe(II), Fe(III), and Cl synthesized by GR synthesis method..... 80
TABLE 4-10	Pseudo first-order rate constants of PCE reduction by solids containing Fe(II), Fe(III), Cl, and Mg synthesized by GR synthesis method..... 82
TABLE 4-11	Pseudo first-order rate constants of PCE reduction by solids containing Fe(II), Fe(III), Cl, and SO ₄ synthesized by GR synthesis method..... 85
TABLE 4-12	Pseudo first-order rate constants of PCE reduction by solids containing Fe(II), Fe(III), Cl, and SiO ₃ synthesized by GR synthesis method..... 88
TABLE 4-13	The Fe(II) concentration normalized first and second order rate constants for PCE degradation in various slurries made with Fe(II) and 10% cement..... 122
TABLE 4-14	The Fe(II) concentration normalized first and second order rate constants for PCE degradation in various Fe(II) containing 10% cement extracts..... 128
TABLE 4-15	The comparison of d-spacing values of 10% cement slurry solids, unit = Å..... 134
TABLE 4-16	Corresponding d-spacing values of peaks in Figure 4-27 and comparison to CPCX, unit = Å 141

	Page
TABLE 4-17 Corresponding d-spacing values of peaks in Figure 4-28 and comparison to CPCXFe, unit = Å	143

CHAPTER I

INTRODUCTION

In 1980, US Congress promulgated the Comprehensive Environmental Response, Compensation and Liabilities Act (CERCLA) to regulate hazardous waste at both active and properly closed facilities. The main purpose of CERCLA is to clean up hazardous waste sites and it establishes the term of “Superfund”, which refers to both the law and the cleanup program mandated under the law. An essential element in CERCLA is the fund established with the tax revenue that can be used to fund cleanup when the responsible parties are unable to do so or are not able to be identified. The Superfund Amendments and Reauthorization Act (SARA) in 1986 was an extension and modification of CERCLA. Under CERCLA, EPA is authorized to take any necessary actions whenever any hazardous substance is actually or potentially released into the environment and wherever an imminent and substantial danger to public health by any actually or potentially released pollutant or contaminant. However, these actions by EPA may be implanted only at sites on the National Priority List (NPL), which identifies the most dangerous hazardous waste sites that are eligible for remedial cleanup under Superfund (1).

Among 1,430 former or current NPL sites, tetrachloroethylene (perchloroethene, PCE) has been found in at least 771 of them (2). According to EPA, the exact number of

This dissertation follows the style of *Environmental Science and Technology*.

NPL sites contaminated by this substance is not known. PCE is a synthetic chemical that is widely used for dry cleaning of fabrics and for metal degreasing. It is also used to make other chemicals and is used in some consumer products, such as water repellents, silicone lubricants, fabric finishers, spot removers, adhesives, and wood cleaners. Exposure to very high concentrations of PCE can cause dizziness, headaches, sleepiness, nausea, unconsciousness, etc. Moreover, the International Agency for Research on Cancer (IARC) has determined that PCE is probably carcinogenic to humans (3).

Conventional remediation technologies, such as bioremediation, soil vapor extraction, incineration, passive/reactive treatment wells, advanced oxidation processes, or activated carbon sorption, have been applied to remediate sites contaminated by PCE and other chlorinated organic compounds (4). However, these technologies have not worked well in destroying it, because PCE is very resistant to both biotic and abiotic degradation under aerobic conditions (5-7).

PCE and other chlorinated aliphatic compounds are suspected to undergo reductive dechlorination under anoxic conditions (8, 9). These transformations are caused by both microbial activities and abiotic geochemical reactions that usually involve inorganic Fe(II) or sulfide (10-12). Reductive dechlorination of PCE and other chlorinated aliphatic compounds has been investigated by many researchers. Intensive research related to abiotic reductive dechlorination of chlorinated aliphatic compounds has included investigations of zero-valent metals (13-24), Fe(II) in combination with Portland cement (23-25), and iron and sulfide minerals (10,11,26-40).

Fe(II)-based degradative solidification/stabilization (Fe(II)-DS/S) technology has been recently developed (23). DS/S is the modification of conventional solidification/stabilization (S/S), which has been an important part of environmental technology at superfund sites in the United States since the passage of hazardous waste control acts (23). The reductive degradation of PCE is enhanced in Fe(II)-DS/S at high pH. Unfortunately, the active reductant for reductive degradation of PCE in Fe(II)-DS/S has not been identified.

The principal goal of this research was to identify the active agents for PCE degradation as well as the conditions that enhance the formation of the active agents in the Fe(II)-DS/S system.

Three objectives were pursued to achieve this research goal. First, conditions that lead to maximizing production of the active agents were identified by measuring the ability of various chemical mixtures to degrade PCE. To achieve this objective, various kinds of solids were synthesized including solids synthesized from Portland Cement Extract (PCX) that has been treated to remove calcium, cement hydration products, solids produced from synthesized cement extract (SCX), and solids prepared with addition of major cement extract elements. These activities were compared to ones for Fe(II)-DS/S, i.e. mixtures of Fe(II) and Portland cement.

Second, instrumental analyses were used to identify compounds in chemical mixtures that have high activities. Analyses to be used include X-Ray Diffraction (XRD), Scanning Electron Microscopy (SEM), and SEM with Electron-Dispersive Spectrometry (SEM-EDS). Solids to be analyzed by these methods were chosen to be

those with more rapid PCE degradation as measured in experiments associated with the first objectives.

Third, the variability of PCE degradation rate by Fe(II)-DS/S using different types of ordinary Portland cement (OPC) was examined and the solids produced were examined by instrumental analyses (XRD, SEM, SEM-EDS).

CHAPTER II

BACKGROUND

2.1 Cement hydration products and layered double hydroxides (LDHs)

2.1.1 Portland cement: General

Anhydrous Portland cement is produced by heating mixtures of limestone and clay, or other materials (41). The initial product is called “clinker”, and it is eventually made into cement by grinding to a fine powder and mixing with a small amount (about 5%) of gypsum to slow down set (42). Gypsum regulates the rate of setting cement and affects the rate of cement strength during hardening processes (41).

Clinkers consist of about 67% of CaO, 22% of SiO₂, 5% of Al₂O₃, 3% of Fe₂O₃, and 3% of other constituents. These formulas do not imply the chemical form of these elements. Allite, belite, aluminate, and ferrite are the four major phases of these elements in clinkers (41).

Allite (Ca₃SiO₅ = C₃S, tricalcium silicate) is the major components of clinkers and represents 50 to 70% of the mass in clinkers. It is responsible for the early stage of development of strength in cement, which lasts up to 28 days. Belite (Ca₂SiO₄ = C₂S, dicalcium silicate) is the second major component of clinkers and represents 15 to 30% of clinker mass. The later stage of cement strength is mostly influenced by belite. Clinkers contain 5 to 10% of their mass as aluminate (Ca₃Al₂O₆ = C₃A, tricalcium aluminate) and 5 to 15% as ferrite (2Ca₂AlFeO₅ = C₄AF, tetracalcium aluminoferrite). The ratio of Al to Fe varies in cements (41)

The modified chemical composition of Portland cement results in the variability of the properties, such as specific surface area, the rate of hardening, or the degree of compressive strength (41, 42).

2.1.2 Cement hydration products and layered double hydroxides

When Portland cement is mixed with water, its four major phases (C_3S , C_2S , C_3A and C_4AF) are totally changed and it sets and hardens. The degree of cement hydration is very important in determining the strength of cement. If the cement to water ratio is very low, strength will be low. However, a ratio of cement to water that is too high creates a high volume of capillary pores, which damages strength and impermeability (42).

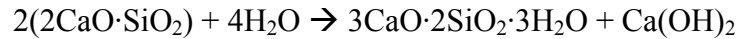
The hydration of the calcium silicate phases (C_3S and C_2S) forms calcium silicate hydrate (C-S-H) and Portlandite ($Ca(OH)_2$). C-S-H represents any amorphous or semi-crystalline calcium silicate hydrate. A large percentage (70%) of C_3S turns into C-S-H in 28 days and all of it is converted within a year. A smaller percentage (30%) of β - C_2S is converted into C-S-H in 28 days and 90% is converted within a year (41). The structure of C-S-H is similar to that of 1.4-nm tobermorite ($C_5S_6H_9$, approx.) and the ratio of Ca/Si is between 0.88 and 1.45 (43). C-S-H is the predominant cement hydration product and it controls the chemical properties of hydrated cement due to its high surface area (44).

The hydration of C_3A and C_4AF forms mostly aluminite-ferrite-tri (AFt) and aluminate-ferrite-mono (AFm) phases. C_3A in the presence of water and calcium sulfate forms Ettringite (AFt, $3CaO \cdot Al_2O_3 \cdot 3CaSO_4 \cdot 32H_2O$) within 30 minutes and then

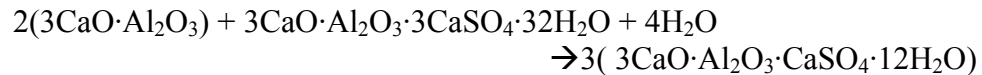
Ettringite and unhydrated C_3A form monosulfate (AFm, $3CaO \cdot Al_2O_3 \cdot CaSO_4 \cdot 12H_2O$) (41, 42). Hydration of C_3A also forms tetracalcium aluminate hydrate (AFm, $4CaO \cdot Al_2O_3 \cdot 13H_2O$) in the presence of calcium hydroxide. It can also form hydrogarnet ($3CaO \cdot Al_2O_3 \cdot 6H_2O$), which is subsequently converted from $2CaO \cdot Al_2O_3 \cdot 8H_2O$ and $4CaO \cdot Al_2O_3 \cdot 19H_2O$ (42). The hydration reaction of C_4AF is very similar to that of C_3A . In general, C_4AF reacts much more slowly than C_3A (41). The hydration reaction rates of C_4AF decrease with increasing Fe(II) contents (45).

In the presence of free-chloride, the hydration of C_3A forms $C_3A \cdot CaCl_2 \cdot 10H_2O$, called “Friedel’s salt” (46). Friedel’s salt is also an AFm phase. Friedel’s salt is more stable than hydroxylaluminate AFm, which has variable water contents ($4CaO \cdot Al_2O_3 \cdot xH_2O$) and can be converted into hydrogarnet and gibbsite. When chloride ions diffuse into cement, AFm serves as a “sink” for chloride so that chloride ion diffusion further into the solid is delayed. The mixtures of Friedel’s salt and hydroxylaluminate AFm keep pH above 12 through substitution of Cl^- for OH^- . Friedel’s salt is very stable at $20^\circ C$ over a wide range of Cl^- concentration, from 14.5 mM to about 8 M, in aqueous phases. Intrusion of CO_2 is a main mechanism to destabilize AFm, but other hydration products, such as Portlandite or C-S-H gel, are still able to buffer the system. Therefore, AFm phases are able to maintain their stability locally and keep reacting with adjacent Cl^- ions. All aluminate hydrates will be converted to Friedel’s salt in the same chloride concentration ranges, so that Friedel’s salt formation is largely dependent on the Al content of cement (47) for a given Cl content. Table 2-1 summarizes some of the cement hydration reactions

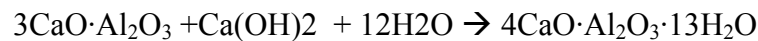
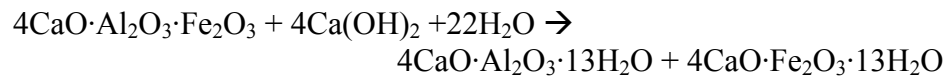
TABLE 2-1 Hydration reactions for Portland cement mineral phases (48)

Tricalcium silicate:**Dicalcium silicate:****Tricalcium aluminate and Gypsum:**

then



then

**Tetracalcium aluminoferrite:**

Hydrated Portland cement generally consists of 70% C-S-H, 20% Portlandite, 7% Ettringite/monosulfate, and 3% minor phases. Porous hydrated Portland cement has up to 200 m²/g of specific surface area (42). The XRD pattern of typical hydrated Portland cement is shown in figure 2-1.

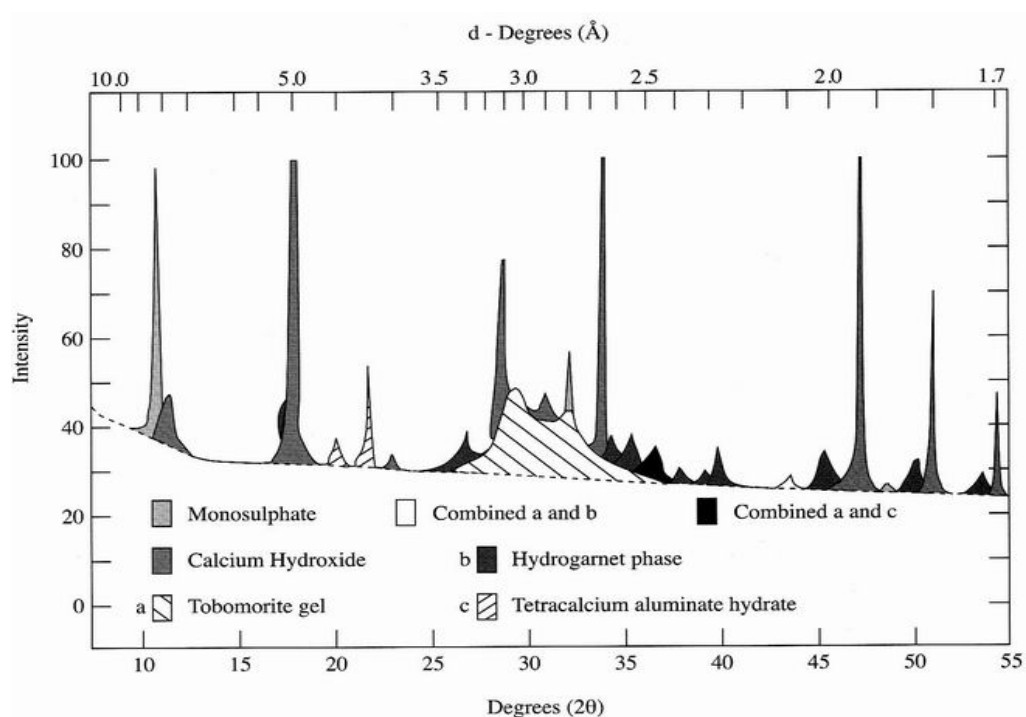
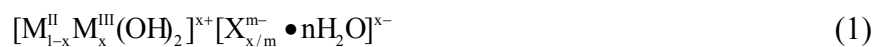


FIGURE 2-1 Schematic X-ray diffractogram of Portland cement paste (49).

AFm phases are examples of compounds called layered double hydroxides (LDHs) (50, 51). LDH are compounds that have sheets of metal hydroxides with anions in the interlayer. They are referred as hydrotalcite-like compounds or pyroaurite-like compounds. Divalent and trivalent metal cations are present in the sheet and to some degree, the divalent cations can substitute for trivalent cations. The divalent and trivalent cations are randomly distributed in an edge-sharing octahedral sheet, forming hydroxylated $M(OH)_2$ sheets similar to those of brucite, $Mg(OH)_2$. The excess positive charge created by isomorphous substitution is balanced by the presence of anions in the interlayers. General formula of an LDH is:



where M^{II} is a divalent cation, M^{III} a trivalent cation, and X an anion (52-55). The schematic structure of LDH is shown in figure 2-2.

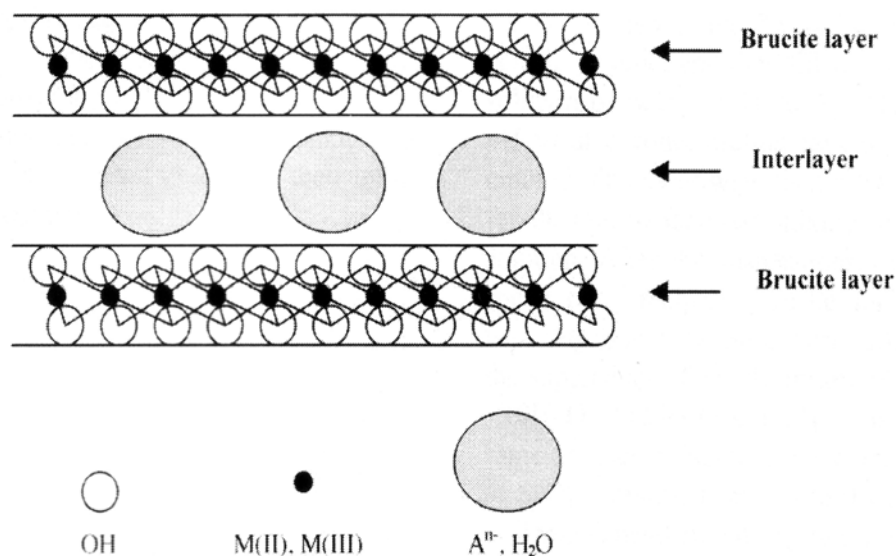


FIGURE 2-2 Schematic representation of a LDH structure (55).

Various cations are found in natural or synthetic LDH. Divalent cations include Mg, Mn, Fe, Co, Ni, Cu, Zn, and Ca. Trivalent cations include Al, Cr, Mn, Fe, Co, and Ni. A diversity of interlayer anions is also reported in LDH and they include halides (F-, Cl-, Br-, I-), oxo-anions (nitrate, sulfate, chromate, selenate, selenite, carbonate), complex anions (ferrocyanide), and organic anions (alkyl-sulfate, carboxylic acid, porphyrins) (53-56)

As we can see from the formula of AFm phases, $[\text{Ca}_2(\text{Al}, \text{Fe})(\text{OH})_6]^+ \cdot x^- \cdot m\text{H}_2\text{O}$, a divalent cation for AFm phases is Ca^{2+} and a trivalent cation is Al^{3+} and/or Fe^{3+} . Commonly found interlayer anions are OH^- , Cl^- , SO_4^{2-} , and CO_3^{2-} (41).

The unique characteristic of LDHs is high anion exchange capacities. It is possible to exchange anions in the interlayer with various kinds of other anions (52, 53). The selectivity of LDH for monovalent anions is $\text{OH}^- > \text{F}^- > \text{Cl}^- > \text{Br}^- > \text{NO}_3^- > \text{I}^-$, and divalent anions are more highly selected than monovalent anions (57). Interlayer spacing of LDHs vary, depending on the size and structure of the anions. LDHs, thus, can have a large surface area, 20-120 m^2/g to 800 m^2/g , and high anion exchange capacity, 2-5 meq/g, due to the characteristics of anions in the interlayers (53, 54). These properties of LDHs result in interesting applications including use as catalysts, electrochemical agents, separation media, and adsorbent (54, 55, 58, 59).

A naturally occurring LDH is Green Rust (GR), which is found as the product of steel corrosion at near neutral conditions and as precipitates in anaerobic soils and sediments (60). GRs formed during steel corrosion are stable up to $\sim \text{pH } 13$ (61). Commonly found anions in the interlayers of GR are Cl^- , SO_4^{2-} , and CO_3^{2-} (60). There are two types of GR, rhombohedral GR1 and hexagonal GR2, based on features of X-ray diffraction. GR1 has planar anions, such as chloride and carbonate and GR2 has three-dimensional anions such as sulfate (62).

2.1.3 Morphology of cement hydration products and LDHs

The microscopic examination of minerals elucidates their microstructure on a scale of micrometers or below and can include characteristics such as composition, surface topography, crystallography, etc (63). Petrographic examination of cement identifies the type, composition, and nature of cement pastes, as well as aids the estimation of the life of concrete (64).

The predominant cement hydration product is the C-S-H gel. It can be amorphous so that it can be difficult to identify through X-ray diffraction alone. Scanning electron microscopic examination shows that it is often found as filaments or tubular structures (Type I) soon after mixing with water and then changes to honeycomb structures (Type II). At the late stage of cement hydration, the shape of the gel has a more massive appearance (Type III) and then it develops a featureless shape (Type IV). Features are not found after 28 days, even at the scale of 100 nm scale (41, 42).

The morphology of Portlandite and hydrated calcium aluminate is hexagonal. Friedel's salt and tetracalcium aluminate hydrate, which are LDHs, are difficult to distinguish due to a similar maximum intensity peak position as well as the same shape. However, they can be distinguished by their size. Crystals of Friedel's salt are typically 2 to 3 μm , while hydration products of C_3A are typically less than 1 μm . Portlandite is also hexagonal in shape, but it is much larger than Friedel's salt, with maximum lengths of about 100 μm . Ettringite and monosulfate form acicular crystals, with sizes generally below 1 μm (42, 65).

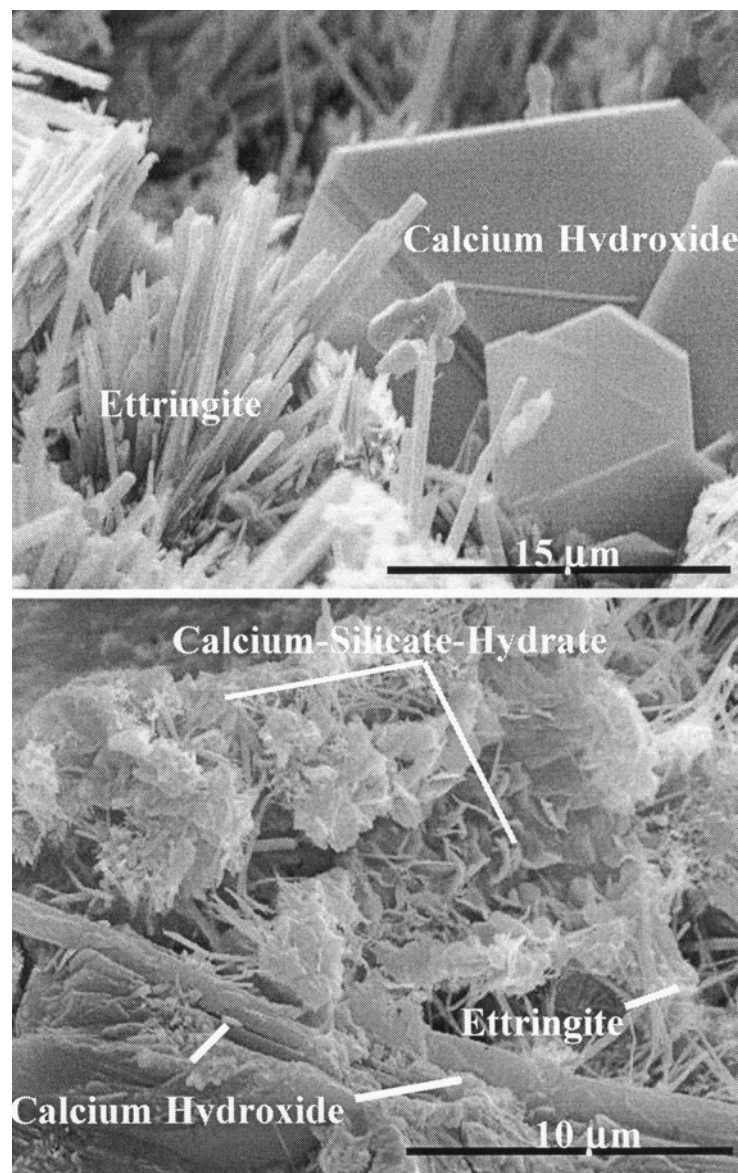


FIGURE 2-3 SEM image shows hexagonal shape of calcium hydroxide, needle-like Ettringite, and sheet-like calcium silicate hydrates (64).

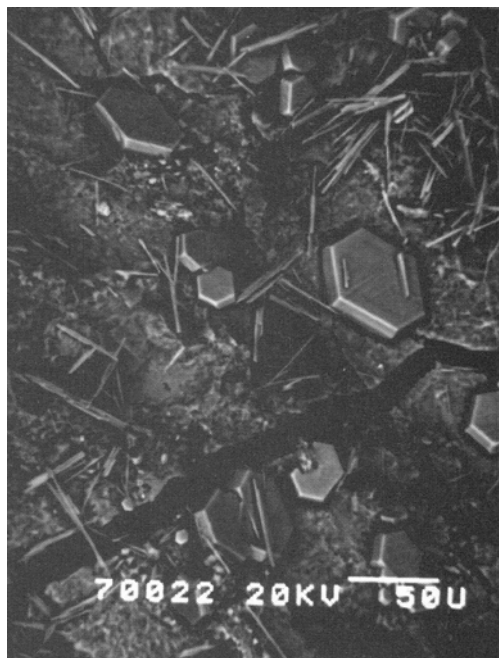


FIGURE 2-4 SEM image of hexagonal Friedel's salt and Ettringite needles (42).

The structure of LDHs is stacking edge sharing octahedral planes with divalent and isomorphously substituted trivalent cations in the center and hydroxyl groups in the vertices and charge balancing anions between octahedral planes (66). In general, crystals having thin flat plane shapes indicate LDHs (67).

For example, green rust sulfate, $\text{GR}(\text{SO}_4^{2-})$, has the shape of hexagonal thin plates with sizes of several micrometers (figure 2-5(a)) (68-70). Although green rust carbonate, $\text{GR}(\text{CO}_3^{2-})$ and green rust chloride, $\text{GR}(\text{Cl}^-)$ do not show perfect hexagonal shapes in figure 2-5(b) and (c), they also have thin flat characteristics. $\text{GR}(\text{CO}_3^{2-})$ particles are very compact platy shapes and have very large thickness, about $0.7\mu\text{m}$ (68, 70). Figure 2-6 shows synthesized Cu substituted MgAILDH in laboratory. They also have thin plate shapes, similar with $\text{GR}(\text{Cl}^-)$ (71).

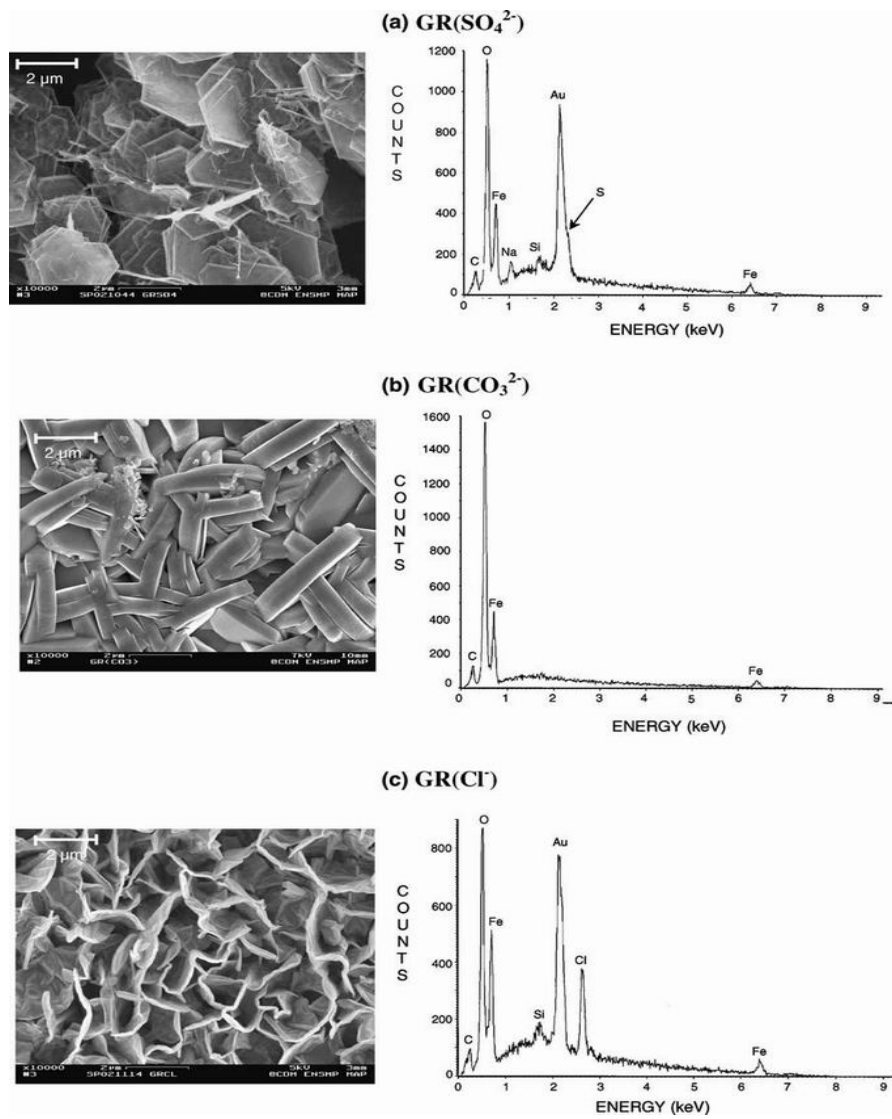


FIGURE 2-5 SEM images and EDS spectra of electrodeposited GR (69).

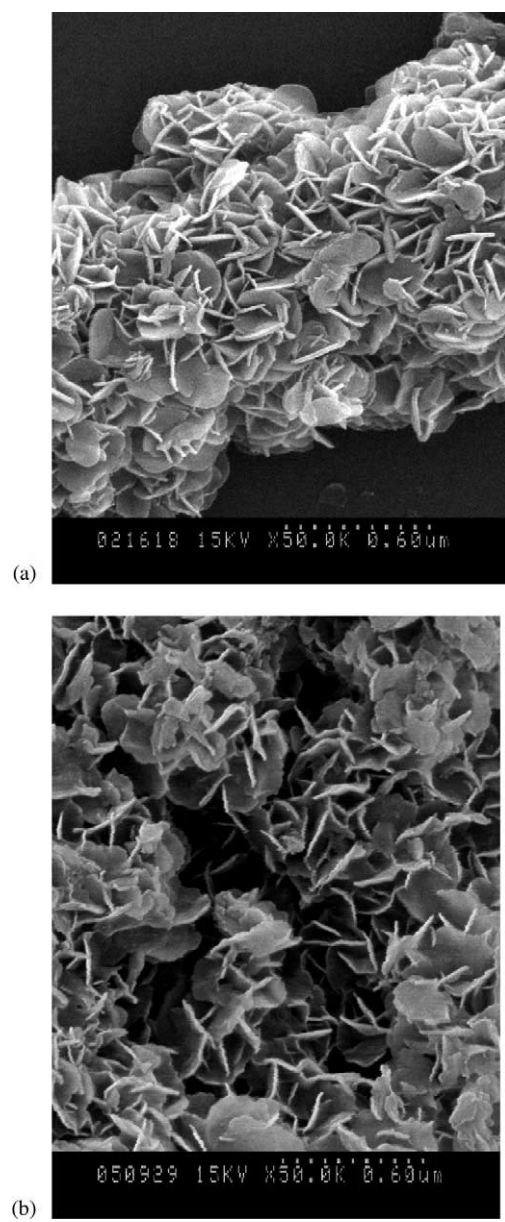


FIGURE 2-6 SEM micrographs of CuLDH (71).

2.2 Reductive dechlorination

2.2.1 Biotic reductive dechlorination

Reductive dechlorination is a major mechanism under anaerobic conditions for biological removal of harmful, toxic chlorinated organic solvents from contaminated environments. Usually, chlorinated organic compounds are very recalcitrant under aerobic conditions, but sometimes they can be degraded to less substituted compounds. In reductive dechlorination, a hydrogen is substituted for a chlorine atom.

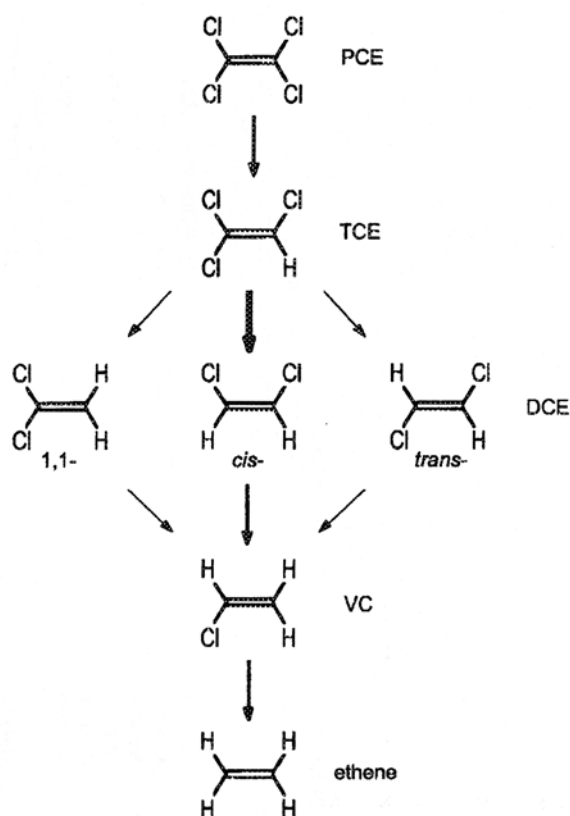


FIGURE 2-7 Reductive dechlorination pathway of PCE (72).

There are two categories of biotic reductive dechlorination; cometabolic dechlorination, and metabolic dechlorination (72-74). In cometabolic processes, microbes do not directly use chlorinated organic compounds as their energy sources. Instead, they utilize other electron donors in their energy-producing reactions, and create enzymes or cofactors to degrade contaminants. For example, PCE was degraded to ethane by introducing acetate, glucose, formate, methanol, lactate, or sucrose as electron donors (75-78). A site that is contaminated by petroleum hydrocarbons and chlorinated solvents can be cleaned up through cometabolic processes. In this case, microbes gain energy through metabolizing petroleum hydrocarbons and synthesize enzymes that can degrade chlorinated organic contaminants in reactions that do not yield energy to the organism.

In metabolic dechlorination, a chlorinated organic compound serves as a terminal electron acceptor in reactions that provide for energy storage and growth (72). *Dehalococcoides ethenogenes* strain 195 is known as halorespiration bacteria, and it is able to dechlorinate PCE to ethane (79).

Microbial dechlorination occurs usually under methanogenic conditions (72, 80, 81). However, polychlorinated methane and ethane are also able to undergo biotransformation under various redox zones, such as a sulfate-reducing conditions, or Fe(III) -reducing conditions (80, 82, 83).

Even though various kinds of electron donors are being investigated, the actual electron donor in dechlorination is hydrogen, which is available directly or through fermentation of fed electron donors (84, 85). Ferguson (85) demonstrated a hydrogen

effect on anaerobic biotransformations of chlorinated compounds. He shows that PCE dechlorination does not occur when acetate is the only electron donor. However, PCE is converted to less chlorinated compounds after H₂ is injected. PCE also starts to degrade soon after adding H₂ in the case when cultures did not previously receive other electron donors. Table 2-2 shows reactions with various electron donors that produce H₂.

TABLE 2-2 Catabolic H₂-releasing reactions of biotic reductive dechlorination (78)

H ₂ -releasing reactions	
acetate ⁻	+ 4H ₂ O → 2HCO ₃ ⁻ + 4H ₂ + H ⁺
propionate ⁻	+ 3H ₂ O → acetate ⁻ + HCO ₃ ⁻ + H ⁺ + 3H ₂
butyrate ⁻	+ 2H ₂ O → 2acetate ⁻ + H ⁺ + 2H ₂
ethanol	+ H ₂ O → acetate ⁻ + H ⁺ + 3H ₂
methanol	+ 2H ₂ O → HCO ₃ ⁻ + H ⁺ + 3H ₂
lactate	+ 2H ₂ O → acetate ⁻ + HCO ₃ ⁻ + H ⁺ + 2H ₂

In contrast to other halorespiring bacteria, *Desulfuromonas chloroethenica* uses acetate as an electron donor, instead of H₂, and reduces PCE to *cis*-DEC (86, 87).

Along with electron donors, temperature is an important factor as well. Anaerobic reductive dechlorination occurs typically in the temperature range between 20 °C and 37 °C (72). The rate of degradation significantly decreases (88) or is stopped (89, 90) below 10 °C. However, microbial reductive dechlorination of PCE is observed even under thermophilic conditions (91).

Several remediation technologies apply biotic reductive dechlorination. First, natural attenuation is an economically favorable remediation process in which indigenous microorganisms use contaminants as their energy sources and degrade them to harmless products without any engineering modifications. When natural attenuation is

applied as a remediation processes at contaminated sites with chlorinated solvents, important controlling factors are subsurface redox conditions and availability of soil organic carbons, which could serve as electron donors to indigenous microorganisms (92). Natural attenuation could be a feasible choice for a site contaminated by both petroleum hydrocarbons and chlorinated solvents.

Another application for bioremediation of chlorinated organics is sequential bioremediation. Figure 2-8 shows a schematic of a sequential bioremediation process. In an anaerobic zone, PCE is dechlorinated to *cis*-DCE, followed by an aerobic zone in which *cis*-DCE is biomineralized to CO₂ by a cometabolic oxidation. An electron donor, such as methanol, is added to stimulate reductive dechlorination in the anaerobic zone, while oxygen and an additional substrate are added to the aerobic zone (93).

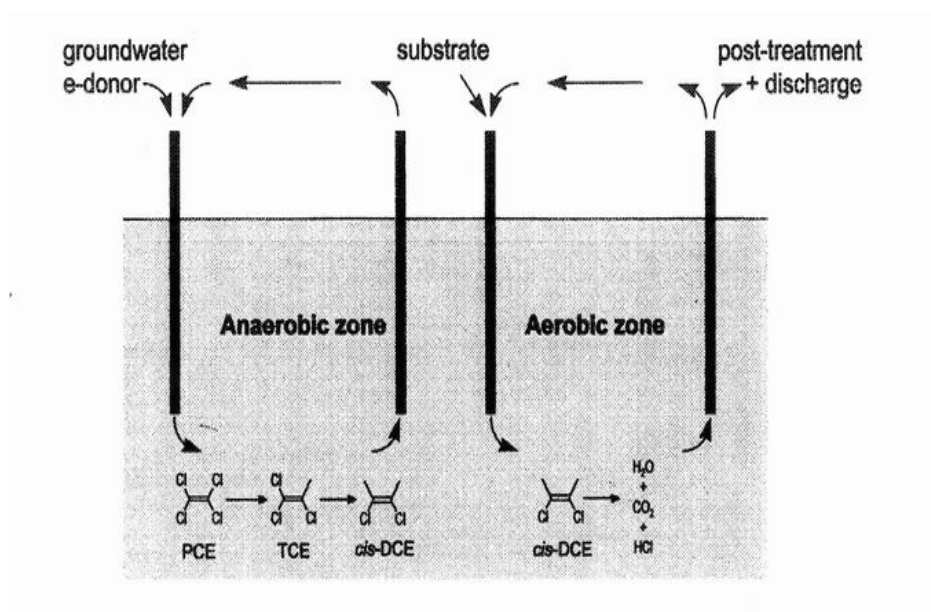
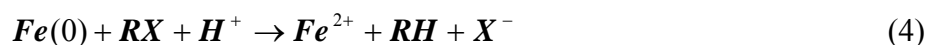
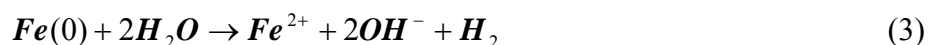


FIGURE 2-8 Schematic sequential bioremediation processes (72).

A third approach to bioremediation of chlorinated organics is bioaugmentation, which is the process where suitable microorganisms are added to contaminated sites when indigenous microorganisms are unable to perform dechlorination. Both biological and chemical factors at contaminated sites are important to successfully conducting bioaugmentation (72). Gregory and co-workers (94) demonstrate that the anaerobes, such as those found in acetate-enriched or lactate-enriched methanogenic cultures, are able to degrade chlorinated aliphatic compounds in combination with Fe(0), which produces H₂. Microbes use this hydrogen as their electron donor for energy production. Fe(0) by itself also reduces chlorinated aliphatic compounds.



Permeable reactive zones or barriers in aquifers are economical and promising remediation technologies. As contaminated groundwater passes through the zones, contaminants are chemically and biologically degraded, sorbed and/or precipitated (95). One type of reactive zone is produced by using biological sludge cake to fill remediation wells or trenches (95-97). Biological sludge cake is a good material for this purpose due to its abundance of carbon sources, sufficient carbon bioavailability for reductive dechlorination, and its low cost. PCE is degraded to less chlorinated products such as vinyl chloride (VC) in upstream anaerobic zones by methanogenic microorganisms and VC is aerobically co-metabolized in downstream zones (refer to figure 2-9).

Ex-situ bioremediation technologies applying biotic reductive dechlorination mechanisms such as the anaerobic filter (98) or biofilm (99) are also reported.

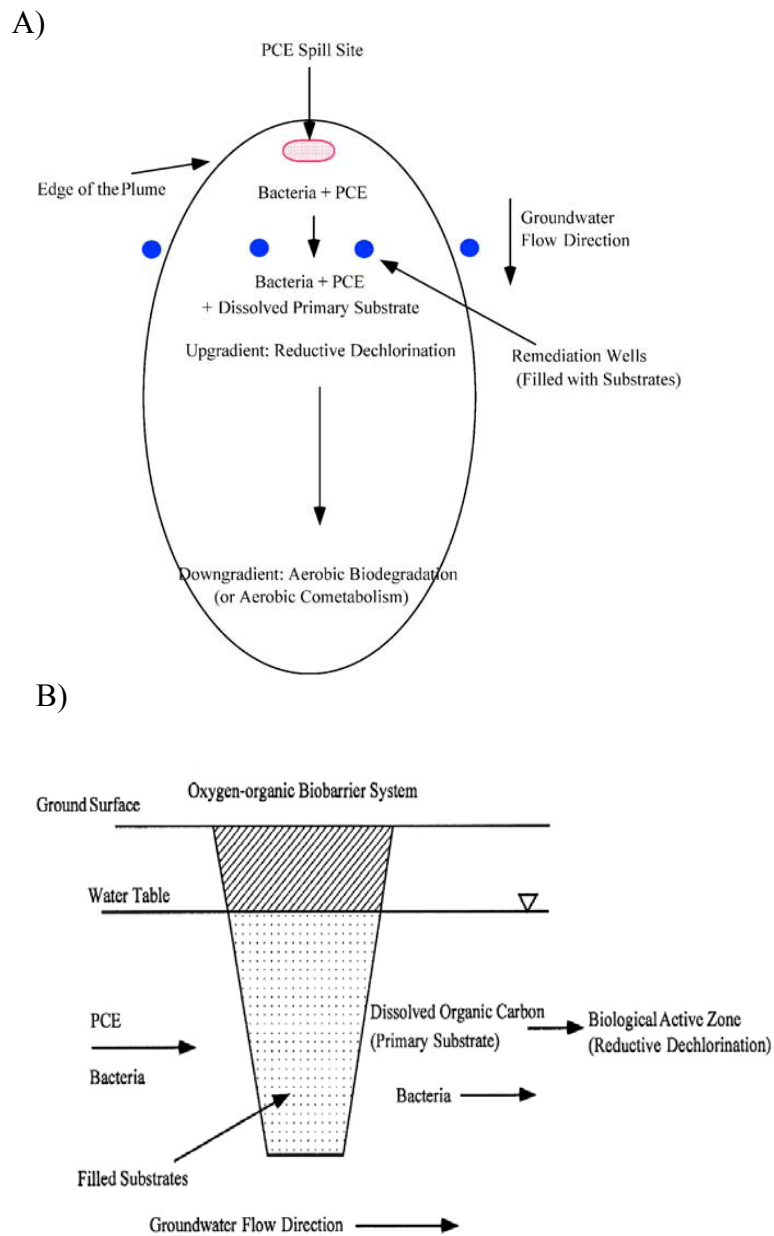


FIGURE 2-9 Schematic diagrams of (A) biobarrier and (B) the trench system (95).

2.2.2 Abiotic reductive dechlorination

Biotic reductive dechlorination sometimes does not completely dechlorinate contaminants, so that more harmful daughter products accumulate, such as *cis*-DCE and VC, which are very toxic to microorganisms. The only microorganism known to completely degrade PCE to ethane is *Dehalococcoides ethenogenes* strain 195. Appropriate environments, such as temperature, nutrient, oxygen, moisture content, and substrate, are required for successful application of natural attenuation (72).

Due to several limitations of biotic reductive dechlorination, abiotic reductive dechlorination could be a promising alternative for remediation of chlorinated solvents. Abiotic reductive dechlorination could be achieved by addition of chemical reductants such as iron-bearing minerals, hydrogen sulfide, iron sulfides, and zero-valent metals, such as iron, zinc. Abiotic reductive dechlorination occurs presumably through three reactions; hydrogenolysis (chloride substitution for hydrogen), reductive elimination (dichloroelimination), and hydrogenation (reduction of multiple bonds) (13) (refer to figure 2-9). The ratios of the rates of these different reactions determine the distribution of products (13).

The first step in abiotic reductive dechlorination is a one-electron transfer from the reductant that results in removal of chloride and the formation of an alkylchloride radical. This intermediate radical undergoes several reactions, such as hydrogenolysis, reductive elimination and dimerization. Hydrogen is attached to the intermediate alkyl radical from the surrounding environment during hydrogenolysis. Another chloride that is attached to an adjacent radical carbon could be lost and an alkene would be formed in a

process called reductive elimination.. This would decrease the possibility of further reduction (7). If there is not a good proton donor, dimerization of the radical can be important. However, dimerization is not favored in dilute solution (100).

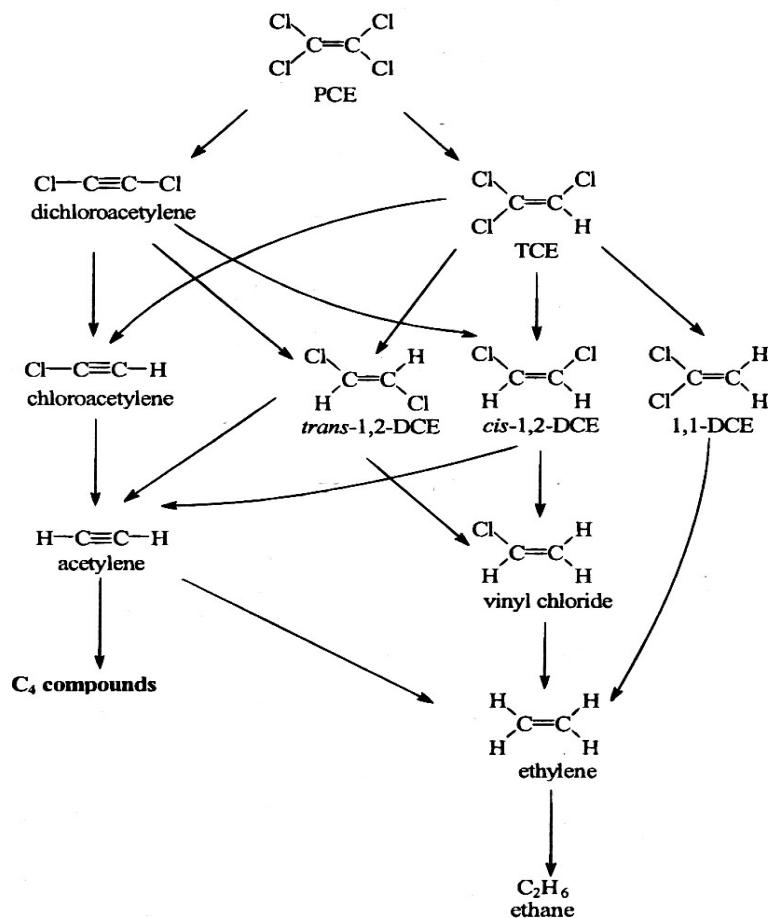


FIGURE 2-10 Hypothesized reaction pathways for the chlorinated ethylenes and other intermediates during reduction by Fe(0) (13).

Several reductants have been investigated for abiotic reductive dechlorination for decades, such as Fe(II) in cement slurry (19-25), iron and sulfide minerals (10, 11, 26-

40), and zero-valent metal (13-22). All of them have shown the ability to dechlorinate chlorinated organic compounds and their dechlorination pathways have been investigated.

2.2.2.1 Fe(II)-based degradative solidification and stabilization

Many hazardous materials, especially those that are recalcitrant to chemical, biological, and thermal processes, have been treated by solidification and stabilization (101). Wastes are stabilized and detoxified by binding to reagents, such as cement. They can also be solidified by changing the physical characteristic of wastes, such as strength, compressibility, permeability. The principle purpose of solidification and stabilization is not only reduction of toxicity and mobility of contaminants but also improvement in physical properties of stabilized wastes (1).

There are six possible physical and chemical mechanisms that affect the effectiveness of solidification and stabilization; macroencapsulation, microencapsulation, absorption, adsorption, precipitation, and detoxification. One or more of these mechanisms can be employed (1). The most widely used principle binder is Portland cement. Pozzolans, lime and soluble silicate are also used as binders (1).

Degradative solidification and stabilization (DS/S) is the modification of conventional solidification and stabilization. The advantage of DS/S is that wastes are contained as well as degraded, for example, inorganic pollutants are immobilized while chlorinated organic pollutants are degraded. Therefore, DS/S will be a promising

technology for sites that are contaminated by both inorganic and organic pollutants (e.g., chlorinated aliphatic compounds) (23).

Hwang (23, 24) developed the DS/S system that uses Fe(II) as a reductant for reductive dechlorination of PCE. He used Portland cement as a binder. He chose Fe(II) as a reductant because Fe(II) showed the highest removal efficiency for PCE of the five reductants tested (sulfide, polysulfide, dithionite, pyrite and Fe(II)). It is popular reductants at S/S sites, and it is inexpensive (23).

PCE is degraded by pseudo-first order kinetics in slurries of Portland cement that contain Fe(II). This combination is called Fe(II)-based DS/S (Fe(II)-DS/S). The reductive elimination pathway is the major one for PCE degradation in Fe(II)-DS/S and the optimum pH is 12.1 (23).

Reductive dechlorination of carbon tetrachloride (CT) (24), and 1,1,1-trichloroethane (1,1,1-TCA) (25) by Fe(II)-DS/S also follows pseudo-first order kinetics. The optimum pH for degradation of CT is pH 13 and the optimum for 1,1,1-TCA degradation is pH 12.5 . Reductive dechlorination of CT follows a hydrogenolysis pathway in which chloroform (CT) and methylene chloride (MC) are produced as daughter products (24).

The effect of initial concentration of target compounds has also been investigated (24, 25). The rate of degradation is described by a saturation model:

$$R_0 = \frac{v_{\max} [\text{substrates}]_0}{(K_m + [\text{substrates}]_0)} \quad (5)$$

where, R_0 = initial degradation rate; v_{\max} = maximum degradation rate; K_m = the half-saturation constant. The value of v_{\max} and K_m are obtained by nonlinear regression. Figure 2-11 shows the saturation behavior for reductive dechlorination of 1,1,1-TCA. The saturation behavior in Fe(II)-DS/S suggests that reductive dechlorination of target compounds might occur on the surface through their adsorption on reactive sites.

Hwang (23) assumed that the possible active reductant in Fe(II)-DS/S might be similar to GR, based on the observation that increased PCE degradation rates were obtained when Fe(III) was added along with Fe(II) to Portland cement slurries.

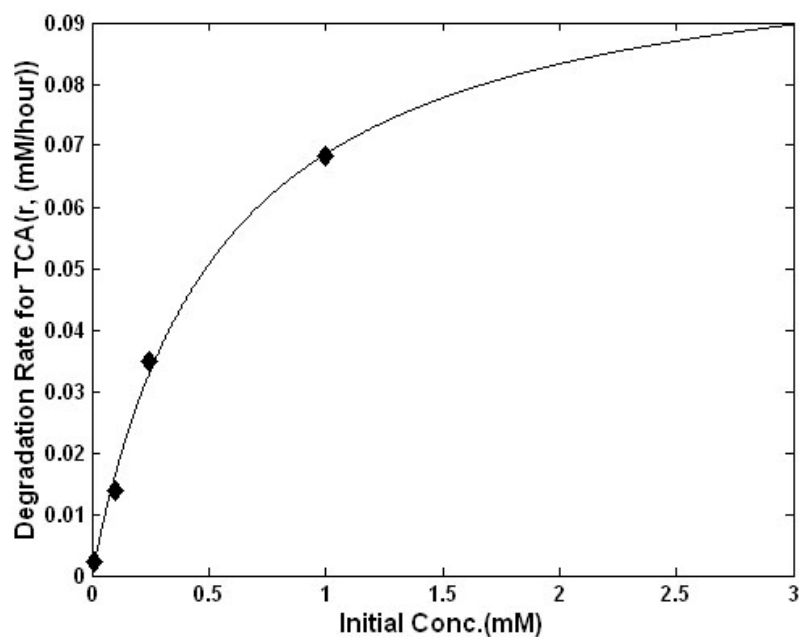


FIGURE 2-11 Dependence of initial degradation rates on initial substrate concentration (25).

2.2.2.2 Iron and sulfide minerals

In anoxic subsurface environment, dissimilatory Fe(III)-reducing bacteria (DIRB) and sulfate-reducing bacteria (SRB) plays an important role on the formation of reduced iron and sulfide minerals, such as pyrite (102) and magnetite (103, 104).

Sulfide minerals are very sensitive to oxidation so that they cannot be present in a great amount under aerobic conditions. The reduction of sulfate to sulfide requires a sulfate source, SRB (e.g., *Disulfovibrio*), a carbon source for microorganisms, and anaerobic environments (102).

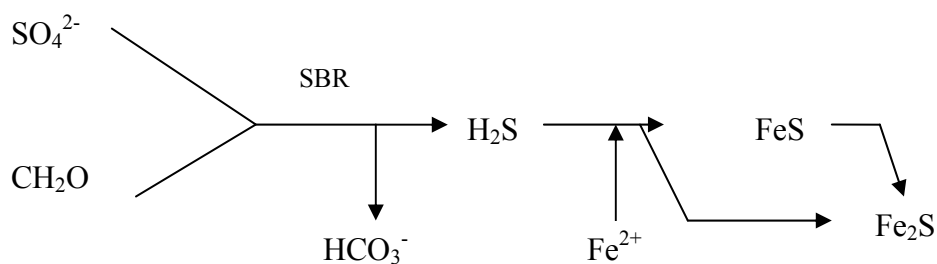


FIGURE 2-12 The reaction and schematic diagrams of pyrite formation (102).

Fe(III)-(hydro)oxides (e.g., hydrous ferric oxide, goethite, hematite, magnetite) and structural Fe(III) in clay minerals can be reduced by DIRB (105). Even SRB, RS-1 (discovered by Sakaguchi and co-workers in 1993), is able to form magnetite (103). Bioavailability of Fe(III)-oxides to DIRB increases by the addition of Fe(III)-binding ligands, such as lactate or ethylenediaminetetraacetic acid (EDTA) (106).

The rate of Fe^{2+} release is very dependent on microbial physiological conditions so that high cell concentrations and the cultivation of cells in nutrient-rich media can increase Fe^{2+} releasing rate (105).

Magnetite is the most commonly formed mineral produced by dissimilatory Fe reduction (37, 104). It is mainly formed via reductive dissolution of ferrihydrite, which can be facilitated by the presence of Cl^- (104, 107-109). The second major pathway of the formation of magnetite is the oxidation of GR, which is commonly found as an intermediate of corrosion processes (110).

Microbial reduction of Fe(III) and/or sulfate plays an important role in degradation of chlorinated solvents in the subsurface due to the reducing ability of iron or sulfide minerals. Those minerals have been intensively investigated (10, 11, 26-40). Understanding the effect of minerals on reductive dechlorination of chlorinated solvents helps to predict the role of abiotic processes in natural attenuation (36).

Green rust is a LDH that has a large surface area due to its interlayer and can act as a reductant for CT (26), PCE, TCE, *cis*-DCE, and VC (27). Its ability as a reductant is dramatically improved when metals, such as Ag, Au, and Cu (28) for CT and Ag, Cu, Pb,

and Pt (29) for PCE, are added to GR. Reductive dechlorination with GR and modified GR follows either the hydrogenolysis or the reductive elimination pathway (27, 29).

Butler and Hayes demonstrate the reductive dechlorination of hexachloroethane (HCA), PCE, TCE, and chlorinated ethane by iron sulfide. Most of them were degraded with the half-lives of hours to days. The rate limiting steps were electron transfer and chloride bond cleavage (30-32). The reductive ability of iron sulfide for HCA also increases with addition of a soft transition metal, such as Ni(II), Cu(II), Zn(II), Cd(II), and Hg(II) (33). Methanogenic activities also improve the reducing power of FeS for transforming 1,1,1-TCA (34). Reductive dechlorination of CT, PCE, and TCE by pyrite is also observed (10, 35, 36).

Iron oxides, such as magnetite and goethite, show the ability to degrade chlorinated aliphatic compounds (36-38). The additions of Fe(II) to magnetite (36) and Cu(II) to goethite (38) enhance degradation of chlorinated aliphatic compounds. The reactive surface bound Fe(II) species are able to be regenerated by transition metals, which are contaminants in aquifers, or, by Fe(II), which is produced by DIRB. This results in maintaining reductive ability over long periods (36, 38). Reductive dechlorination of chlorinated aliphatic compounds is observed by iron-bearing clay minerals, such as biotite and vermiculite (11, 39, 40).

2.2.2.3 Zero-valent metals and Permeable reactive barriers

Reductive dechlorination of chlorinated solvents by zero-valent metal (ZVM) (13, 14, 19-22) has been an active research area since Gillham and coworkers (111)

proposed zero-valent iron (ZVI) as a reductant. Since then, permeable reactive barriers (PBR) employing ZVI are the most commonly applied technology for *in-situ* ground water remediation, because they are inexpensive (100). Degradation reactions occur at the metal surface (111, 112,). There are three possible pathways for reductive degradation in PBR (figure 2-13). According to Matheson and Tratnyek (100), the direct electron transfer from metal to sorbed organic compounds (figure 2-13(A)) is a principal reductive dechlorination mechanism. The dissociation of water, resulting in the formation of hydrogen reaction, is also a possible reaction pathway, due to the observation of increasing pH (figure 2-13(B)) (111).

Rate constants are proportional to specific surface area (surface area of iron per solution volume) (111, 112). Therefore, first-order rate constants are normalized by a specific area concentration (k_{SA}) in order to describe the kinetics of dechlorination by zero-valent iron more generally (14). The rate-determining step of reductive dechlorination in a PBR is mass transport of the target compounds to the metal surface. Other factors that affect the long-term operation of PBRs are the formation of precipitates on the metal surface (decreasing permeability), sulfide (affecting redox chemistry of iron), and bacterial activities (oxidizing and reducing Fe) (100).

Frequently found precipitates in PBRs are Fe (oxy)hydroxides, such as goethite, magnetite, and ferrihydrite, green rust, amorphous FeS, and calcium and Fe carbonate (113-115). They are formed as a result of Fe corrosion and deteriorate iron reactivity due to clogging pores (114, 115). Fe corrosion is developed either geochemically (114) or microbially (115).

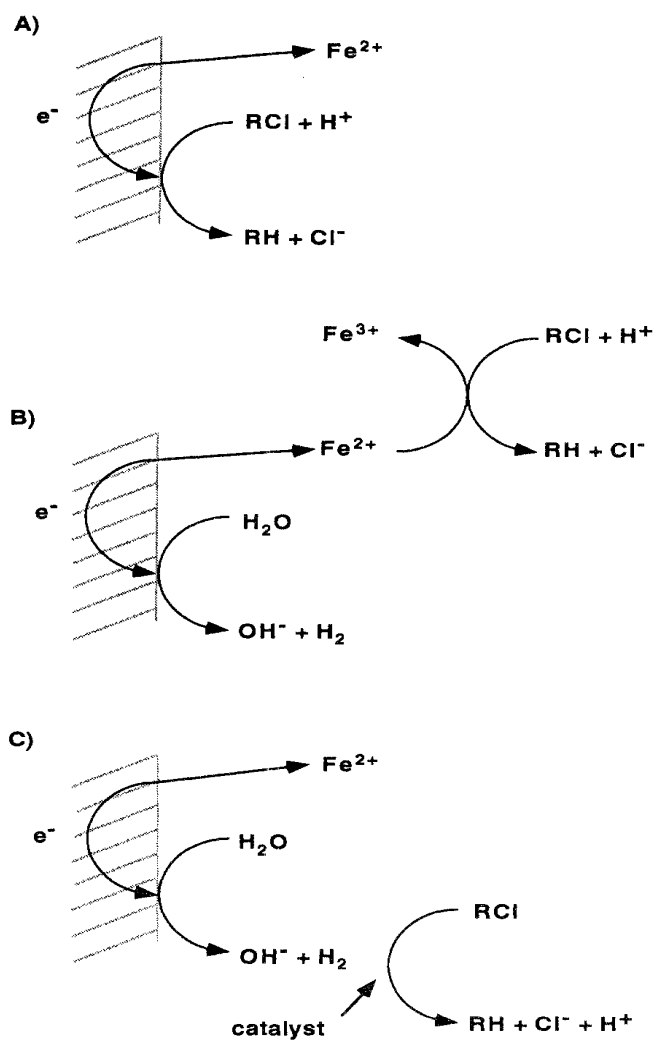
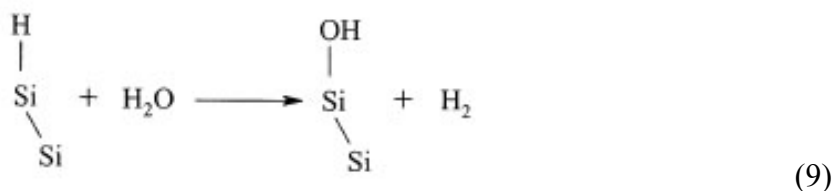


FIGURE 2-13 Scheme showing proposed pathways for reductive dehalogenation in anoxic Fe^0 - H_2O systems. (A) direct electron transfer from iron metal at the metal surface; (B) reduction by Fe^{2+} , which results from corrosion of the metal; (C) catalyzed hydrogenolysis by the H_2 that is formed by reduction of H_2O during anaerobic corrosion (100).

Modified ZVMs can be produced by adding metals such as Pd, Cu, Ni and Pt, which form a metallic coating on the ZVM surface. These bimetallic reductants can be applied to reductive dechlorination. (15-17). Metal catalysts might reduce the activation energy for reductive dechlorination, so that reaction rates increase (15).

Zero-valent silicon/iron (Si^0/Fe^0) can also serve as a reductant for reductive dechlorination (18). Even though the oxidative dissolution of Si^0 forms silicon dioxide (SiO_2) on the surface of silicon after a long exposure to humid air, the removal reaction of hydrogenated silicon and silicon oxide is catalyzed by hydroxide ion (OH^-).



It might be a great advantage to operate a PBR with Si^0/Fe^0 because consumption of hydroxide ion by silicon keeps pH from increasing. Iron oxide precipitation on the zero-valent iron surface can be prevented through the pH buffering ability of Si^0 thereby avoiding the problems of reduced permeability and reactivity found in Fe^0 -PBRs (18).

According to Arnold and Roberts (13), reductive β -elimination is a major reaction for dechlorination of PCE, TCE, *cis*- and *trans*-DCE and hydrogenolysis of *cis*- and *trans*-DCE to acetylene. The rate of reductive dechlorination by ZVI increases with increasing degree of chlorination, that is, the degradation rate of PCE is about 5 times faster than that for TCE and 3 to 60 times faster than that for DCE isomers (19, 20).

2.3 X-ray diffraction

X-ray diffraction (XRD) is the most widely used method to identify unknown minerals and determine crystal structures. Each mineral has its own atomic arrangement and distances between crystal planes, thus, it shows its unique XRD pattern (116). Mineral samples with particle sizes less than 50 μm in the diameter are scanned through diffraction angle and plots of x-ray intensity versus twice diffraction angle (2θ) are obtained. Bragg's law is used to relate the location of x-ray peaks in the plots with distances between diffracting crystal plans (117). Bragg's law (117) is

$$\frac{d}{n} = \frac{\lambda}{2 \sin \theta} \quad (10)$$

where, d = perpendicular distance between diffracting planes to diffracting angle; θ = diffracting angle; n = order of diffraction, usually n is unknown, so it set as 1; λ = wavelength of x-ray radiation; d/n = d -value. These d -values resulting from XRD are characteristics of each mineral and used to identify the minerals.

The wavelength of x-ray is between 0.1 and 10 \AA and depends on the energy of the electron and the materials it hits. When x-rays hit the target materials, two kinds of x-ray beams are emitted. White radiation is a continuous spectrum of x-ray (figure 2-14(A)) and characteristic x-ray (figure 2-14(B)) is characteristic of the target element that produces the x-ray (118). The continuous spectrum of x-ray is background noise and has to be removed by filtering. Along with the continuous spectrum, K_{β} must be also removed to have monochromatic x-rays of K_{α} , which has the greatest intensity. Table 2-3 present the wavelengths of characteristic x-ray commonly used as targets and suitable thickness. Copper is the most frequently used target.

Fluorescent x-radiation, resulting from an excited element in the specimen by primary x-ray beams, increases background noise and, thus, reduces the clarity of x-ray diffraction. To avoid unwanted fluorescent effects, a proper target should be chosen. For example, if the sample contains high amounts of iron, copper would be not a good target. Cobalt or iron radiation would be better. However, copper radiation gives a higher intensity than cobalt and iron. Another way to reduce fluorescent effect while using copper as target is to put a crystal monochromator between the specimen and the counter (118).

XRD data are collected in a series of books called the Joint Committee on Powder Diffraction Standards (JCPDS) X-ray Powder Data File (PDF). This book lists d-values with relative intensity along with crystallography, physical property and optical data of each mineral (119). Minerals can be identified by either Hanawalt or chemical index. Three strongest peaks are listed in the Hanawalt index. Under the assumption of possible chemical compositions of suspected minerals, search chemical index until the three strongest peaks get matched (120).

TABLE 2-3 X-ray wavelengths and suitable filters to give $K_{\beta 1}/K_{\alpha 1} = 1/100$ (118)

Target element	Wavelength (\AA)				β filter	Thickness (mm)	High fluorescence from		
	$K_{\alpha 1,2}$	$K_{\alpha 1}$	$K_{\alpha 2}$	K_{β}					
Mo	0.7107	0.7093	0.7135	0.6323	Zr	0.08	Y	Sr	Ru
Cu	1.5418	1.5405	1.5443	1.3922	Ni	0.015	Co	Fe	Mn
Co	1.7902	1.7889	1.7928	1.6207	Fe	0.012	Mn	Cr	V
Fe	1.9373	1.9360	1.9399	1.7565	Mn	0.011	Cr	V	Ti

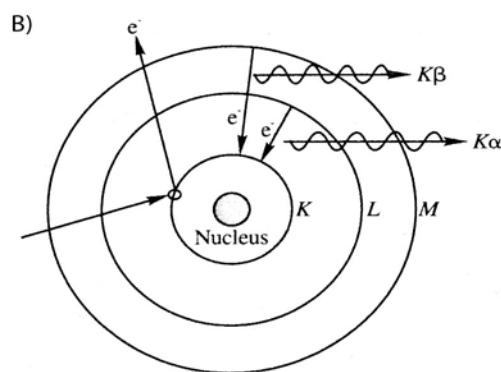
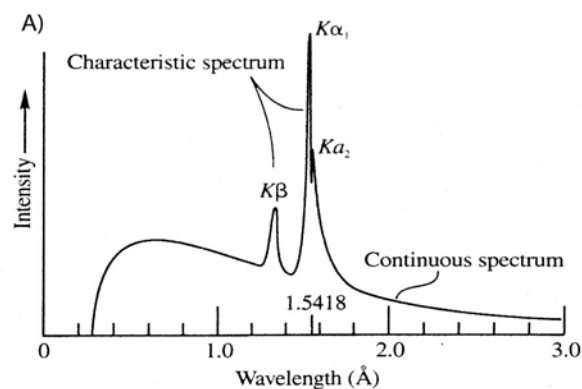


FIGURE 2-14 X-ray spectra. (A) Intensity of X-rays emitted by a copper target operated at 50 kV. The characteristic spectrums (peaks) are superimposed on the continuous spectrum. (B) The characteristic spectrum is produced when electrons are dislodged from the K shell and electrons from outer shell drop in to occupy the vacancy (119).

The quantitative interpretation of diffraction patterns is possible because intensity of diffraction is related to the number of planes. The relative intensity can give an estimation of mineral concentrations. There are two methods to estimate the concentrations of a mineral. One is the internal standard method, which uses a calibration curve and the other is the standard addition method, where known amounts of material are added to the sample. The second method does not require a calibration curve to determine the concentration of minerals, but uses the ratio of the relative intensity (120). The relative intensity is also affected by other factors, such as particle size, crystal perfection, and chemical composition, variations in sample packing, crystal orientation, and presence of amorphous substances (121). Therefore, quantification of minerals by XRD is very difficult (120).

2.4 Electron microscopy

Scanning electron microscopy (SEM) and electron probe microanalyzer (EPMA) can examine the surface of heterogeneous organic and inorganic materials at a micrometer (μm) or submicrometer scale. Both instruments use very finely focused electron beams to examine specimens. The types of electron beams include secondary electrons, backscattered electrons, auger electrons, characteristic x-rays, and photons of various energies (figure 2-15). SEM often uses secondary electrons and backscattered electrons to produce images. EPMA uses mainly characteristic x-ray to yield both qualitative and quantitative compositional analyses of micrometer scale area of a specimen (63).

The useful features of SEM yield high resolution and a three-dimensional image, while EPMA can gather compositional information nondestructively, as well as create compositional mapping. The energy-dispersive spectrometer (EDS) is the most commonly used x-ray analyzer (63).

The components of an SEM are the three lens systems, electron gun, electron collector, visual and recording cathode ray tubes (CRT), and the electronics associated them (figure 2-16). An electron gun produces an electron beam having the range of 1 to 40 KeV of the energy and then three electron lenses generate a finely focused beam, which forms a spot less than about 10 nm on the specimen surface. Two pairs of scan coils control the magnification, which is defined as the ratio of the linear size of the viewing screen to the linear size of the raster on the specimen. This is done by controlling the deflection distance of the raster of the beam on the specimen. The electron detector collects the signal and the camera records the images (63).

Samples used in SEM are required to eliminate or reduce the electric charge and image distortion. The electric charge is generated when the high energy of the beam scans the surface of samples. Samples are usually coated with conductive materials, such as gold, platinum, palladium, or carbon, to reduce the electric charge on the surface of samples (63).

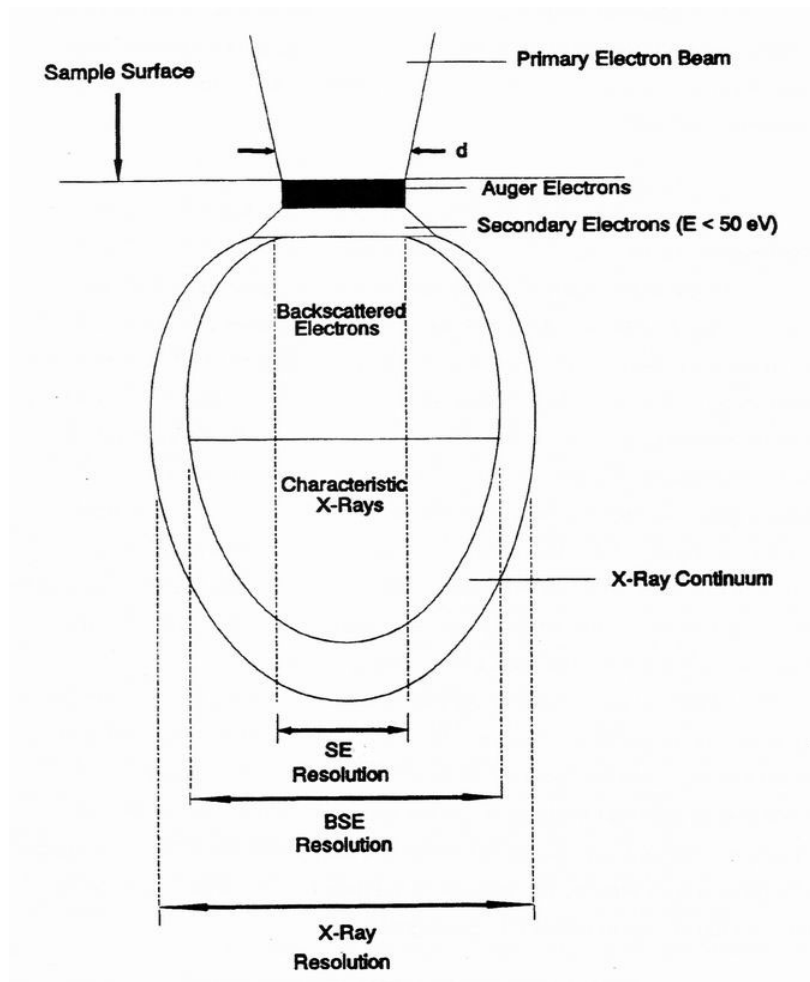


FIGURE 2-15 Types of signals resulting from the interaction of an electron beam with a sample (63).

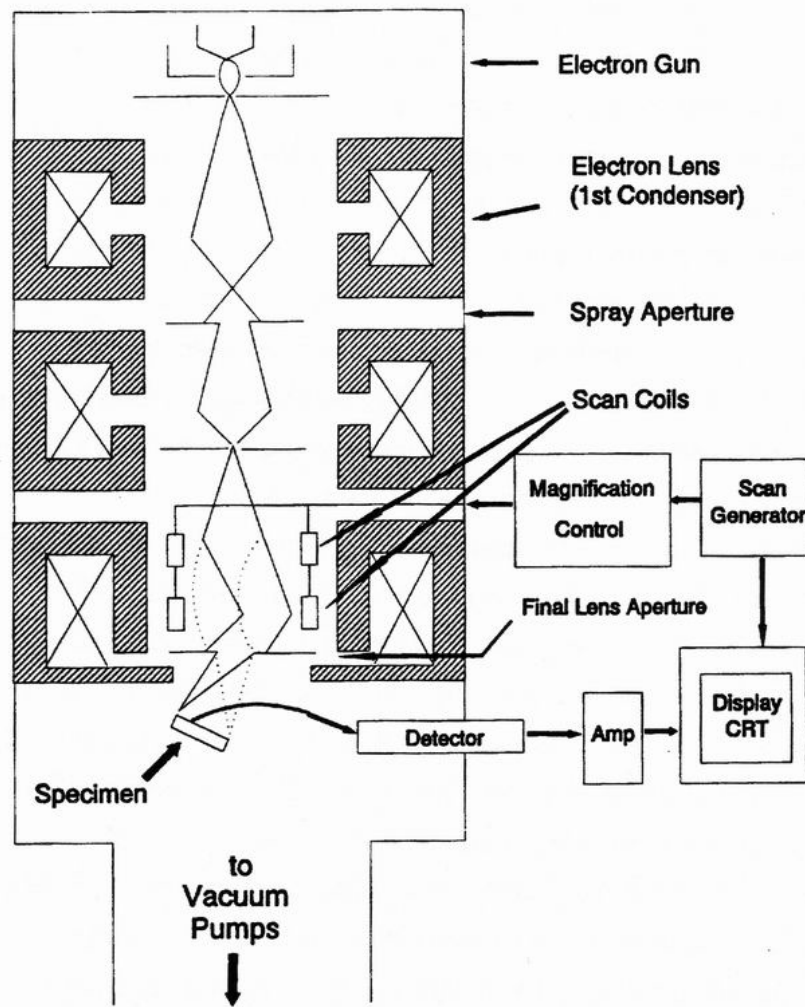


FIGURE 2-16 Schematic of SEM showing the electron column, the deflection system, and the electron detectors (63).

Relatively accurate quantitative analysis of elements above Na can be achieved, but this is more difficult for elements below Be in the periodic table. The detection limit of x-ray analysis is normally 50-100 part per millions (ppm) (122). The concentration of a given element in the analyzed region is proportional to x-ray intensities emitted by a

specimen (63). In addition, each element has its own characteristic wavelength, so that differentiated quantum energy can be obtained using the following equation,

$$E(\text{KeV}) = \frac{12.396}{\lambda} \quad (11)$$

where, λ = wavelength of each photon, Å. For example, NiK_α is 1.659 Å and quantum energy for Ni is 7.471 (= 12.396/1.659) KeV. Thus, typical x-ray spectrum can be obtained by the plot of quantum energy (x-axis) versus intensity (y-axis), providing qualitative or semi-quantitative analyses of a selected region of a specimen (122).

CHAPTER III

METHODOLOGY

3.1 Materials

Tetrachloroethylene (99.9+%, HPLC grade, Aldrich) was used as a target organic compound. Portland cement (Capitol Cement, Lehigh, and Quikrete for type I and Txi for type I/II) and ferrous chloride (99+%, tetrahydrate, Aldrich) were used as DS/S agents. Synthetic cement extract solutions were made using the following chemicals (ACS or higher grade): aluminum chloride (hexahydrate, 98+%, Sigma), boric acid (Matheson), barium chloride (dehydrate, 100.3%, Fisher Scientific), beryllium sulfate (tetrahydrate, 99+%, Fluka), calcium chloride (dihydrate, 99.5%-105.0%, ACS grade, EM), ferric chloride (hexahydrate, 98+%, Sigma), cupric chloride (dehydrate, 99+%, Aldrich), magnesium chloride (hexahydrate, 99+%, EM), magnesium sulfate (heptahydrate, 98+%, EM), manganous sulfate (monohydrate, 98.6+%, Fisher Scientific), nickel sulfate (hexahydrate, Aldrich), strontium chloride (hexahydrate, 99+%, Fluka), zinc chloride (anhydrous, 98+%, EM), sodium silicate (ACS grade, Fisher Scientific). The following chemicals were used to synthesize cement hydration products of monosulfate, Friedel's salt, Kuzel's salt and tetracalcium aluminate hydrate: calcium chloride (dihydrate, 99.5%-105.0%, ACS grade, EM), sodium aluminate (anhydrous, EM), calcium sulfate (dehydrate, 101.5%, ACS grade, Sigma), aluminum chloride (hexahydrate, 98+%, Sigma). Sodium chloride (100.8%, ACS grade, Mallinckrodt) and sodium sulfate (99.9%, ACS grade, Sigma) were used to adjust chloride and sulfate

concentrations in synthetic cement extract (SCX). Sodium carbonate (99.0%, ACS grade, Sigma) was used to remove calcium in Portland cement extract (PCX). De-aerated deionized water was prepared by purging water purified by the Barnstead Nanopure system with nitrogen for at least 12 hours in an anaerobic chamber (Coy Laboratory Product) that contained 5% hydrogen and 95% nitrogen. Ferrous chloride stock solutions were prepared daily in de-aerated deionized water in the anaerobic chamber. PCE stock solution was prepared daily in methanol (99.8%, HPLC grade, EM). Calcium hydroxide (Fisher Scientific) and sodium hydroxide (97+%, ACS grade, EM) were used to maintain pH around 12. Hydrochloric acid (36.5%-38%, ACS grade, EM) was used to dissolve cement.

3.2 Analytical procedures

PCE was analyzed by gas chromatography (Hewlett-Packard 5890 GC with a combination of DB-5 column (30m × 0.35mm i.d. × 0.25µm film thickness, J & W Scientific), and an electron capture detector (ECD)). Aqueous samples were separated from solid phases by centrifuging the reaction vials at 2000 rpm (739 g) for 3 min (International Equipment CO., model CS centrifuge). PCE in the liquid phase was extracted with hexane (99.9%, HPLC grade, EM) containing 1,2-dibromopropane (1,2-DBP, 97%, Aldrich) as an internal standard.

Solid phases containing potential active agents were characterized by X-ray Diffraction and Scanning Electron Microscope with Electron-Dispersive Spectrometer. Rigaku automated diffract meter using Cu K α radiation ($\lambda=1.5406\text{\AA}$) was used to obtain

the powder X-ray patterns (Geology Department and Texas Transport Institute at Texas A&M University). The sample was scanned between 5θ and 60θ with scan speed $3\theta/\text{minute}$ for XRD analysis. JEOL 6400 Scanning Microscope (Microscopy and Image center at Texas A&M University) was used to analyze morphology and chemical compositions of the sample.

Ferrozine method (123) was used for Fe(II) and total iron analysis (UV-VIS spectrophotometer, Hewlett Packard G1103A).

3.3 Experiment procedures

3.3.1 Reactor system

A completely mixed batch reactor was used for the PCE degradation test. The clear borosilicate glasses were used with screw caps lined with three layers: Teflon, lead foil, and Teflon-lined rubber septum (23, 27, 36).

3.3.2 Preparation of 10% (w/v) PCX

Portland cement was dissolved by mixing it with strong acid (2.2N HCl) on the shaking table for at least 24 hours. After 24 hours, the mixture of Portland cement and acid were transferred to several 250-ml plastic centrifuge bottles and centrifuged at 6000 rpm (6650g) for 5 min (Beckman, model J-6M centrifuge, JS-7.5 rotor). Supernatant was filtered with filter paper ($2\mu\text{m}$ quantitative filter paper, VWR scientific products) to remove the visible suspension and solids at the bottom of bottle were discarded. The filtered solution was called a Portland cement extract (PCX) and was used to prepare the

potential active agent. In order to remove oxygen, PCX was purged with nitrogen for at least 24 hours in an anaerobic chamber that contained 5% hydrogen and 95% nitrogen.

3.3.3 Identification of conditions that promote formation of the active agents

Activity tests of all synthesized solids were conducted as one-point kinetic experiments in an anaerobic chamber. Ferrous chloride was used as the ferrous iron source and the reaction pH was around 12. PCE controls were prepared in duplicate and all solid samples were prepared in triplicate. A control contained de-aerated deionized water and PCE. A volume (10 μ l) methanolic PCE stock solution was added to the suspension (24.3 μ l) of the potential active agent to achieve an initial concentration of 0.242 mM. As soon as PCE was spiked, three-layered closures capped the vials. Then the vials were placed on the tumbler that provides end-over-end rotation at 7 rpm at room temperature. PCE concentration in the liquid phase was measured as a function of time.

3.3.3.1 Ca effect

PCX prepared from 100 g/L Portland cement (10% w/v) was pretreated with sodium carbonate to remove calcium. The pH of the mixture of was adjusted to 10 and mixed for 2 hours. Supernatant of this carbonate-pretreated PCX (CPCX) was taken after centrifugation. Two types of solids were prepared using CPCX. One was a mixture of Fe(II), calcium chloride and CPCX and another was a mixture of Fe(II) and CPCX. The pH values of both were adjusted to 11.7 by adding 5 N NaOH after putting all

components together. The mixtures were allowed to react for 2 and 24 hours as shown in figure 3-1.

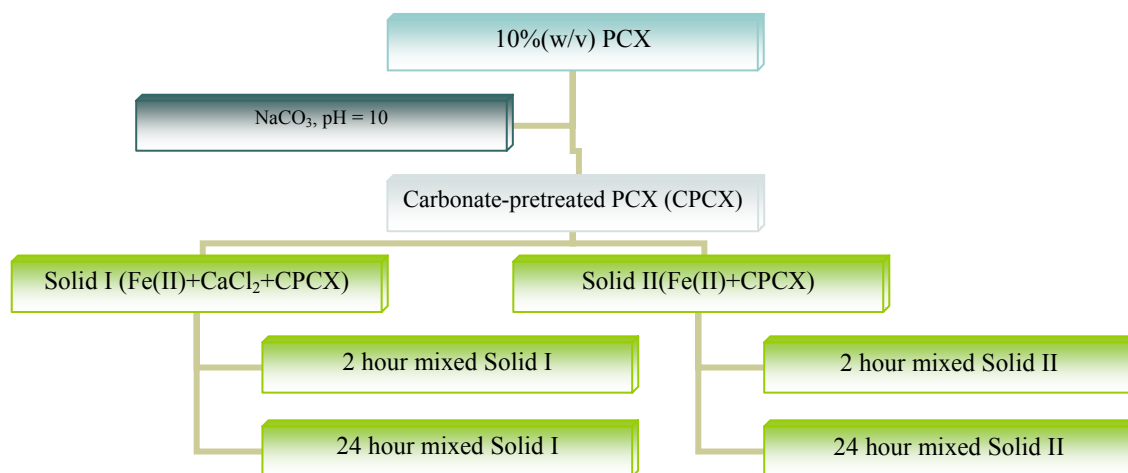


FIGURE 3-1 Schematic diagram of method of synthesizing solids to examine effect of calcium.

Abilities of solids produced from CPCX to degrade PCE were examined over a range of pH (10, 10.5, 11, 11.5, 11.7, 12, 12.5, and 13), CPCX concentrations (4.5%, 8.6%, 17.3%, and 34.5% of weight to volume) and PCX contents (6%, 8%, and 10% of weight to volume).

Experiments to evaluate the effect of pH on activity of solids produced from CPCX were conducted by first preparing 20% (w/v) PCX by dissolving Portland Cement in 4.1N HCl. Then, 20% (w/v) PCX was evaporated passing dry air through the solution until its total volume was reduced by half. Air was dried by passing it through a column

filled with desiccant. The resulting PCX content was 34% (w/v) after evaporation. Sodium carbonate was added to 34% (w/v) PCX to prepare CPCX. The pH was adjusted with 5 N HCl and 5 N NaOH to the desired values (10, 10.5, 11, 11.5, 11.7, 12, 12.5, 13).

Experiments to examine the effects of concentration of PCX and CPCX were prepared by first preparing a 20% (w/v) PCX solution by dissolving Portland Cement in 4.1 N HCl. Then, 20% (w/v) PCX was evaporated by passing dry air through it until its total volume was reduced by half. The resulting PCX content was 34.5% (w/v) after evaporation. Sodium carbonate was added to 34.5% (w/v) PCX to prepare CPCX. The concentrated CPCX (34.5% w/v) was diluted to make 4.3%, 8.6%, and 17.3% CPCX. Fe(II) was added to each CPCX solution and pH was adjusted to 11.8. The mixture was mixed for 24 hours in the anaerobic chamber. Two dilutions (6% and 8% w/v) of PCX were prepared from the concentrated solution (10% w/v). Fe(II) and Ca(OH)₂ were added and mixed with PCX for 2 hours in the anaerobic chamber. After mixing, solid mixtures were centrifuged at 6000 rpm for 5 min and solids from the upper were taken for the PCE degradation test.

3.3.3.2 Effect of cement hydration product

Monosulfate (124), Friedel's salt (125), tetracalcium aluminate hydrate (125) and Kuzel's salt (126) were synthesized in the lab to examine the effect of cement hydration products (CHPs) on solid activities. Each cement hydration product was mixed with ferrous or both ferrous and ferric iron to synthesize ferrous containing solid mixtures as indicated in Table 3-1. The suspensions were adjusted to the desired pH

(11.7 or 12.1). Along with ferrous-containing solids, each cement hydration product without ferrous and/or ferric addition was examined to measure its activity in degrading PCE. In the case of Friedel's salt, two different mixing times, 10 days and 7 days, were used to synthesize the solid.

TABLE 3-1 The procedure to examine the effect of cement hydration product

CHPs	2 hr mixing		24 hr mixing	
	Fe(II)	Fe(III)	Fe(II)	Fe(III)
C ₄ AH _x	39.2mM		39.2mM	
	39.2mM	47.8mM	39.2mM	47.8mM
10d mixed Friedel	39.2mM		39.2mM	
	39.2mM	47.8mM	39.2mM	47.8mM
7d mixed Friedel	39.2mM		39.2mM	
	39.2mM FeCl ₂		39.2mM FeCl ₂	
Kuzel	39.2mM FeSO ₄		39.2mM FeSO ₄	

3.3.3.3 Effect of synthetic cement extract (SCX)

Synthetic cement extract (SCX) was prepared with the composition described by Table 3-2. The concentrations of the elements in table 3-2 are the same as those measured in PCX (10%) (127). Each stock solution was made in 0.01N HCl. Ferrous iron was mixed with SCX for 3 days in the anaerobic chamber to produce reactive solids. Three different kinds of SCX were prepared. One contained all elements of PCX. The second excluded only one element of PCX, and the third excluded all major PCX elements (Ca, Mg, Al, and SO₄). PCE degradation tests were conducted after a 3-day mixing period. The pH was adjusted to 12.0 with 1.25M Ca(OH)₂ for SCX containing full PCX elements and with 5N NaOH for SCX that excludes individual elements.

TABLE 3-2 Stock solution of each element consisting in SCX and element compositions of SCX in each experiment

Chemical	Conc mM	MW	stock mM	g/100ml	added amt mL
CaCl ₂	1000	147.02		14.70	
AlCl ₃	47.8	241.4	477.8	11.53	10
MgSO ₄	6.98	246.48	698	17.20	1
MgCl ₂	15.25	203.3	152.5	3.10	10
MnSO ₄	0.41	169.01	41	0.693	1
SrCl ₂	1.07	266.62	107	2.85	1
Na ₂ SiO ₃	1.62	284.2	162	4.60	1
H ₃ BO ₃	0.35	61.83	35	0.216	1
BaCl ₂	0.05	244.28	5	0.122	1
BeSO ₄	0.005	177.14	5	0.0886	0.1
CuCl ₂	0.02	170.48	20	0.341	0.1
FeCl ₃	0.4	270.3	40	1.08	1
NiSO ₄	0.04	262.86	4	0.105	1
ZnCl ₂	0.24	136.28	24	0.327	1
Cl _{TotSCX}	2178				
SO _{4TotSCX}	7.44				
Ca(OH) ₂	1250	74.09		9.26	
FeCl ₂	39.2	198.8	196	3.896	20

Exp	Ca	Al	Mg	Fe(III)	Mn	Cu	Zn	Ni	SiO ₃	Sr	B	Ba	Be
30													
31													
32													
33													
34													
35													
36													
37													
38													
39													
40													
41													
42													
43													
44													

No filled box indicates the absence of an element in each experiment

3.3.3.4 Effect of major cement extract element

Fe(III), Mg, Al, SO₄, and/or SiO₃ were used to synthesize another set of solids that potentially could contain high concentrations of the active agent. Fe(II) and Cl were always added to the mixtures because they were presumed to be the critical elements for the formation of the active agent (127) and PCE degradation tests were performed with the solids produced after mixing for 3 days in the anaerobic chamber. The concentrations of these elements other than Fe(III), presented in table 3-3, were chosen as the same as ones in section 3.3.3.3. The lower concentration of Fe(III) to be used (0.4mM) was the same as in table 3-2. The higher concentration of Fe(III) (13.1 mM) was chosen to make the ratio of Fe(II) to Fe(III) equal to 3, which was the same ratio found in chloride green rust (GR(Cl)), which was a presumable active agent in Fe(II)-DS/S system. These solids were synthesized in two ways. One way simply mixed the necessary elements at once (table 3-3) and the other applied a method used to synthesize GR (128) (Table 3-4). The effect of the concentration of ferric iron (0.4mM, 2mM, 4mM, 6mM, 8mM, and 10mM) and the effect of mixing time (2h, 12h, 1d, 2d, and 3d) on the activity of solids were examined for solids prepared with the simple technique.

TABLE 3-3 Different element compositions for the simple mixing method in which solids were synthesized from major element of PCX

Exp	Element(mM)						
	Fe(II)	Fe(III)	Cl	Mg	Al	SO ₄	SiO ₃
47	39.2	0.4	2178				
48	39.2	0.4	2178	22.2			
49	39.2	0.4	2178		47.8		
50	39.2	0.4	2178	22.2	47.8		
51	39.2	13.1	2178				
52	39.2	13.1	2178	22.2			
53	39.2	13.1	2178		47.8		
54	39.2	13.1	2178	22.2	47.8		
55	39.2	0.4	2178			7.44	
56	39.2	0.4	2178		47.8	7.44	
57	39.2	13.1	2178			7.44	
58	39.2	13.1	2178		47.8	7.44	
59	39.2	0.4	2178				1.62

TABLE 3-4 Different element compositions and element addition orders for the GR synthesis method in which solids were synthesized from major element of PCX

(a) Solid consisting of Fe(II), Fe(III), and Cl

	Element addition order	1 st	2 nd		3 rd	4 th
	Element	Cl	Fe(II)	Fe(III)	OH ^a	Adjust pH ^b
Exp.71-75	Conc.	2.17M	39.2mM	8.7mM	70mM	12.0
Exp.76-80					110mM	

	Element addition order	1 st		2 nd	3 rd	4 th
	Element	Fe(II)	Fe(III)	OH ^a	Cl	Adjust pH ^b
Exp. 81-85	Conc.	39.2mM	8.7mM	70mM	2.17M	12.0
Exp. 86-90					110mM	

^aNaOH addition rate (Vol_{Total} = 50000μL)

- i. 10.0μL/sec
- ii. 33.3μL/sec
- iii. 83.3μL/sec
- iv. 167μL/sec
- v. 50000μL/sec

^bpH raising rate

- i. When 70mM NaOH was added – 3.33μL/sec of 5M NaOH was added to raise pH to 12.0
- ii. When 110mM NaOH was added – 1.67μL/sec of 5M NaOH was added to raise pH to 12.0

Table 3-4 Continued

(b) Solids consisting of Fe(II), Fe(III), Cl, and one major element, Mg, SO₄, or SiO₃, of PCX

Exp.	Element addition order	1 st	2 nd		3 rd /4 th			5 th	
	Element	Cl	Fe(II) and Fe(III) addition		Rest elements	OH ^c	Adjust pH ^d		
			Fe(II)	Fe(III)					
91-96	Conc.	2.17M	39.2mM	0.4mM	Mg	22.2mM	70mM	12.0	
97-102			39.2mM	8.7mM	Mg	22.2mM	70mM		
103-108			39.2mM	0.4mM	Mg	22.2mM	110mM		
109-114		2.17M	39.2mM	0.4mM	8.7mM	SO ₄	7.44mM	70mM	12.0
115-120						SO ₄	7.44mM	70mM	
121-126						SO ₄	7.44mM	110mM	
127-132						SiO ₃	1.62mM	70mM	
133-138		SiO ₃	1.62mM	70mM					
139-144		SiO ₃	1.62mM	110mM					

^cNaOH addition rate (Vol_{Total} = 50000μL)

- i. 20.0μL/sec
- ii. 83.3μL/sec
- iii. 50000μL/sec

^dpH raising rate: 3.33μL/sec of 5M NaOH was added to raise pH to 12 , except SO₄ and SiO₃ addition in the case of 110mM NaOH used (pH raising rate = 1.67μL/sec)

3.3.4 Identification of the active agents through instrumental analyses (XRD, SEM and SEM-EDS)

Solids presented in table 3-4 underwent instrumental analyses. Fe(II), Fe(III) and Cl might be the most important elements that affect formation of the active agent. The synthesis method and pH were also expected to affect the formation of the active agent. Thus, solids 1-1, 1-2 and 2 (table 3-4) were chosen to examine solids formed under two different pH values and two different synthesis methods. FSCX solid (solid 3) was examined to investigate whether SCX makes the same solid as PCX did. MSCX solid

(solid 4) was chosen to investigate whether major elements of PCX (Ca, Mg, Al, and SiO₃) have an effect on the formation of the active agent. PCX w/ Fe(II) (solid 5) and PCS w/ Fe (II) (solid 7) were previously investigated for PCE degradation (23, 127) and were also chosen for the instrumental analyses. Solids synthesized with only PCX (10%) and calcium hydroxide (Solid 6) showed no activity for PCE degradation in a preliminary experiment and they were also examined to observe the role of Fe(II) on the formation of the active agent.

All solids undergoing instrumental analyses were dried in the anaerobic chamber after synthesis. Solids 1 through 4 in table 3-4 were synthesized using the same method as in section 3.3.3. Solid 5 was prepared by mixing ferrous iron, PCX (10%) and calcium hydroxide. Sufficient calcium hydroxide was added to increase the pH to around 12, which was the optimum pH of Fe(II)-DS/S. After adding reagents, the solutions were mixed on the magnetic stirrer for a couple of hours in an anaerobic chamber. Centrifugation was used to attempt to separate the potential active agent from inactive solids. A previous experiment (127) showed that higher levels of activity were observed for solids separated by centrifugation. Two layers of solids were formed after centrifugation- a light blue solid at the top and a white solid at the bottom. The white solid probably consists of lime and other cement hydration products. The light blue solid might contain higher levels of the active agent. Therefore, the colored solid from the top layer was taken and dried in an anaerobic chamber for instrumental analysis (XRD, SEM, SEM-EDS).

Solid 7 was also prepared by mixing ferrous iron and Portland cement to produce a slurry with solid/solution mass ratio of 0.1. Portland cement (2.33 g) and de-aerated deionized water (23.3 mL) was added to clear borosilicate glasses with the three-part closure (Teflon tape, lead foil tape, Teflon-lined rubber septum). Ferrous iron was added to the Portland cement slurries at the same concentration as used in the PCX experiment. All preparations were conducted in an anaerobic chamber. The glass vials and closures were equilibrated in an anaerobic chamber before conducting the sample preparations. After ferrous iron was added to the cement slurry, the vials were mixed on the shaking table for 5 days outside of the anaerobic chamber. After 5 days, the sample vials were taken into the anaerobic chamber and then transferred to several 250-ml plastic centrifuge bottles. These bottles were tightly sealed with parafilm before taken out from an anaerobic chamber. These bottles were centrifuged at 6000 rpm (6650 g) for 5 min and the top layer solid were taken (figure 3-2). This solid was dried in an anaerobic chamber for instrumental analysis (XRD, SEM, SEM-EDS). The pH was adjusted to 12 using 5N HCl.

TABLE 3-5 Solids to be analyzed by XRD and SEM with EDS

	Solid	Fe(II)	Fe(III)	NaOH	pH
1-1	Fe(II)(III)Cl (GR method)	39.2mM	0.4mM	70mM	neutral
1-2	Fe(II)(III)Cl (GR method)	39.2mM	0.4mM	110mM	12
2	Fe(II)(III)Cl (simple mixing)	39.2mM	0.4mM		12
3	FSCX ^a	39.2mM	0.4mM		12
4	MSCX ^b	39.2mM	0.4mM		12
5	PCX w/ Fe(II)	39.2mM			11.7
6	PCX w/o Fe(II)				11.7
7	PCS ^c w/ Fe(II)	39.2mM			12

^a = Full Element Synthetic Cement Extract, which contains all elements of PCX

^b = Minor Element Synthetic Cement Extract, which excludes major elements of PCX, Ca, Mg, Al, and SiO₃

^c = 10% (w/v) Portland Cement Slurry

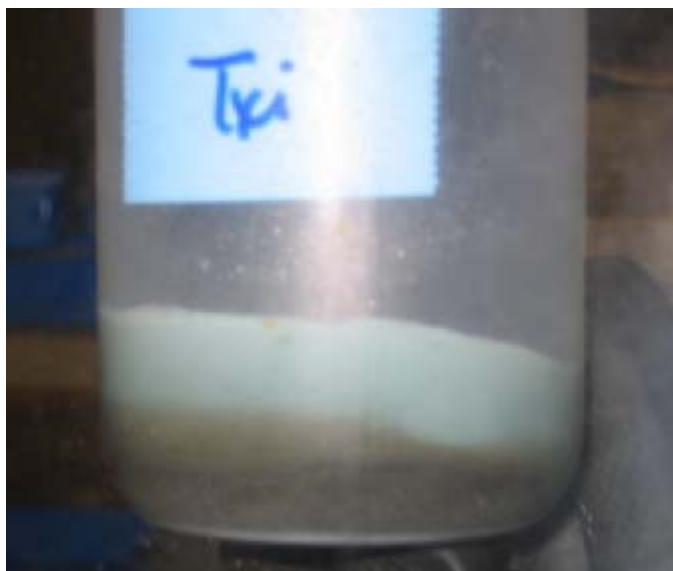


FIGURE 3-2 Two layers of solids after centrifugation of Fe(II) containing PCS solids.

3.3.5 Examination of variability of Ordinary Portland Cement (OPC)

Portland cements from three different cement manufacturers were chosen to examine the variability of cement source on activity of solids produced by mixing them in 10% slurries with Fe(II). PCE degradation kinetics was measured in tests using at least 10 samples obtained at well-spaced times. Solids were also produced with 10% PCX for comparison. Kinetic constants were obtained through nonlinear regression using Matlab. These constants were compared to previous results by Hwang (23) and Ko (127). Instrumental analysis (XRD, SEM, SEM-EDS) was applied to solids produced by the various OPCs using the same procedures as in section 3.3.4.

CHAPTER IV

RESULTS AND DISCUSSION

4.1 Identification of conditions that promote formation of the active agents through solid activity tests

4.1.1 Evaluation of kinetic constants

PCE degradation by Fe(II)-based DS/S previously showed pseudo-first order kinetics (23, 127). Apparent kinetic constants were determined that considered partitioning of PCE to gas, liquid and solid phases (23);

$$\frac{dC_l}{dt} = -\frac{k}{\left(1 + H \frac{V_g}{V_l} + K_s\right)} C_l = -\frac{k}{P} C_l = -k_{app} C_l \quad (12)$$

where C_l : PCE concentration in the liquid phase

k : corrected pseudo-first-order-rate coefficient

H : dimensionless Henry's law constant for PCE

V_g and V_l : volume of the gas and liquid phases

K_s : solid phase partition coefficient of PCE (ratio of mass of PCE in all solid phases to mass of PCE in aqueous phase)

P : partitioning factor = $1 + HV_g/V_l + K_s$

k_{app} : apparent pseudo-first-order-rate coefficient

The exponential function was assumed to be valid based on the previous experiments that showed first-order degradation kinetics (23, 127). The exponential function ($C_l = C_0 \exp(-k_{app} t)$) was transformed to the natural log function ($\ln C_l = \ln C_0 - k_{app} t$), which is the same form as a linear function with $\ln C_l$ as a y-axis, t as a x-axis, and $-k_{app}$ as a slope, and then the values of k_{app} in one-point solid activity

tests with known values of PCE concentration in liquid phase and time were obtained through hand-calculation in the natural log function. The 95% confidence intervals for the rate constants were calculated using an equation of the confidence interval on the slope for simple linear regression. The error of estimated solid concentration normalized rate constants was calculated using Taylor Series.

4.1.2 Effect of Ca

Table 4-1 shows the pseudo first-order rate constants of PCE reduction with carbonate-pretreated PCX (CPCX) solids. After pretreatment of carbonate to remove Ca in PCX, the same Ca concentration as PCX was added to one set of experiments (CPCX solid I, exp. 1 and 2) and not to another (CPCX solid II, exp. 3 and 4) to examine Ca effect on PCE degradation. In addition to the Ca effect, mixing time effects (2 and 24 hours) on the formation of active agents were also examined. As shown in table 4-1, Ca and mixing time did not affect the rate of PCE degradation. The pseudo-first order rate constants normalized by solids, Fe(II), and Fe(III) were observed to have values that had the same order of magnitude. Based solely on results shown in table 4-1, neither the presence of Ca nor solid mixing time affected the observed rates. Therefore, it appears that these factors do not enhance the formation of the active agents.

Table 4-2 shows composition of the solids produced in experiments with CPCX and PCX produced with different concentrations of Portland cement. As CPCX concentration was increased, the concentration of Fe(II) in the solids decreased and the concentration of Fe(III) in the solids increased. The total concentration of solids also

increased. Solid phases that do not contain Fe(II) might be more formed to a greater extent with cement extracts formed with higher concentrations of cement. This might be most extensive in the 34.5% CPCX (exp. 8). In addition, some of Fe(III) might be associated with non-active agents. Although concentrations of Fe(II) in the solids decreased with increasing PCX contents, the concentration of Fe(III) also decreased, resulting in reduced total iron concentrations. The composition of iron in the solids could also be affected by how they were prepared. Solids were centrifuged and only the top layer of solids were collected and used to conduct PCE reduction tests. More ferrous iron might have been contained in the solids in the bottom layer.

Behavior of the observed rate constants in systems with CPCX and PCX are shown in figure 4-1 and 4-2. The pseudo first-order rate constants for CPCX that were normalized by concentration of solids and Fe(III) (k_{solid} and $k_{\text{Fe(III)}}$) decreased with increasing CPCX contents from 4.5 to 17.3%. However, k_{solid} and $k_{\text{Fe(III)}}$ suddenly increased by 2 times and 5 times, respectively, as CPCX contents increased from 17.3% to 34.5%. The pseudo first-order rate constant for CPCX normalized by Fe(II) concentration ($k_{\text{Fe(II)}}$) gradually increased with increasing CPCX contents from 4.5 to 17.3% and then increased by the factor of 10 from 17.3% to 34.5%. The values of $k_{\text{Fe(II)}}$ were the most dependent on CPCX contents.

The observed rate constants (k_{solid} , $k_{\text{Fe(III)}}$, and $k_{\text{Fe(II)}}$) of PCX solids increased as PCX contents increased. As PCX concentration increased by 2%, k_{solid} , $k_{\text{Fe(III)}}$, and $k_{\text{Fe(II)}}$ values increased by 1.5, 3, and 2 times, respectively. The values of $k_{\text{Fe(III)}}$ were the most dependent on PCX contents.

In exp. 5 to 8, solids were formed in the absence of Ca and pH was adjusted with 5N NaOH. In exp. 9 to 11, solids were formed in the presence of Ca and pH was adjusted with 1.25M Ca(OH)₂. These modifications might cause the different PCE removal behaviors and less activity of CPCX solids. It probably indicates that the elemental compositions of cement extract strongly affect the formation of active agents. The dependence on chemical compositions in cement extract was also observed when KOH was used to adjust pH instead of Ca(OH)₂ (127). In the experiment that used KOH, the value of $k_{\text{Fe(II)}}$ was one order of magnitude lower than that when Ca(OH)₂ was used even though solid concentrations in the experiments with KOH were much higher than those with Ca(OH)₂. That might indicate that KOH leads to formation of more non-active solid phases.

Although there was not much effect of Ca (exp. 1 and 2 compared to 3 and 4, table 4-1), solids formed from CPCX and PCX showed different behaviors in terms of PCE removal. Ca extracted from cement in PCX and foreign Ca added to CPCX could act differently. Ca added to CPCX might not become a component of active agents. Active agents formed in PCX and CPCX systems might be different. In addition, PCE degradation rates of PCX were more strongly affected by cement extract concentrations than those of CPCX. The lack of Ca might lead to form active agents which are less sensitive to the element composition and element concentration.

TABLE 4-1 Pseudo first-order rate constants for PCE reduction by Fe(II)-PCX solids with and without Ca

Exp.	Solid	Mixing time Hour	pH	k_{solid}^c L/(g×d)	$k_{\text{Fe(II)}}^d$ (mM×d) ⁻¹	$k_{\text{Fe(III)}}^e$ (mM×d) ⁻¹
1	CPCX solid I ^a	24	11.6	1.3E-03 (±51%)	1.2E-03 (±51%)	7.2E-03 (±51%)
2		2	11.7	2.0E-03 (±7.7%)	1.9E-03 (±7.9%)	2.0E-02 (±7.9%)
3	CPCX solid II ^b	24	11.7	1.9E-03 (±47%)	1.4E-03 (±47%)	1.7E-02 (±47%)
4		2	11.7	1.1E-03 (±51%)	5.0E-04 (±52%)	7.5E-03 (±52%)

^a Carbonate-pretreated PCX adding 39.2mM FeCl₂ and 1M CaCl₂

^b Carbonate-pretreated PCX adding only 39.2mM FeCl₂

^c $k_{\text{solid}} = k_{\text{app}}/\text{solid conc.}$

^d $k_{\text{Fe(II)}} = k_{\text{app}}/\text{Fe(II) conc.}$

^e $k_{\text{Fe(III)}} = k_{\text{app}}/\text{Fe(III) conc.}$

k_{app} = pseudo-first order rate constant, unit = day⁻¹

Initial PCE concentration was 0.242mM

A sampling time for individual experiment was 4 days for exp. 1 and 3; and 3 days for exp. 2 and 4

Uncertainties represent 95% confidence limits expressed in % relative to estimate k

TABLE 4-2 Iron and solid concentrations in different cement extract contents of 24hour-mixed CPCX solid II and Fe(II)-PCX solid

Exp.	Cement content %(w/v)	pH	Fe(II) mM	Fe(III) mM	Fe(II)/ Fe(III)	Fe(T) mM	solid conc g/L
5	4.5% CPCX	11.9	37.7	3.15	12.0	40.8	6.01
6	8.6% CPCX	11.8	35.2	4.22	8.34	39.4	8.34
7	17.3% CPCX	11.8	32.1	9.58	3.35	41.7	13.8
8	34.5% CPCX	11.7	20.2	14.5	1.39	34.7	60.2
9	6% PCX	11.7	23.7	16.6	1.43	40.3	52.1
10	8% PCX	11.7	23.1	9.83	2.35	32.9	73.0
11	10% PCX	11.7	15.8	5.17	3.06	21.0	80.3

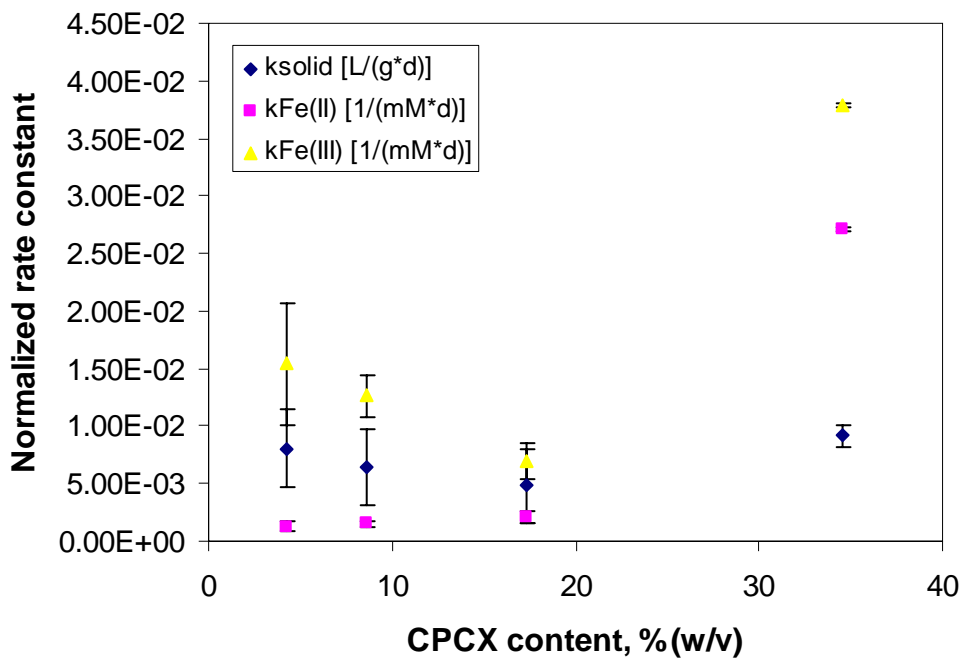


FIGURE 4-1 The variation of normalized pseudo first-order rate constants with respect to CPCX contents. Solid = 24h CPCX solid II, $[PCE]_0 = 0.242\text{mM}$, and sampling time = 3.5 days. Error bar represents 95% confidence interval.

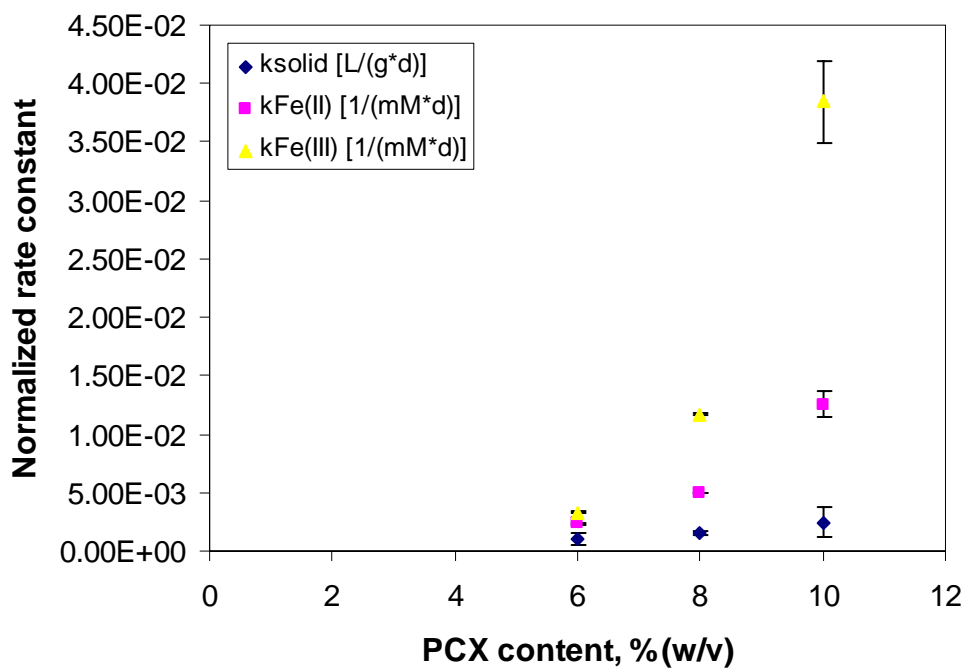


FIGURE 4-2 The variation of normalized pseudo first-order rate constants with respect to PCX contents. Solid = Fe(II)-PCX solid, $[PCE]_0 = 0.242\text{mM}$, and sampling time = 4 days. Error bar represents 95% confidence interval.

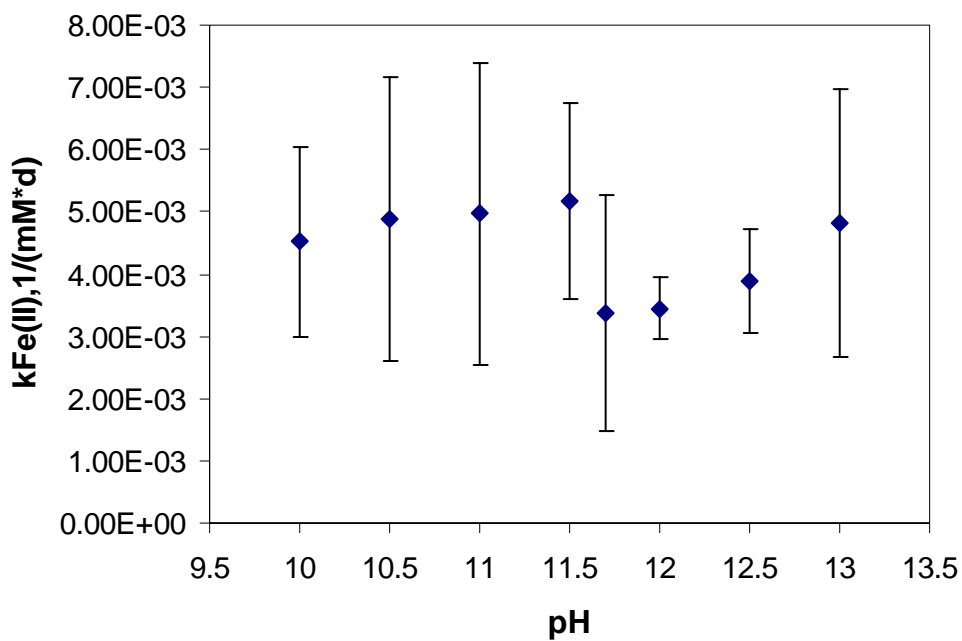


Figure 4-3 The effect of pH on pseudo first-order rate constants normalized with Fe(II) concentration ($k_{Fe(II)}$). Solid = 24h CPCX solid II, CPCX content = 34%(w/v), $[PCE]_0 = 0.242\text{mM}$, and sampling time = 3 days. Error bar represents 95% confidence interval.

Figure 4-3 shows the effect of pH on activity of solids produced by 24 hour mixing of 34% CPCX (solid II). The trend of pseudo first-order rate constants in CPCX was totally different from those reported for Fe(II)-DS/S (23). PCE reduction in Fe(II)-DS/S was the highest at pH 12.1. The effect of pH on rate constants for PCE degradation fitted well with a normal distribution function (23). Optimal pH of PCE reduction by CPCX was 11.5. $k_{\text{Fe(II)}}$ values increased with pH up to 11.5, sharply decreased and then continued to increase up to pH 13. The differences between the highest (pH 12.1) and lowest (pH 10.6) $k_{\text{Fe(II)}}$ in Fe(II)-DS/S were about the factor of 10. However, the highest (pH 11.5) and lowest (pH 11.7) $k_{\text{Fe(II)}}$ in CPCX were smaller than Fe(II)-DS/S, i.e., $k_{\text{Fe(II)}}$ at pH 11.5 was about 1.5 time faster than pH 11.7. $k_{\text{Fe(II)}}$ values in all pH range, from 10.5 to 13, fell into the same order of magnitude. $k_{\text{Fe(II)}}$ of CPCX solids was about one order of magnitude faster than Fe(II)-DS/S solids at pH 10.5 and three time faster at pH 11.5. CPCX and Fe(II)-DS/S solids showed the similar activities at pH 12 and 12.5.

Results of experiments show that Ca affects the formation of active agents, based on the comparisons of PCE reduction behaviors and solid activities among CPCX, Fe(II)-PCX and Fe(II)-DS/S systems. Those experiments might indicate that formation of the active agent is very sensitive to chemical composition of cement extracts.

4.1.3 Effect of cement hydration products

Table 4-3 shows the results of PCE reduction experiments using a mixture of Fe(II) and/or Fe(III) and cement hydration products (tetracalcium aluminate, Friedel's salt, and Kuzel's salt). When no iron was added to the suspensions of cement hydration

products (CHP), PCE was degraded negligibly or not at all (exp. 12, 17, 22, and 25). When both Fe(II) and Fe(III) were added to C₄AHx suspensions and mixed for 2 hours in the anaerobic chamber, PCE was not degraded (exp. 23). Suspensions of Kuzel's salt mixed for 2 hours with ferrous sulfate showed no activity in degrading PCE (exp. 28). Solid concentrations of Kuzel's salt were not directly measured due to messing up the vial location in the oven during solid drying processes. Generally, the location of sample vials in the oven was recorded in the lab note before oven-drying in order to track down samples because paper labeling of glass vial samples was unreadable after solid drying. In the case of Kuzel's salt, the vial samples were disturbed and lost their original location so that they could not be identified through their location. Therefore, all solid masses after drying were averaged and their standard deviations were less than 5%. Averaged solid mass was applied to calculate solid concentrations.

TABLE 4-3 Pseudo first-order rate constants for PCE reduction by cement hydration products (tetracalcium aluminate, Friedel's salt, and Kuzel's salt) by themselves, with Fe(II) and with both Fe(II) and Fe(III)

Exp.		Solid	pH	k_{solid} L/(g×d)	$k_{\text{Fe(II)}}$ (mM×d) ⁻¹	$k_{\text{Fe(III)}}$ (mM×d) ⁻¹
12	C ₄ AH _x	no Fe(II),Fe(III)	11.8	N/A	N/A	N/A
13		2h Fe(II)	11.8	1.8E-04 (±352%)	1.1E-04 (±352%)	2.1E-03 (±352%)
14		2h Fe(II)+Fe(III)	11.8	N/A	N/A	N/A
15		24h Fe(II)	11.8	5.5E-04 (±53%)	3.3E-04 (±53%)	6.2E-02 (±53%)
16		24h Fe(II)+Fe(III)	11.8	1.5E-04 (±463%)	1.2E-04 (±187%)	1.1E-04 (±187%)
17	Friedel's	no Fe(II),Fe(III)	11.8	N/A	N/A	N/A
18	(10d)	2h Fe(II)	11.8	1.8E-04 (±203%)	8.9E-05 (±203%)	7.3E-04 (±203%)
19		2h Fe(II)+Fe(III)	11.8	2.1E-04 (±62%)	1.3E-04 (±62%)	2.5E-05 (±62%)
20		24h Fe(II)	11.8	4.5E-04 (±119%)	2.3E-04 (±119%)	7.2E-04 (±119%)
21		24h Fe(II)+Fe(III)	11.8	3.1E-04 (±135%)	2.0E-04 (±135%)	6.6E-05 (±135%)
22	Friedel's	no Fe(II),Fe(III)	12.0	7.3E-04 (±40%)		
23	(7d)	2h Fe(II)	12.1	1.8E-03 (±20%)	3.3E-04 (±20%)	7.8E-03 (±20%)
24		24h Fe(II)	12.1	2.0E-03 (±32%)	4.2E-04 (±32%)	5.2E-03 (±32%)
25	Kuzel	no Fe(II),Fe(III)	12.1	N/A	N/A	N/A
26		2h FeCl ₂	12.1	2.7E-03*	2.6E-03 (±44%)	2.5E-02 (±44%)
27		24h FeCl ₂	12.1	5.0E-04*	4.3E-04 (±70%)	2.4E-03 (±70%)
28		2h FeSO ₄	12.1	N/A	N/A	N/A
29		24h FeSO ₄	12.1	2.2E-03*	1.8E-03 (±21%)	7.0E-02 (±21%)
11		10% (w/v) PCX	11.7	2.5E-03 (±54%)	1.3E-02 (±9.2%)	3.8E-02 (±9.2%)

*solid concentrations in Kuzel's salt (exp. 26 to 29) were not directly measured. k_{solid} was calculated with estimated solid concentration; $k_{\text{solid}} = k_{\text{app}}/\text{estimated solid conc.}$; the way of estimating solid concentration was explained in the text.

N/A = not able to estimate kinetic constants because no reduction of PCE was observed

Initial PCE concentration was 0.242mM

Sampling times for individual experiment: 4 days for exp. 12 to 16; 3 days for exp. 17 to 21; 13 days for exp. 22 to 24; and 3.8 days for 25 to 29.

Uncertainties represent 95% confidence limits expressed in % relative to estimate k

The values of $k_{\text{Fe(II)}}$, in CHP suspensions were one order to three orders of magnitude lower than those in experiments with Fe(II)-PCX solids (exp. 11). Addition of 48 mM Fe(III), which is the same concentration as sum of Fe(III) and Al in PCX, did not improve the solid activities. The mixing time did not affect the solid activities, either.

When cement is mixed with water, its components become hydrated and are changed into other solid phases, called cement hydration products. Four major cement components (C_3S , C_2S , C_3A and C_4AF) are changed to C-S-H gel (calcium silicates) and AFm or AFt phases (calcium aluminates). XRD analysis of Fe(II)-PCX solids found that the three highest intense peaks (8.14Å, 4.13 Å, and 2.76 Å) were similar to those in LDHs containing Cl as interlayer anions, such as Friedel's salts (127). Therefore, PCE reduction tests with CHP were conducted under the hypothesis that CHPs might influence the formation of the active agent or they, themselves, might be the active agent. However, these experiment set did not show any activity of CHPs as dechlorinating agents.

Results of this experiment indicate that the mechanism of solid formation might be different in Fe(II)-PCX suspensions and Fe(II)-DS/S . The particle size and chemical compositions of CHP solids formed in the presence of Fe(II) (Fe(II)-PCX and Fe(II)-DS/S) might be different from those formed in the absence of Fe(II), even when Fe(II) were added later such as was done in these experiments with CHP.

4.1.4 Effect of synthetic cement extract

Table 4-4 presents results of experiments with synthetic cement extracts. FSCX (exp. 30) solids showed less activity than Fe(II)-PCX solids (exp. 11, 45 and 46) as seen in values of $k_{\text{Fe(II)}}$ that are about 50% lower (Table 4-4). Although the composition of FSCX simulated PCX as close as possible, the same activities were not obtained. This could result from different chemical compositions of solid phases in each system. It was not guaranteed that all elements were incorporated into solids to the same degree in experiments with FSCX as in experiments with PCX. In other words, chemical compositions of FSCX solids could be different from Fe(II)-PCX solids. Another possible reason could be different Ca contents, because 5 N NaOH was used to adjust pH with FSCX, while Ca(OH)_2 was used with PCX.

The absence of silicate (exp. 35) had the most influence on the solid activity of compounds tested and the absence of calcium had the least influence (exp. 43). Solid activities of FSCX without silicate and calcium, measured in terms of $k_{\text{Fe(II)}}$, were about 80% and 40% less than full FSCX solids (exp. 30), respectively. However, all of the elements removed from PCX had similar effects, because their Fe(II)-normalized rate constants were the same order of magnitude.

When major constituents of PCX (Ca, Al, and Mg) were not added to the synthetic extract, the solids produced (exp. 44) had similar activity as those produced with FSCX (exp. 30). However, significant amounts of TCE were detected, with concentrations as high as 10% of the initial PCE concentration. This might indicate that the PCE degradation pathway of MSCX solids was different from solids produced by Fe(II)-DS/S,

where no TCE was detected (23). This might also indicate that solid phases formed with MSCX (exp. 44) might be different from ones in formed under other conditions (exp. 30 to 43).

TABLE 4-4 Pseudo first-order rate constants of PCE reduction by various kinds of synthetic cement extracts

Exp.	Solid	pH	k_{solid} L/(g×d)	$k_{\text{Fe(II)}}$ (mM×d) ⁻¹	$k_{\text{Fe(III)}}$ (mM×d) ⁻¹	TCE ^e mM
30	FSCX ^a	12.0	9.7E-04 (±26%)	6.1E-03 (±26%)	1.2E-02 (±26%)	
31	FSCX w/o Be	12.0	4.9E-04 (±26%)	2.9E-03 (±6.4%)	7.4E-03 (±6.4%)	
32	FSCX w/o BeBa	12.0	4.8E-04 (±83%)	2.9E-03 (±54%)	5.7E-03 (±54%)	
33	FSCX w/o BeBaB	12.0	1.2E-03 (±80%)	6.2E-03 (±52%)	1.1E-02 (±52%)	
34	FSCX w/o BeBaBSr	12.0	9.7E-04 (±144%)	5.8E-03 (±94%)	1.0E-02 (±94%)	
35	FSCX w/o SiO ₃	12.0	2.6E-04 (±32%)	1.2E-03 (±32%)	5.6E-03 (±32%)	
36	FSCX w/o Cu	12.0	8.2E-04 (±80%)	4.4E-03 (±66%)	1.9E-02 (±66%)	
37	FSCX w/o Ni	12.0	5.8E-04 (±35%)	2.7E-03 (±35%)	1.1E-02 (±35%)	
38	FSCX w/o Zn	12.0	3.5E-04 (±44%)	1.8E-03 (±44%)	5.3E-03 (±44%)	
39	FSCX w/o Mn	12.0	4.2E-04 (±18%)	2.2E-03 (±16%)	1.3E-02 (±16%)	
40	FSCX w/o Fe(III)	12.0	5.0E-04 (±18%)	3.1E-03 (±16%)	6.5E-03 (±16%)	
41	FSCX w/o Mg	12.0	5.8E-04 (±7.4%)	3.2E-03 (±7.4%)	9.0E-03 (±7.4%)	
42	FSCX w/o Al	12.0	4.3E-04 (±9.9%)	2.5E-03 (±9.9%)	7.7E-03 (±9.9%)	
43	FSCX w/o Ca	12.0	6.3E-03 (±30%)	3.5E-03 (±30%)	4.7E-02 (±30%)	

Table 4-4 Continued

Exp.	Solid	pH	k_{solid} L/(g×d)	$k_{\text{Fe(II)}}$ (mM×d) ⁻¹	$k_{\text{Fe(III)}}$ (mM×d) ⁻¹	TCE ^e mM
44	MSCX ^b	12.0	1.2E-02 (±15%)	3.8E-03 (±15%)	4.1E-02 (±15%)	0.02
45 ^d	PCX ^c + FeCl ₂	11.8	6.1E-03 (±19%)	1.1E-02 (±4.9%)	1.1E-01 (±4.9%)	
46 ^d	PCX ^c + FeSO ₄	12.2	6.0E-03 (±17%)	1.5E-02 (±14%)	1.5E-01 (±14%)	
11	PCX ^c + FeCl ₂	11.7	2.5E-03 (±54%)	1.3E-02 (±9.2%)	3.8E-02 (±9.2%)	

^a all PCX elements are added, Full element Synthetic Cement Extract (FSCX)

^b all PCX elements are added other than Ca, Mg, and Al, Minor element Synthetic Cement Extract (MSCX)

^c 10% (w/v) PCX

^d data referenced from Ko's thesis (127)

^e approximate estimation of TCE conc. in liquid phase

Initial PCE concentration was 0.242mM

A sampling time for individual experiment was 4.5 days for exp. 30 to 34; 4.9 days for exp. 35 to 38; 5.7 days for exp. 39 to 42; and 4 days for exp. 43; 6.9 days for exp. 44

Uncertainties represent 95% confidence limits expressed in % relative to estimate k

4.1.5 Effect of major element of cement extract

4.1.5.1 Simple mixing method

Table 4-5 shows results of the PCE degradation experiments conducted with solids synthesized using major elements of cement extract with a simple mixing technique. Adding Mg, Al, SO₄, or SiO₃ (exp. 48 to 59) to Fe(II)(III)Cl slightly improved solid activities (80%) compared to Fe(II)(III)Cl (exp. 47). Fe(II)(III)Cl solids had values of $k_{\text{Fe(II)}}$ that were one order of magnitude smaller than the values observed with FSCX solids (exp. 30) and two orders of magnitude smaller than those observed with Fe(II)-PCX solids (exp. 45). Fe(II), Fe(III), and Cl might be the most important

elements in forming active agents due to the observation that there was not a significant enhancement to activity of solids when other elements were introduced to cement extract. In addition, they might be the main composition of active agents. One of LDHs are potential active agents in Fe(II)-DS/S (127). LDHs are composed of di and trivalent cations in the octahedral sheets and an anion in interlayers between the sheets. Fe(II) could serve as a divalent cation, Fe(III) as a trivalent cation and Cl as an anion in potential active agents. Other elements could be either substituted for Fe(II), Fe(III), and/or Cl, to some degree, or absorbed on the surface.

TABLE 4-5 Pseudo first-order rate constants of PCE reduction by solids composed of major elements of cement extract

Exp.	Solid ^a	pH	k_{solid} L/(g×d)	$k_{\text{Fe(II)}}$ (mM×d) ⁻¹	$k_{\text{Fe(III)}}$ (mM×d) ⁻¹
47	Fe(II)(III)Cl ^b	12.0	3.4E-03 (±40%)	8.2E-04 (±40%)	1.6E-02 (±40%)
48	Fe(II)(III)ClMg ^b	12.0	4.6E-03 (±26%)	1.5E-03 (±25%)	6.1E-03 (±25%)
49	Fe(II)(III)ClAl ^b	12.0	2.6E-03 (±7.9%)	1.2E-03 (±7.7%)	1.1E-02 (±7.7%)
50	Fe(II)(III)ClMgAl ^b	12.0	1.9E-03 (±31%)	1.3E-03 (±31%)	1.2E-02 (±31%)
51	Fe(II)(III)Cl ^c	12.0	2.5E-03 (±30%)	1.1E-03 (±30%)	5.3E-03 (±30%)
52	Fe(II)(III)ClMg ^c	12.0	1.5E-03 (±36%)	7.5E-04 (±36%)	3.4E-03 (±36%)
53	Fe(II)(III)ClAl ^c	12.0	3.1E-03 (±29%)	1.5E-03 (±28%)	3.8E-03 (±28%)
54	Fe(II)(III)ClMgAl ^c	12.0	1.6E-03 (±23%)	1.1E-03 (±23%)	2.7E-03 (±23%)
55	Fe(II)(III)ClSO ₄ ^b	12.0	5.2E-03 (±67%)	1.7E-03 (±67%)	2.0E-02 (±67%)

Table 4-5 Continued

Exp.	Solid ^a	pH	k_{solid} L/(g×d)	$k_{\text{Fe(II)}}$ (mM×d) ⁻¹	$k_{\text{Fe(III)}}$ (mM×d) ⁻¹
56	Fe(II)(III)ClSO ₄ Al ^b	12.0	2.6E-03 (±26%)	1.1E-03 (±25%)	1.7E-02 (±25%)
57	Fe(II)(III)ClSO ₄ ^c	12.0	2.8E-03 (±3.3%)	1.1E-03 (±3.2%)	4.1E-03 (±3.2%)
58	Fe(II)(III)ClSO ₄ Al ^c	12.0	2.1E-03 (±11%)	1.3E-03 (±11%)	3.0E-03 (±11%)
59	Fe(II)(III)ClSiO ₃ ^b	12.0	4.4E-03 (±33%)	1.3E-03 (±33%)	1.6E-02 (±33%)
30	FSCX	12.0	9.7E-04 (±26%)	6.1E-03 (±26%)	1.2E-02 (±26%)
45	FeCl ₂ +10%(w/v)PCX	11.8	6.1E-03 (±19%)	1.1E-02 (±4.9%)	1.1E-01 (±4.9%)

^aeach solid was named after its composition

^bInitial Fe(III) concentration was 0.4mM

^cInitial Fe(III) concentration was 13.1mM

Initial PCE concentration was 0.242mM

A sampling time for individual experiment was 8.5 days for exp. 48; 7 days for exp. 48 to 54 and 59; 5.6 days for exp. 55 to 58

Uncertainties represent 95% confidence limits expressed in % relative to estimate k

The compositions of solids formed in mixtures of Fe(II), Fe(III) and Cl are shown in Table 4-6 and results of PCE reduction experiments are shown in table 4-7. Higher Fe(III) concentrations resulted in lower iron recoveries (Table 4-6). When 0.4 mM Fe(III) was added, 98% of iron was recovered, but only 70% of iron was recovered when 13.1 mM Fe(III) was added. The color of the solution after digesting solids with 1.2 N HCl was darker at higher Fe(III) concentrations., and some solid phases would not dissolve. Higher Fe(III) concentrations might have caused another solid phases to form, such as magnetite or ferrihydrite that was resistant to dissolution in HCl.

Fe(III) concentration did not have a much effect on solid activities as shown in table 4-7. Values of $k_{\text{Fe(II)}}$ increased 50% at 6 mM Fe(III) (exp 63), compared to 0.4 mM (exp 47, 60). Values of $k_{\text{Fe(II)}}$ that were one order of magnitude smaller than those observed with FSCX (exp 30) and two order of magnitude smaller than those observed with PCX (exp 45) were observed in Fe(II)(III)Cl solids having different Fe(III) concentrations (exp 60 to 65).

The mixing time used to synthesize solids did not have much affect on the formation of the active agents as shown in table 4-8. Values of $k_{\text{Fe(II)}}$ were slightly higher (30%) with a 1-day mixing time, compared to 3-day mixing time, which had the lowest activity. An active agent could be formed in 2 hours and might reach the best activity within a day based on the solid activity test presented in table 4-8.

TABLE 4-6 Iron and solid concentrations of solids containing Fe(II), Fe(III), and Cl with the different initial Fe(III) concentration

Exp.	Solid	Initial				Solid conc g/L
		Fe(III) conc. mM	Fe(II) mM	Fe(III) mM	Fe(II)/ Fe(III)	
60	Fe(II)(III)Cl	0.4	36.2	2.77	13.1	9.25
61		2	35.6	3.66	9.73	11.4
62		4	36.2	3.89	9.30	12.9
63		6	34.4	3.77	9.13	12.2
64		8	35.0	6.37	5.49	12.4
65		10	34.6	3.55	9.77	12.0

TABLE 4-7 Pseudo first-order rate constants of PCE reduction by solids containing Fe(II), Fe(III), and Cl with different initial Fe(III) concentrations

Exp.	Solid	Initial Fe(III) conc. mM	pH	k_{solid} L/(g×d)	$k_{\text{Fe(II)}}$ (mM×d) ⁻¹	$k_{\text{Fe(III)}}$ (mM×d) ⁻¹
60	Fe(II)(III)Cl	0.4	12.0	3.3E-03 (±23%)	8.3E-04 (±23%)	1.1E-02 (±23%)
61		2	12.0	3.1E-03 (±53%)	9.8E-04 (±51%)	9.5E-03 (±51%)
62		4	12.0	2.6E-03 (±34%)	9.2E-04 (±32%)	8.6E-03 (±32%)
63		6	12.0	3.6E-03 (±83%)	1.3E-03 (±83%)	1.2E-02 (±83%)
64		8	12.0	2.9E-03 (±31%)	1.1E-03 (±30%)	5.6E-03 (±30%)
65		10	12.0	3.2E-03 (±56%)	1.1E-03 (±56%)	1.1E-02 (±56%)
47	Fe(II)(III)Cl	0.4	12.0	3.4E-03 (±40%)	8.2E-04 (±40%)	1.6E-02 (±40%)
51	Fe(II)(III)Cl	13.1	12.0	2.5E-03 (±30%)	1.1E-03 (±30%)	5.3E-03 (±30%)
30	FSCX	0.4	12.0	9.7E-04 (±26%)	6.1E-03 (±26%)	1.2E-02 (±26%)
45	FeCl ₂ +10%(w/v)PCX	0	11.8	6.1E-03 (±19%)	1.1E-02 (±4.9%)	1.1E-01 (±4.9%)

Initial PCE concentration was 0.242mM

A sampling time for individual experiment was 7 days

Uncertainties represent 95% confidence limits expressed in % relative to estimate k

TABLE 4-8 Pseudo first-order rate constants of PCE reduction by solids containing Fe(II), Fe(III), and Cl with different solid synthesis mixing time

Exp.	Solid	Mixing time	pH	k_{solid} L/(g×d)	$k_{\text{Fe(II)}}$ (mM×d) ⁻¹	$k_{\text{Fe(III)}}$ (mM×d) ⁻¹
66	Fe(II)(III)Cl	2h	12.0	3.3E-03 (±19%)	9.8E-04 (±19%)	2.3E-02 (±19%)
67		12h	12.0	3.1E-03 (±13%)	1.0E-03 (±12%)	1.3E-02 (±12%)
68		1d	12.0	3.8E-03 (±44%)	1.3E-03 (±44%)	1.9E-02 (±44%)
69		2d	12.0	3.1E-03 (±25%)	1.1E-03 (±24%)	1.8E-02 (±24%)
70		3d	12.0	3.1E-03 (±21%)	9.7E-04 (±17%)	1.9E-02 (±17%)

Initial PCE concentration was 0.242mM

A sampling time for individual experiment was 7.9 days

Uncertainties represent 95% confidence limits expressed in % relative to estimate k

Various conditions for the solid formation with simple mixing methods with major elements of cement extract did not have much affect on the formation of active agents. All solids formed by the simple mixing method had similar solid activities and lower activities than Fe(II)-PCX solids. Although Fe(II), Fe(III), and Cl might be the most important elements to form active agents, other elements were also required to enhance their activity. This further supports the observation that chemical composition of solids might be critical to determining their level of PCE degradation activity.

4.1.5.2 Adaptation of GR synthesis method

Table 4-9 shows the results of PCE degradation by Fe(II)(III)Cl solid synthesized by the method used to synthesize green rust (GR) (m6). As seen in table 4-9, five different NaOH addition rates (10, 33, 83, 167, and 50,000 μ L/sec) did not have much affect on the solid activities synthesized by GR synthesis method. The least active solid was observed in exp. 72, where the solid was synthesized with Cl addition before other elements, 33 μ L/sec of NaOH addition rate, and neutral pH. The most active solid was observed in exp. 83 with Cl addition after all other elements, 83 μ L/sec of NaOH addition rate and neutral pH. The normalized kinetic coefficients ($k_{\text{Fe(II)}}$) of the least active solid was $9.39 \times 10^{-4} \text{ (mMFe(II)} \times \text{d)}^{-1}$ and the most active solid was $3.02 \times 10^{-3} \text{ (mMFe(II)} \times \text{d)}^{-1}$. However, $k_{\text{Fe(II)}}$ for all types of solids in table 4-9 were about the same order of magnitude, one order of magnitude lower than those observed with FSCX (exp. 30), and two order magnitude lower than those observed with PCX (exp. 45).

The GR synthesis method did not increase activities of most solids compared to those formed with simple mixing. An exception was exp. 83 where a solid was synthesized at neutral pH, with OH addition rate of 83.3 μ L/sec and Cl addition after OH. The activities of solids in this experiment were about 3 times higher in terms of k_{solid} and $k_{\text{Fe(II)}}$ than those found with the simple mixing technique. This was observed even though the Fe(III) concentrations of the two solids were different. The GR synthesis method produced solids with 8.7 mM Fe(III) and simple mixing method produced solids with 0.4 mM Fe(III).

TABLE 4-9 Pseudo first-order rate constants of PCE reduction by solids containing Fe(II), Fe(III), and Cl synthesized by GR synthesis method

Exp.	Solid Fe(II)(III)Cl ^a	pH	k _{solid} L/(g×d)	k _{Fe(II)} (mM×d) ⁻¹	k _{Fe(III)} (mM×d) ⁻¹
71	70 ^b (F ^c)_10 ^d	12.0	4.4E-03 (±57%)	1.2E-03 (±57%)	8.3E-03 (±57%)
72	70(F)_33	12.0	3.9E-03 (±35%)	9.4E-04 (±35%)	6.3E-03 (±35%)
73	70(F)_83	12.0	5.3E-03 (±37%)	1.1E-03 (±37%)	8.8E-03 (±37%)
74	70(F)_167	12.0	4.7E-03 (±12%)	1.0E-03 (±9.3%)	3.6E-03 (±9.3%)
75	70(F)_50000	12.0	1.1E-02 (±32%)	2.2E-03 (±32%)	7.7E-02 (±32%)
76	110(F)_10	12.0	2.8E-03 (±66%)	1.1E-03 (±66%)	7.8E-03 (±66%)
77	110(F)_33	12.0	3.0E-03 (±26%)	1.0E-03 (±25%)	1.1E-02 (±25%)
78	110(F)_83	12.0	4.1E-03 (±29%)	1.3E-03 (±28%)	6.5E-03 (±28%)
79	110(F)_167	12.0	3.0E-03 (±28%)	1.1E-03 (±28%)	5.9E-03 (±28%)
80	110(F)_50000	12.0	4.4E-03 (±50%)	1.5E-03 (±50%)	1.4E-02 (±50%)
81	70(L ^e)_10	12.0	5.5E-03 (±17%)	1.5E-03 (±15%)	3.7E-02 (±15%)
82	70(L)_33	12.0	6.7E-03 (±7.8%)	1.6E-03 (±7.6%)	1.2E-02 (±7.6%)
83	70(L)_83	12.0	1.0E-02 (±47%)	3.0E-03 (±47%)	1.8E-02 (±47%)
84	70(L)_167	12.0	5.7E-03 (±20%)	2.1E-03 (±20%)	1.5E-02 (±20%)
85	70(L)_50000	12.0	8.4E-03 (±45%)	2.7E-03 (±44%)	2.0E-02 (±44%)
86	110(L)_10	12.0	2.1E-03 (±40%)	1.1E-03 (±40%)	9.3E-03 (±40%)
87	110(L)_33	12.0	4.2E-03 (±56%)	1.3E-03 (±56%)	1.0E-02 (±56%)
88	110(L)_83	12.0	8.2E-03 (±62%)	2.2E-03 (±62%)	1.9E-02 (±62%)

Table 4-9 Continued

Exp.	Solid Fe(II)(III)Cl ^a	pH	k _{solid} L/(g×d)	k _{Fe(II)} (mM×d) ⁻¹	k _{Fe(III)} (mM×d) ⁻¹
89	110(L)_167	12.0	3.4E-03 (±17%)	1.1E-03 (±17%)	6.9E-02 (±17%)
90	110(L)_50000	12.0	5.3E-03 (±21%)	1.6E-03 (±21%)	2.1E-02 (±21%)
68	Fe(II)(III)Cl	12.0	3.8E-03 (±44%)	1.3E-03 (±44%)	1.9E-02 (±44%)
30	FSCX	12.0	9.7E-04 (±26%)	6.1E-03 (±26%)	1.2E-02 (±26%)
45	PCX	11.8	6.1E-03 (±19%)	1.1E-02 (±4.9%)	1.1E-01 (±4.9%)

^aFe(II)(III)Cl solid was synthesized by adding Fe(II), Fe(III) and Cl; Initial Fe(III) concentration of solid was 8.7mM

^bNaOH concentration

- i. 70 = 70mM NaOH
- ii. 110 = 110mM NaOH

^cNaCl addition order

- (F) NaCl addition before adding other elements
- (L) NaCl addition after adding other elements

^dNaOH addition rate

- i. 10 = 10.0μL/sec
- ii. 33 = 33.3μL/sec
- iii. 83 = 83.3μL/sec
- iv. 167 = 167μL/sec
- v. 5000 = 50000μL/sec

Initial PCE concentration was 0.242mM

A sampling time for individual experiment was 7.7 days for exp. 71 to 75; 6.9 days for exp. 76 to 85; and 7 days for exp. 86 to 90

Uncertainties represent 95% confidence limits expressed in % relative to estimate k

Table 4-10 shows the effect of Mg on the activity of solids synthesized with the GR method (128). As seen in table 4-10, NaOH addition rates (20, 83, and 45,000μL/sec) did not have much affect on the solid activities. The solids formed in exp. 108 showed the best activity among Fe(II)(III)ClMg solids. This experiment was

conducted with addition of 0.4 mM Fe(III), 110 mM NaOH at the rate of 45,000 μ L/sec and 22.2 mM Mg added after NaOH.

Solids formed in exp. 108 were 50% and 75% less active based on $k_{\text{Fe(II)}}$ than solids formed with FSCX (exp. 30) and with Fe(II)-PCX (exp. 45), and had similar activities with solid formed in exp. 83. Mg did not have much improved solid activity. Significant amounts of TCE were detected, with concentrations as high as 5 to 10% of the initial PCE concentration, in exp. 93, 96, and 108, like MSCX solids (exp. 44).

TABLE 4-10 Pseudo first-order rate constants of PCE reduction by solids containing Fe(II), Fe(III), Cl, and Mg synthesized by GR synthesis method

Exp.	Solid Fe(II)(III)ClMg ^a	pH	k_{solid} L/(g \times d)	$k_{\text{Fe(II)}}$ (mM \times d) ⁻¹	$k_{\text{Fe(III)}}$ (mM \times d) ⁻¹	TCE ^f mM
91	70 ^b (0.4 ^c)_20 ^d (BO ^e)	12.0	3.4E-03 (\pm 30%)	1.1E-03 (\pm 30%)	1.5E-02 (\pm 30%)	
92	70(0.4)_83(BO)	12.0	3.5E-03 (\pm 15%)	1.3E-03 (\pm 15%)	2.2E-02 (\pm 15%)	
93	70(0.4)_45000(BO)	12.0	5.0E-03 (\pm 30%)	1.7E-03 (\pm 30%)	2.4E-02 (\pm 30%)	0.01
94	70(0.4)_20(AO)	12.0	3.3E-03 (\pm 30%)	1.6E-03 (\pm 29%)	1.6E-02 (\pm 29%)	
95	70(0.4)_83(AO)	12.0	2.9E-03 (\pm 25%)	1.3E-03 (\pm 25%)	1.9E-02 (\pm 25%)	
96	70(0.4)_45000(AO)	12.0	6.5E-03 (\pm 39%)	2.1E-03 (\pm 39%)	6.0E-02 (\pm 39%)	0.02
97	70(8.7)_20(BO)	12.0	3.7E-03 (\pm 29%)	1.9E-03 (\pm 29%)	6.5E-03 (\pm 29%)	
98	70(8.7)_83(BO)	12.0	3.2E-03 (\pm 28%)	1.6E-03 (\pm 28%)	6.0E-03 (\pm 28%)	
99	70(8.7)_45000(BO)	12.0	3.5E-03 (\pm 17%)	1.8E-03 (\pm 17%)	5.6E-03 (\pm 17%)	
100	70(8.7)_20(AO)	12.0	3.6E-03 (\pm 29%)	1.6E-03 (\pm 29%)	5.0E-03 (\pm 29%)	

Table 4-10 Continued

Exp.	Solid Fe(II)(III)ClMg ^a	pH	k _{solid} L/(g×d)	k _{Fe(II)} (mM×d) ⁻¹	k _{Fe(III)} (mM×d) ⁻¹	TCE ^f mM
101	70(8.7)_83(AO)	12.0	3.9E-03 (±91%)	1.9E-03 (±91%)	6.2E-03 (±91%)	
102	70(8.7)_45000(AO)	12.0	4.3E-03 (±37%)	2.1E-03 (±37%)	7.4E-03 (±37%)	
103	110(0.4)_20(BO)	12.0	6.7E-03 (±20%)	2.6E-03 (±20%)	3.2E-02 (±20%)	
104	110(0.4)_83(BO)	12.0	4.8E-03 (±30%)	2.0E-03 (±39%)	2.1E-02 (±39%)	
105	110(0.4)_4500(BO)	12.0	5.6E-03 (±10%)	2.2E-03 (±10%)	3.7E-02 (±10%)	
106	110(0.4)_20(AO)	12.0	3.0E-03 (±23%)	1.4E-03 (±23%)	1.3E-02 (±23%)	
107	110(0.4)_83(AO)	12.0	5.1E-03 (±6.0%)	2.2E-03 (±5.9%)	2.7E-02 (±5.9%)	
108	110(0.4)_4500(AO)	12.0	6.5E-03 (±23%)	2.9E-03 (±23%)	9.6E-02 (±23%)	0.02
83	70(L)_83(Fe(II)(III)Cl)	12.0	1.0E-02 (±47%)	3.0E-03 (±47%)	1.8E-02 (±47%)	
48	Fe(II)(III)ClMg	12.0	4.6E-03 (±26%)	1.5E-03 (±25%)	6.1E-03 (±25%)	
68	Fe(II)(III)Cl	12.0	3.8E-03 (±44%)	1.3E-03 (±44%)	1.9E-02 (±44%)	
30	FSCX	12.0	9.7E-04 (±26%)	6.1E-03 (±26%)	1.2E-02 (±26%)	
44	MSCX	12.0	1.2E-02 (±15%)	3.8E-03 (±15%)	4.1E-02 (±15%)	0.02
45	PCX	11.8	6.1E-03 (±19%)	1.1E-02 (±4.9%)	1.1E-01 (±4.9%)	

^aFe(II)(III)ClMg solid was synthesized by adding Fe(II), Fe(III), Cl and Mg

^bNaOH concentration

- i. 70 = 70mM NaOH
- ii. 110 = 110mM NaOH

^cFe(III) concentration

- i. 0.4 = 0.4mM Fe(III)
- ii. 8.7 = 8.7mM Fe(III)

^dNaOH addition rate

- i. 20 = 20.0μL/sec
- ii. 83 = 83.3μL/sec
- iii. 45000 = 45000μL/sec

^eMg addition order

- i. BO = Before OH addition
- ii. AO = After OH addition

^festimate of TCE conc. in liquid phase

Initial PCE concentration was 0.242mM

A sampling time for individual experiment was 5.7 days for exp. 91 to 96; 4 days for exp. 97 to 102; 4.6 days for exp. 103 to 107; and 4.2 days for exp. 108

Uncertainties represent 95% confidence limits expressed in % relative to estimate k

Table 4-11 shows the effect of SO_4 on the activity of solids synthesized with the GR method. When sulfate was added after addition of NaOH, solids showed activities that were a little higher than when sulfate was added before addition of NaOH. Solids synthesized at high pH (about 12) showed more activity than those synthesized at neutral pH. Slow addition of NaOH ($20\mu\text{L}/\text{sec}$, and $83.3\mu\text{L}/\text{sec}$) made more active solids than fast addition of NaOH ($50,000\mu\text{L}/\text{sec}$).

The most active solid in this set of experiments was observed in experiment 125, which was conducted with 0.4 mM Fe(III) and 110 mM NaOH . The NaOH was added at the rate of $83.3\mu\text{L}/\text{sec}$. These solids were still less active than those produced with FSCX (exp. 30) and with Fe(II)-PCX (exp. 45). They had values of $k_{\text{Fe(II)}}$, that were about 60% and 80% lower than those for FSCX solids and Fe(II)-PCX solids, respectively

The GR synthesis method was able to make more active solids with normalized rate constants (k_{solid} , $k_{\text{Fe(II)}}$) about 50% higher than those produced by the simple mixing method (exp. 68 and exp. 77). However, certain amounts of TCE were detected, with concentrations as high as 2 to 10% of the initial PCE concentration, in exp. 110, 111, 114, 123. Sulfate did not have much effect on activity.

TABLE 4-11 Pseudo first-order rate constants of PCE reduction by solids containing Fe(II), Fe(III), Cl, and SO₄ synthesized by GR synthesis method

Exp.	Solid Fe(II)(III)ClSO ₄ ^a	pH	k _{solid} L/(g×d)	k _{Fe(II)} (mM×d) ⁻¹	k _{Fe(III)} (mM×d) ⁻¹	TCE ^f mM
109	70 ^b (0.4 ^c)_20 ^d (BO ^e)	12.0	6.0E-03 (±84%)	1.7E-03 (±84%)	2.7E-02 (±84%)	
110	70(0.4)_83(BO)	12.0	2.8E-03 (±16%)	1.0E-03 (±16%)	1.1E-02 (±16%)	0.004
111	70(0.4)_50000(BO)	12.0	4.4E-03 (±13%)	1.2E-03 (±13%)	2.4E-02 (±13%)	0.004
112	70(0.4)_20(AO)	12.0	3.1E-03 (±16%)	9.8E-04 (±16%)	8.3E-03 (±16%)	
113	70(0.4)_83(AO)	12.0	3.5E-03 (±426%)	1.1E-03 (±26%)	1.2E-02 (±26%)	
114	70(0.4)_50000(AO)	12.0	6.6E-03 (±32%)	1.7E-03 (±32%)	2.7E-02 (±32%)	0.02
115	70(8.7)_20(BO)	12.0	4.4E-03 (±11%)	1.3E-03 (±9.2%)	4.4E-03 (±9.2%)	
116	70(8.7)_83(BO)	12.0	3.7E-03 (±14%)	1.4E-03 (±7.3%)	7.3E-03 (±7.3%)	
117	70(8.7)_50000(BO)	12.0	5.1E-03 (±97%)	1.5E-03 (±95%)	1.3E-02 (±95%)	
118	70(8.7)_20(AO)	12.0	5.2E-03 (±39%)	1.6E-03 (±37%)	6.3E-03 (±37%)	
119	70(8.7)_83(AO)	12.0	6.2E-03 (±283%)	1.9E-03 (211%)	6.9E-03 (±211%)	
120	70(8.7)_50000(AO)	12.0	5.8E-03 (±18%)	1.6E-03 (±17%)	9.1E-03 (±17%)	
121	110(0.4)_20(BO)	12.0	6.5E-03 (±13%)	1.9E-03 (±13%)	1.8E-02 (±13%)	
122	110(0.4)_83(BO)	12.0	7.3E-03 (±23%)	2.0E-03 (±22%)	1.3E-02 (±22%)	
123	110(0.4)_5000(BO)	12.0	6.0E-03 (±21%)	1.6E-03 (±21%)	2.1E-02 (±21%)	0.004
124	110(0.4)_20(AO)	12.0	9.4E-03 (±24%)	2.5E-03 (±23%)	2.3E-02 (±23%)	
125	110(0.4)_83(AO)	12.0	9.7E-03 (±31%)	2.6E-03 (±31%)	1.8E-02 (±31%)	
126	110(0.4)_5000(AO)	12.0	5.7E-03 (±36%)	1.9E-03 (±28%)	1.2E-02 (±28%)	

Table 4-11 Continued

Exp.	Solid Fe(II)(III)ClSO ₄ ^a	pH	k _{solid} L/(g×d)	k _{Fe(II)} (mM×d) ⁻¹	k _{Fe(III)} (mM×d) ⁻¹	TCE ^f mM
83	70(L)_83(Fe(II)(III)Cl)	12.0	1.0E-02 (±47%)	3.0E-03 (±47%)	1.8E-02 (±47%)	
55	Fe(II)(III)ClSO ₄	12.0	5.2E-03 (±67%)	1.7E-03 (±67%)	2.0E-02 (±67%)	
68	Fe(II)(III)Cl	12.0	3.8E-03 (±44%)	1.3E-03 (±44%)	1.9E-02 (±44%)	
30	FSCX	12.0	9.7E-04 (±26%)	6.1E-03 (±26%)	1.2E-02 (±26%)	
45	PCX	11.8	6.1E-03 (±19%)	1.1E-02 (±4.9%)	1.1E-01 (±4.9%)	

^aFe(II)(III)ClMg solid was synthesized by adding Fe(II), Fe(III), Cl and SO₄

^b: NaOH concentration

i. 70 = 70mM NaOH

ii. 110 = 110mM NaOH

^c: Fe(III) concentration

i. 0.4 = 0.4mM Fe(III)

ii. 8.7 = 8.7mM Fe(III)

^d: NaOH addition rate

i. 20 = 20.0μL/sec

ii. 83 = 83.3μL/sec

iii. 50000 = 50000μL/sec

^e: SO₄ addition order

i. BO = Before OH addition

ii. AO = After OH addition

^festimate of TCE conc. in liquid phase

Initial PCE concentration was 0.242mM

A sampling time for individual experiment was 7 days for exp. 109 to 114; 4.9 days for exp. 115 to 120; and 5.6 days for exp. 121 to 126

Uncertainties represent 95% confidence limits expressed in % relative to estimate k

Table 4-11 shows the effect of SiO₃ on the activity of solids synthesized by the GR method. Solids synthesized at high pH (about pH 12) and at neutral pH showed similar activities. NaOH addition rates and a silicate addition order were not important factors in forming more active solids.

The highest solid activities in this set of experiments were observed in exp. 140 and 143. Exp. 140 was conducted with 0.4 mM Fe(III), 110 mM NaOH, NaOH addition rate of 83.3 μ L/sec and silicate addition before NaOH. Exp. 142 was conducted with 0.4 mM Fe(III), 110 mM NaOH, NaOH addition rate of 20.0 μ L/sec, and silicate addition after NaOH. The activities in these experiments were lower than those observed for FSCX solids (exp. 30) and Fe(II)-PCX solids (exp. 45). Values of $k_{\text{Fe(II)}}$, were about 60% of those observed for FSCX solids and 80% of those observed for Fe(II)-PCX solids.

The GR synthesis method was able to make solids with normalized rate constants (k_{solid} , $k_{\text{Fe(II)}}$) that were about 50% higher than those obtained with the simple mixing method (exp. 68 and exp. 77), but TCE was detected in many experiments using the GR synthesis method..

Silicate and sulfate had the almost same effect on the solid activities. Like, Mg and sulfate, silicate also did not improve solid activities to a major extent.

TABLE 4-12 Pseudo first-order rate constants of PCE reduction by solids containing Fe(II), Fe(III), Cl, and SiO₃ synthesized by GR synthesis method

Exp.	Solid Fe(II)(III)ClSiO ₃ ^a	pH	k _{solid} L/(g×d)	k _{Fe(II)} (mM×d) ⁻¹	k _{Fe(III)} (mM×d) ⁻¹	TCE ^f mM
127	70 ^b (0.4 ^c)_20 ^d (BO ^e)	12.0	5.2E-03 (±5.7%)	1.2E-03 (±5.7%)	2.1E-02 (±5.7%)	
128	70(0.4)_83(BO)	12.0	7.4E-03 (±18%)	1.9E-03 (±18%)	8.1E-02 (±18%)	
129	70(0.4)_50000(BO)	12.0	5.0E-03 (±30%)	1.3E-03 (±30%)	2.3E-02 (±30%)	0.003
130	70(0.4)_20(AO)	12.0	4.7E-03 (±12%)	1.6E-03 (±12%)	5.0E-02 (±12%)	
131	70(0.4)_83(AO)	12.0	6.6E-03 (±21%)	2.2E-03 (±21%)	3.4E-02 (±21%)	0.003
132	70(0.4)_50000(AO)	12.0	4.5E-03 (±46%)	1.6E-03 (±46%)	6.2E-03 (±46%)	0.01
133	70(8.7)_20(BO)	12.0	6.0E-03 (±34%)	2.2E-03 (±34%)	7.0E-03 (±34%)	
134	70(8.7)_83(BO)	12.0	7.0E-03 (±76%)	1.7E-03 (±76%)	7.1E-03 (±76%)	
135	70(8.7)_50000(BO)	12.0	6.1E-03 (±43%)	2.3E-03 (±43%)	1.0E-02 (±43%)	
136	70(8.7)_20(AO)	12.0	6.2E-03 (±73%)	2.2E-03 (±73%)	8.3E-03 (±73%)	
137	70(8.7)_83(AO)	12.0	8.9E-03 (±83%)	2.5E-03 (±83%)	9.0E-03 (±83%)	
138	70(8.7)_50000(AO)	12.0	7.1E-03 (±9.5%)	2.2E-03 (±9.5%)	2.3E-02 (±9.5%)	
139	110(0.4)_20(BO)	12.0	4.0E-03 (±31%)	1.7E-03 (±31%)	1.5E-02 (±31%)	
140	110(0.4)_83(BO)	12.0	8.6E-03 (±17%)	2.6E-03 (±17%)	4.0E-02 (±17%)	0.003
141	110(0.4)_5000(BO)	12.0	6.1E-03 (±6.2%)	1.6E-03 (±5.6%)	1.7E-02 (±5.6%)	0.03
142	110(0.4)_20(AO)	12.0	6.4E-03 (±11%)	2.6E-03 (±11%)	2.8E-02 (±11%)	
143	110(0.4)_83(AO)	12.0	7.1E-03 (±22%)	2.3E-03 (±22%)	2.0E-02 (±22%)	0.01
144	110(0.4)_5000(AO)	12.0	4.1E-03 (±55%)	1.3E-03 (±55%)	3.1E-02 (±55%)	0.01

Table 4-12 Continued

Exp.	Solid Fe(II)(III)ClSiO ₃ ^a	pH	k _{solid} L/(g×d)	k _{Fe(II)} (mM×d) ⁻¹	k _{Fe(III)} (mM×d) ⁻¹	TCE ^f mM
83	70(L)_83(Fe(II)(III)Cl)	12.0	1.0E-02 (±47%)	3.0E-03 (±47%)	1.8E-02 (±47%)	
59	Fe(II)(III)ClSiO ₃	12.0	4.4E-03 (±33%)	1.3E-03 (±33%)	1.6E-02 (±33%)	
68	Fe(II)(III)Cl	12.0	3.8E-03 (±44%)	1.3E-03 (±44%)	1.9E-02 (±44%)	
30	FSCX	12.0	9.7E-04 (±26%)	6.1E-03 (±26%)	1.2E-02 (±26%)	
45	PCX	11.8	6.1E-03 (±19%)	1.1E-02 (±4.9%)	1.1E-01 (±4.9%)	

^aFe(II)(III)ClMg solid was synthesized by adding Fe(II), Fe(III), Cl and SiO₃

^b: NaOH concentration

iii. 70 = 70mM NaOH

iv. 110 = 110mM NaOH

^c: Fe(III) concentration

iii. 0.4 = 0.4mM Fe(III)

iv. 8.7 = 8.7mM Fe(III)

^d: NaOH addition rate

iv. 20 = 20.0μL/sec

v. 83 = 83.3μL/sec

vi. 50000 = 50000μL/sec

^e: SiO₃ addition order

iii. BO = Before OH addition

iv. AO = After OH addition

^festimate of TCE conc. in liquid phase

Initial PCE concentration was 0.242mM

A sampling time for individual experiment was 5.8 days for exp. 127 to 132; 4.9 days for exp. 133 to 138; and 4.5 days for exp. 139 to 144

Uncertainties represent 95% confidence limits expressed in % relative to estimate k

The solid activity was not changed by synthesis methods (GR synthesis method or simple mixing method). For some cases when NaOH was added at a rate of 50000μL/sec there were significant amounts of TCE were detected, with concentrations ranging from 5 to 12 % of initial PCE concentration. TCE concentrations were particularly high when silicate was added to Fe(II)(III)Cl solids. Although silicate was a

major element in ordinary Portland cement (OPC), silicate alone might not facilitate formation of the active solid. Solids prepared with additional Mg showed the best activities of the three compounds tested (Mg, SO_4 , SiO_3). However, experiments with these solids also showed accumulation of TCE.

4.2 Identification of the active agents through instrumental analyses

4.2.1 10% Portland cement slurry (10% PCS)

Figure 4-4 showed the x-ray diffraction (XRD) pattern for 10% PCS with and without Fe(II). CPCS stands for Capitol Portland cement slurry. The major solid phases found through XRD analysis in solids from a 10% cement slurry containing Fe(II) (10% CPCSFe) were calcium chloroaluminate hydrates (Friedel's salt), calcium aluminate hydrates and calcium aluminum silicate hydrates.

The peaks of Friedel's salts and calcium aluminate hydrates were very close and similar with one another, especially the first highest intensity peak having d-values of 7.8 Å. However, these solids could be easily distinguished by their second and third highest intensity peaks of 3.9 and 3.8 Å. Peaks circled in figure 4-4(a) and (b) show the distinctive differences between solids containing Fe(II) and solids not containing Fe(II). The intensity of the peak of 2.87 Å at $31^\circ \theta$ is higher in CPCSFe. Ettringite was identified in the solids from the 10% cement slurry that did not contain Fe(II) (CPCS). Most Ettringite peaks disappeared in CPCSFe.

In general, Ettringite can be formed within 30 minutes when cement is mixed with water (41, 42). Introducing Fe(II) into the cement slurry system might facilitate the

formation of Friedel's salts rather than Ettringite, so that the formation of Ettringite was either inhibited or decelerated.

Typical XRD patterns of the amorphous phase were observed between 25° and 40° 2θ (41). These patterns indicated CSH gel, which constitutes about 90%, of cement hydration products.

Adding Fe(II) did not make any new solids that could be identified by XRD. Fe(II) might be incorporated into Friedel's salts through isomorphous substitution for calcium or adsorbed onto their surfaces.

(a)

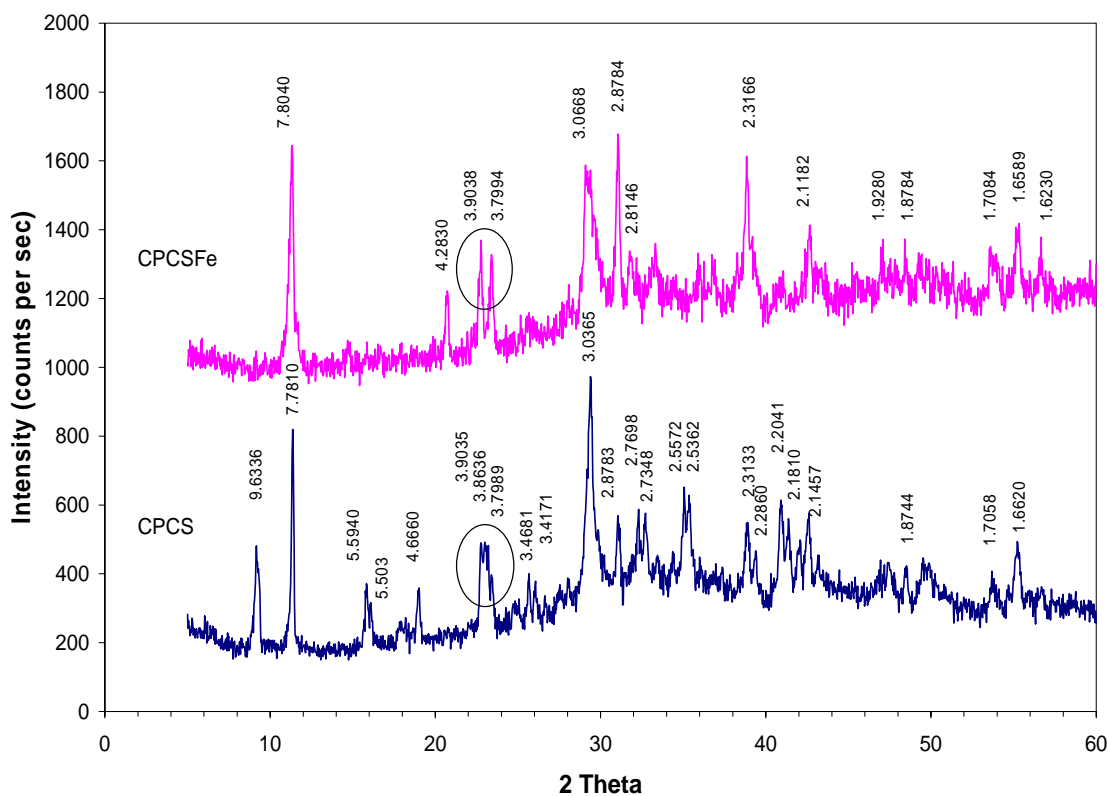


FIGURE 4-4 X-ray patterns of 10% Capitol cement slurry. (a) CPCSFe = 10% Capitol Portland cement slurry with Fe(II); CPCS = 10% Capitol Portland cement slurry without Fe(II); unit of d-spacing values = Å. (b) Mineral identification using software program, JADE, of CPCS. (c) Mineral identification using software program, JADE, of CPCSFe. Note: Backgrounds of figure (b) and (c) were adjusted by JADE. Thanks to the Texas Transportation Institute for the use of the Rigü automatic diffract.

(b)

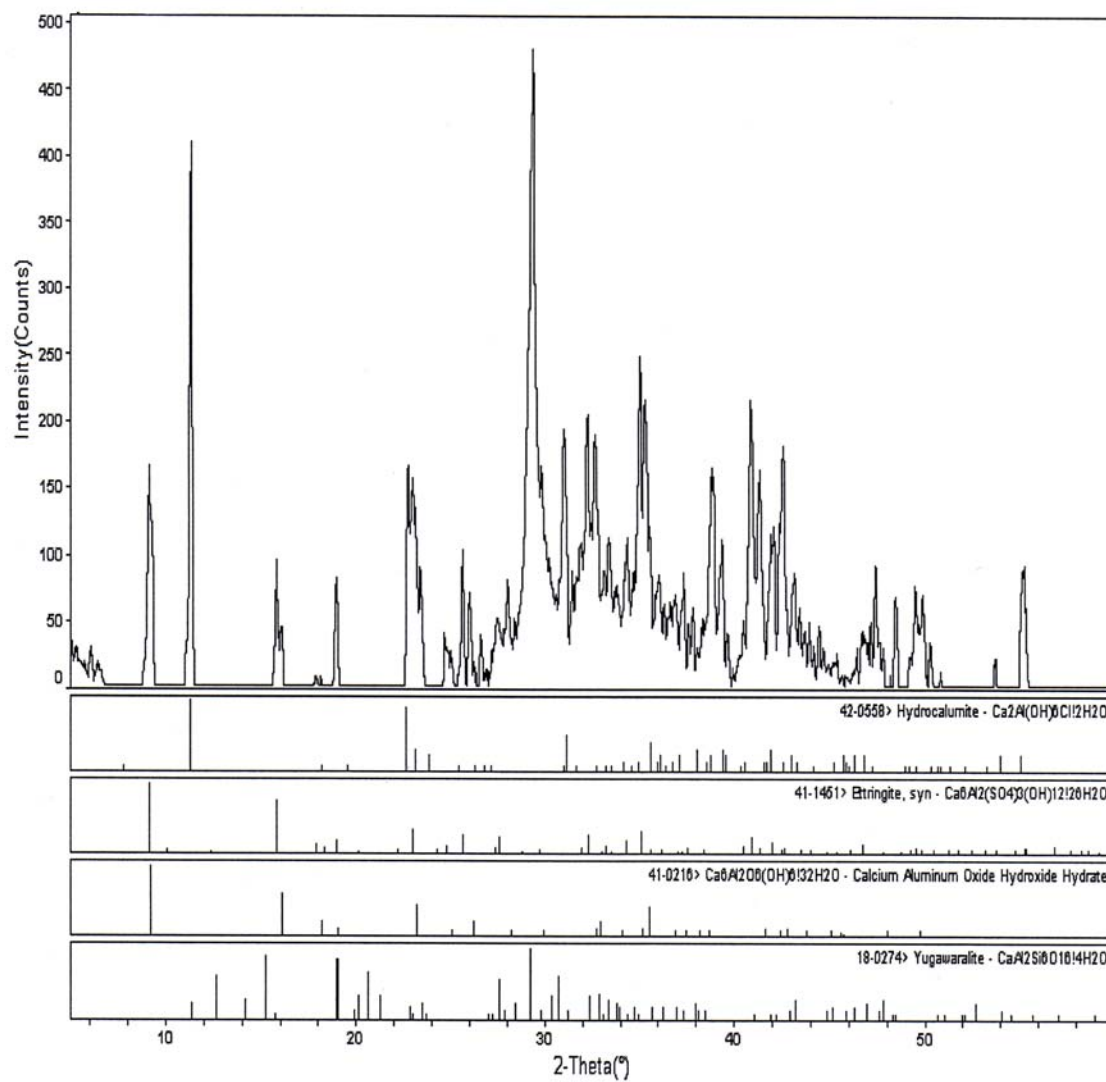


FIGURE 4-4 Continued

(c)

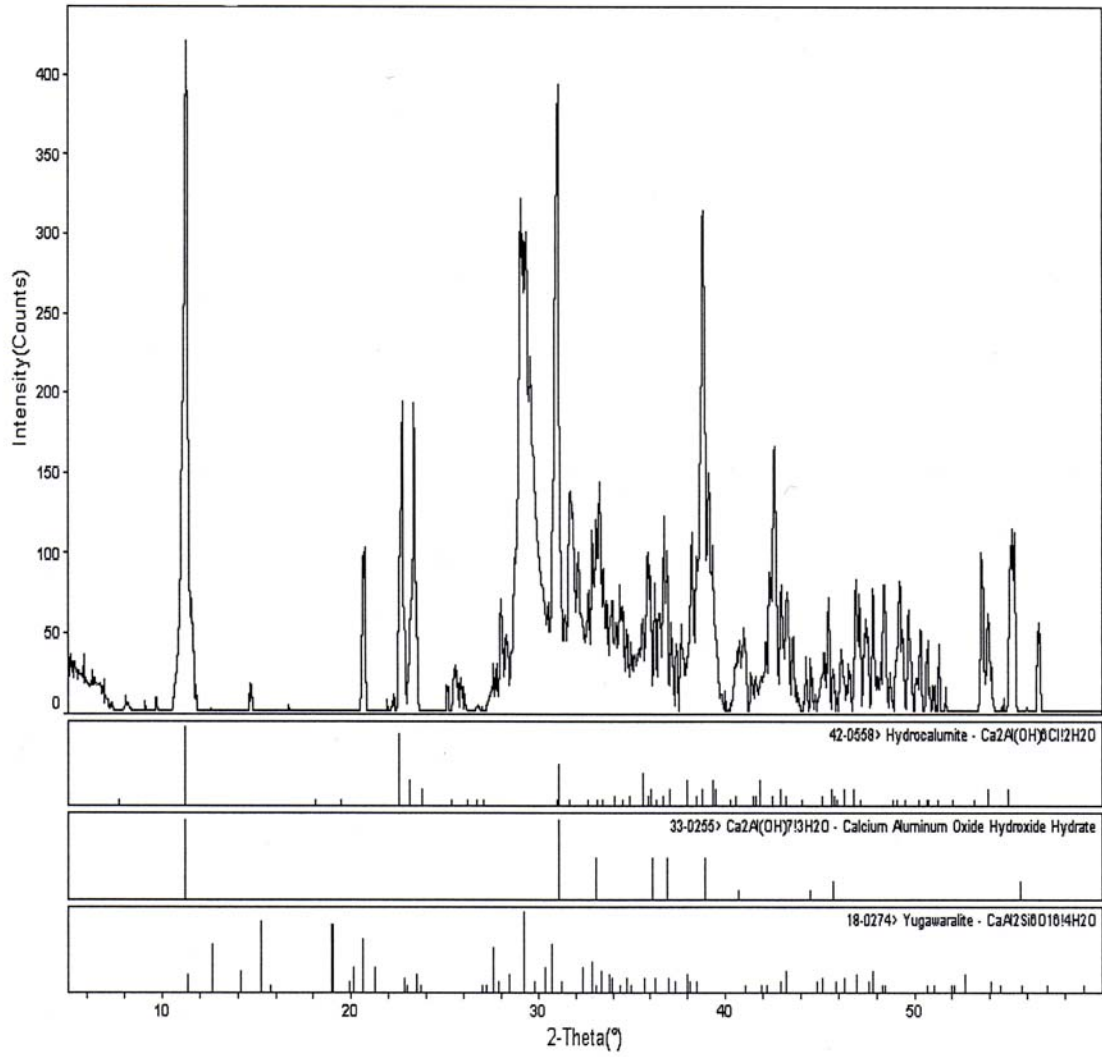


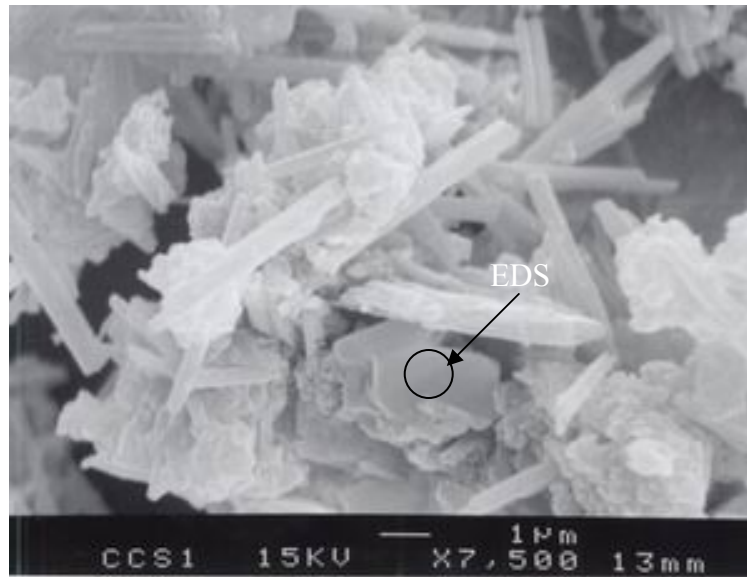
FIGURE 4-4 Continued

Figure 4-5 through 4-7 showed scanning electron microscopic (SEM) images and energy dispersive spectrometer (EDS) spectra of 10 % CPCS without (figure 4-5 and 4-6) and with (figure 4-7) Fe(II). EDS spectra were taken from a hexagonal particle. Needle-like crystals of Ettringite and hexagonal plates of Friedel's salt were found in cement slurry systems. In figure 4-6, a very low peak of Fe was observed. It might come from substitution of Fe(III) for Al in Friedel's salt or in calcium aluminate hydrates, which has a layered structure.

The particle sizes of the hexagonal plates typically vary from a few micrometers to around 50 μm (64). The SEM images show that the particle sizes were reduced when Fe(II) was added. These phenomena might be related to the activities of the solids for PCE degradation.

Major elements in hexagonal plates were Ca, Al, Si, and Cl. S might be present but its peaks would not be clearly observed because of overlap with Au peaks. Fe was also detected in hexagonal plates when Fe(II) was added

Based on XRD, SEM and EDS analyses, the possible active solids for PCE degradation might be AFm phases, such as Friedel's salt, calcium aluminate hydrates and/or calcium aluminum silicate hydrates. Fe(II) could be adsorbed on the surfaces of those solids or incorporated into their structure through isomorphous substitution.



Capitol Cement Slurry without Fe(II):CCS1

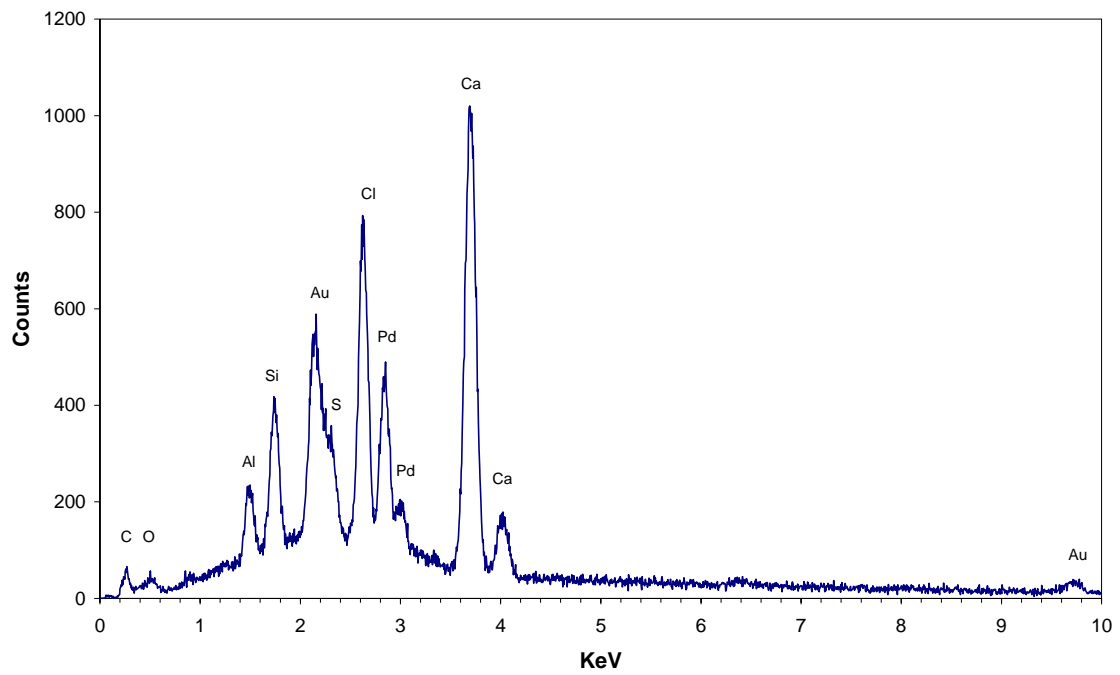
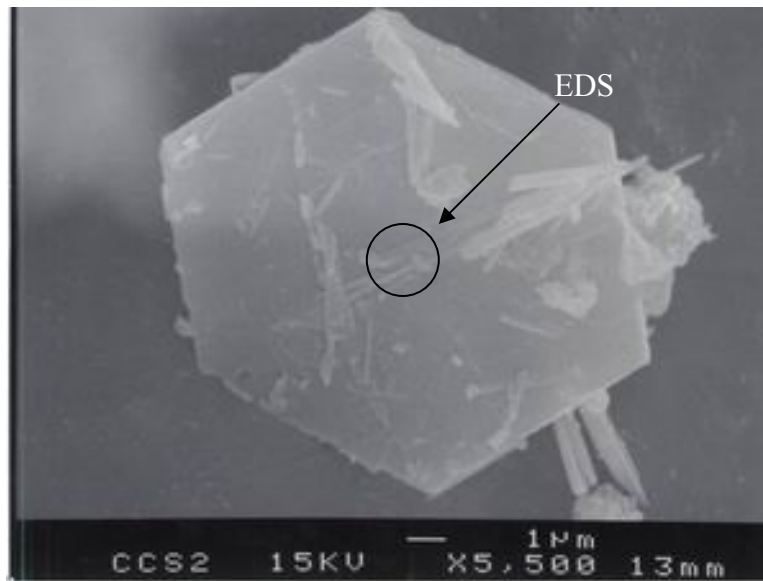


FIGURE 4-5 The first SEM image and EDS of Capitol cement slurry without Fe(II).



Capitol Cement Slurry without Fe(II):CCS2

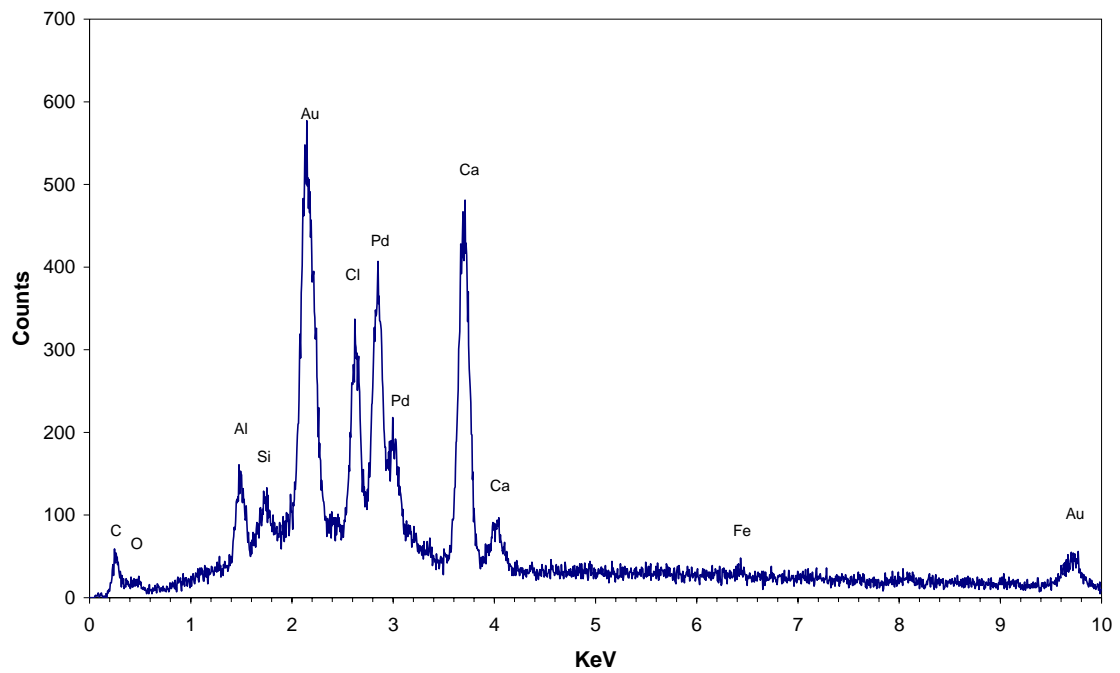
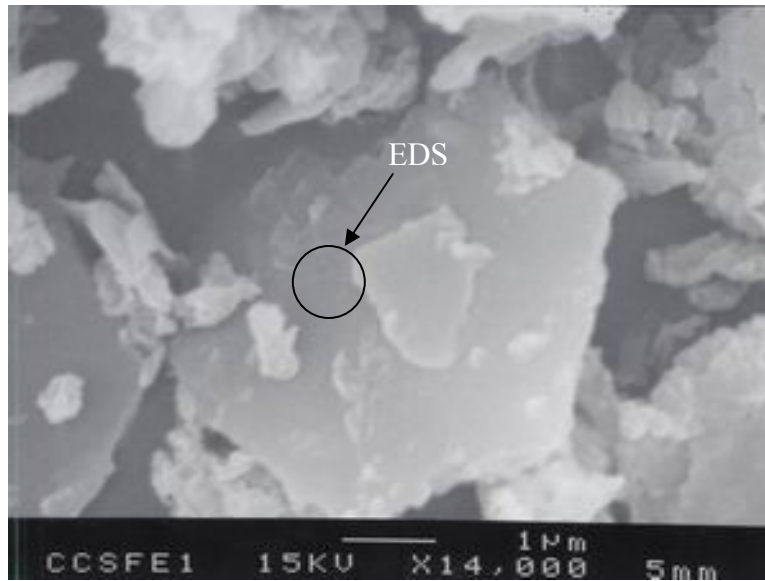


FIGURE 4-6 The second SEM image and EDS of Capitol cement slurry without Fe(II).



Capitol Cement Slurry with Fe(II):CCSFE1

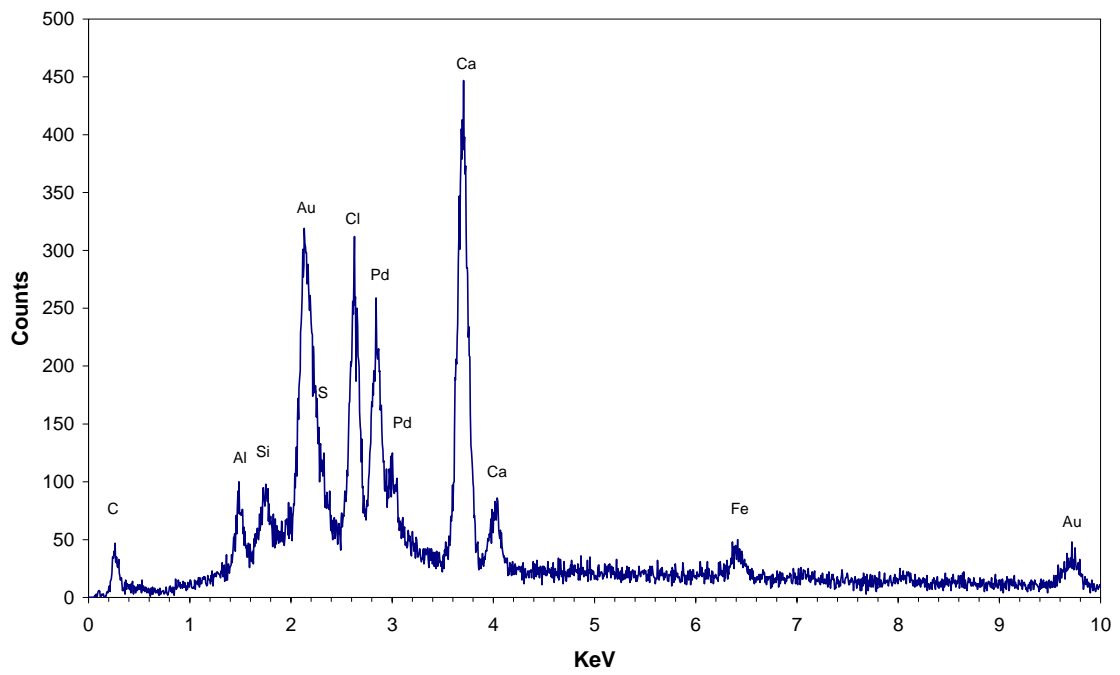


FIGURE 4-7 SEM image and EDS of Capitol cement slurry with Fe(II).

4.2.2 10% Portland cement extract (10% PCX)

Figure 4-8 shows the XRD patterns (figure 4-8(a)) and peak identifications (figure 4-8(b)) of solids formed in 10% PCX. CPCX stands for Capitol Portland cement extract and CPCXFe for Fe(II) containing Capitol Portland cement extract. Portlandite and Friedel's salts were identified in 10% CPCXFe solids to which Fe(II) was added. They were major solids formed in CPCXFe. Peaks of Friedel's salts were more clearly observed when Fe(II) was added to 10% PCX, as was observed for 10% cement slurry solids. The pH in these slurries was increased by addition of 1.25M of $\text{Ca}(\text{OH})_2$, which resulted in considerable amounts of $\text{Ca}(\text{OH})_2$ remaining in the suspension that would also remain after solid separation through centrifugation.

The highest intensity peak in 10% CPCXFe was observed at 38.3° with 2.3481 \AA of d-spacing, which is associated with Friedel's salt (the fourth highest peak in β form Friedel's salt, JCPD 35-105). The highest intensity peak in 10% CPCX was found at about 33.8° with 2.6483 \AA of d-spacing, which is associated with Portlandite. The peak of 2.7662 \AA might come from calcium aluminum silicate hydrates (JCPD 18-274), but the first and second highest intensity peaks (3.1 \AA and 5.8 \AA) of calcium aluminum silicate hydrates were not detected.

Portlandite was a major solid phase detected in CPCX. Peaks of 4.2186 , 3.4139 , 3.1997 , and 2.7962 \AA in figure 4-8(a) were calcium silicate hydrates (JCPD 39-1373) and peaks of 3.0662 , 2.9530 , and 2.8955 \AA were calcium aluminum silicate (JCPD 23-105). The 8.5180 \AA peak might be calcium aluminum oxide sulfite hydrate (the highest intensity peak, JCPD 41-477), but other peaks of calcium aluminum oxide sulfite

hydrate were not matched, other than the one at 4.2186 Å in figure 4-8(a). Intensity and d-spacing values of CPCX were not exactly matched with references. This might be the result of different chemical composition and atomic arrangement of CPCX solids compared to the referenced solids. Portlandite and calcium aluminum silicate probably were the dominant solid phases formed in 10% CPCX. Friedel's salt peaks were not observed in CPCX.

XRD patterns of 10% CPCXFe were similar to those of 10% CPCXFe as seen in figure 4-1. Peaks from either calcium aluminum silicate hydrate or calcium aluminate hydrate in 10% CPCXFe were not observed as strongly as they were for 10% CPCXFe. However, both cement slurries and cement extracts with Fe(II) addition showed the presence of Friedel's salts. XRD patterns of 10% CPCXFe also supported that hypothesis that Friedel's salt is an active agent for dechlorination in Fe(II)-DS/S.

Figure 4-9 to 10 shows scanning electron microscopic (SEM) images and energy dispersive spectrometer (EDS) spectra of 10 % CPCX without (figure 4-9) and with (figure 4-10) Fe(II). EDS spectra were taken from single hexagonal particle. Although SEM images of 10% CPCX did not show the perfect hexagonal shapes observed in 10% CPCX, thin plates having nearly hexagonal angles were observed. Particle sizes in 10% CPCX were 1 to 3 µm, which were smaller than those in 10% CPCX by more than a few micrometers. They were so aggregated so that an image of an individual particle could not be seen.

(a)

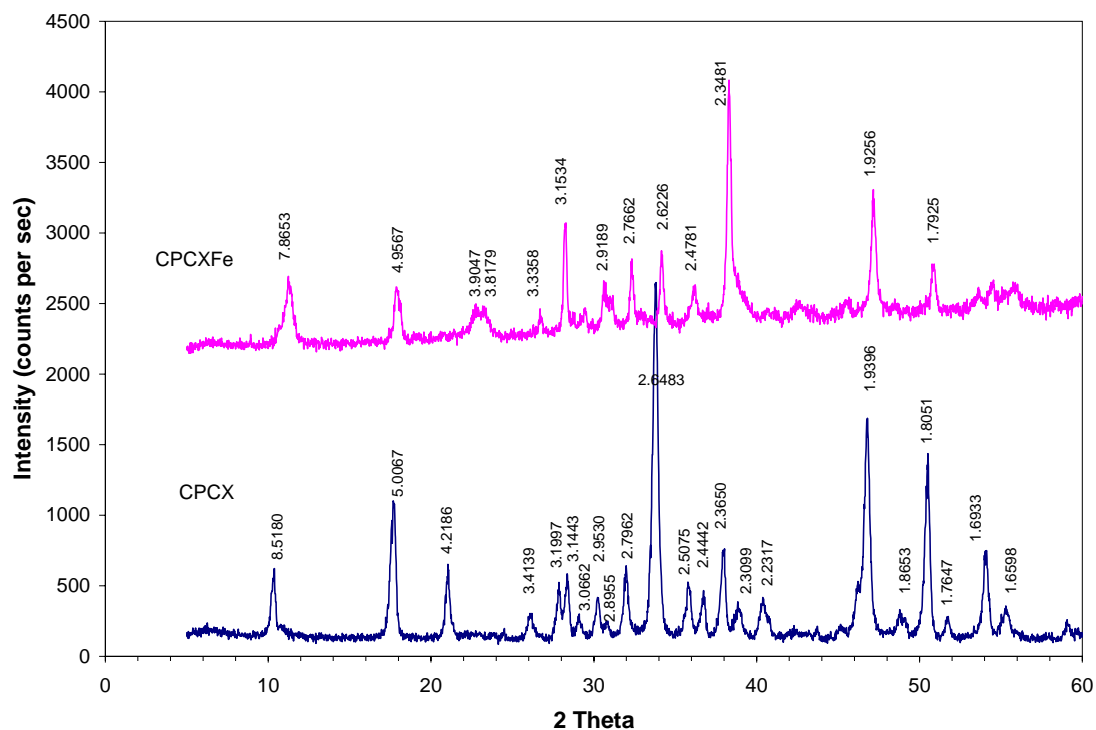


FIGURE 4-8 X-ray patterns of 10% Capitol cement extract. (a) CPCXFe = 10% Capitol Portland cement extract with Fe(II); CPCX = 10% Capitol Portland cement extract without Fe(II); Unit of d-spacing values is Å. (b) Mineral identification using software program, JADE, of CPCXFe. Note: Backgrounds of figure (b) was adjusted by JADE. Thanks to the Texas Transportation Institute for the use of the Rigü automatic diffract.

(b)

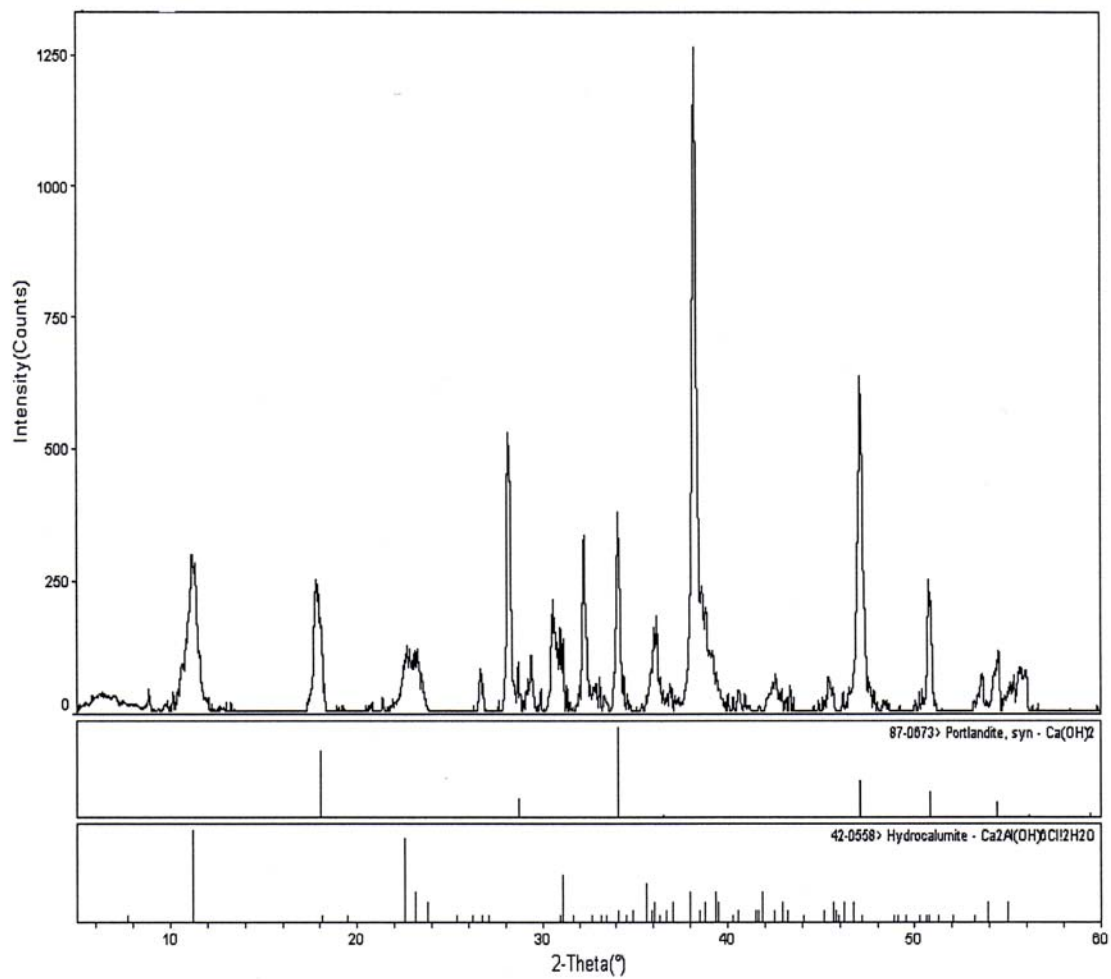
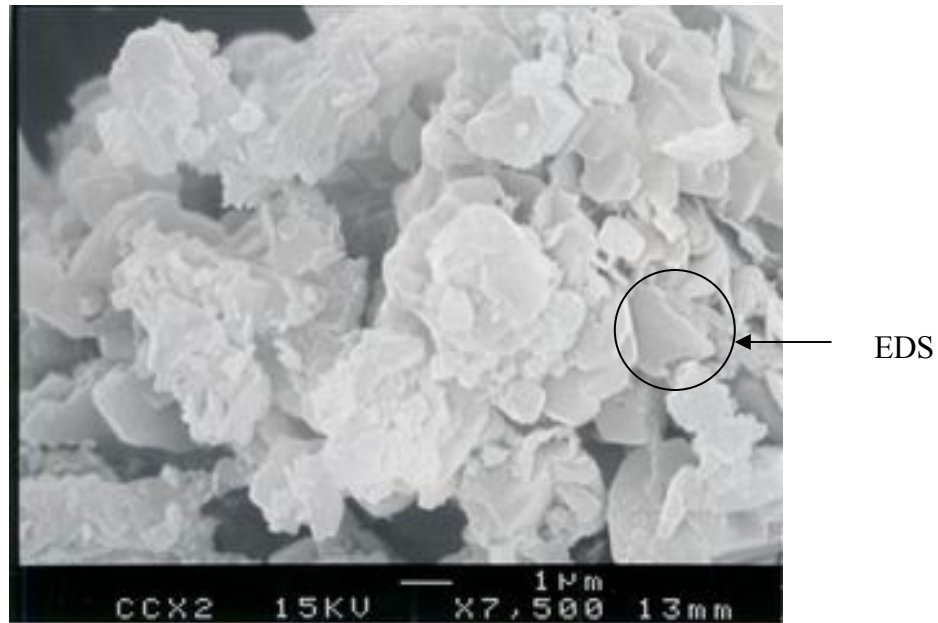


FIGURE 4-8 Continued

High concentrations of Cl were observed in EDS spectra in systems with and without addition of Fe(II). They were the result of the addition of 2.1 N HCl that was used to prepare the cement extracts. Based on EDS spectra, solids in figure 4-9 might be Portlandite. Although Portlandite and calcium aluminum silicate probably were the dominant solid phases formed in 10% CPCX, neither Al nor Si was detected in EDS analysis of circled area in figure 4-9. When cement is hydrated, about 20% of the hydration products are Portlandite (42). Furthermore, high concentrations of Ca(OH)_2 were added to 10% cement extract during solid preparation of CPCX and solids were not separated, unlike preparation of 10% CPCXFe, when the top layer of solids was separated from the other solids. Therefore, significant amounts of Portlandite would be expected to be present in 10% CPCX solids, compared to other solid phases that were not found in SEM and EDS analysis. However, based on XRD analysis, other solid phases are also present in 10% CPCX solids. Along with Ca, and Cl, Fe and Al were detected in 10% CPCXFe solids as well as a low count of Mg and Si. A low degree of substitution of Mg for Ca might have occurred. Peaks found in figure 4-9 might be associated with Friedel's salt or calcium aluminum silicate hydrate. Presence of Si could be the result of a substitution for Al in AFm phases. Another possibility is that Si exists as an interlayer anion in possible LDH that appear as particles with thin hexagonal plate shapes in the SEM.



Capitol Cement Extract without Fe(II):CCX2

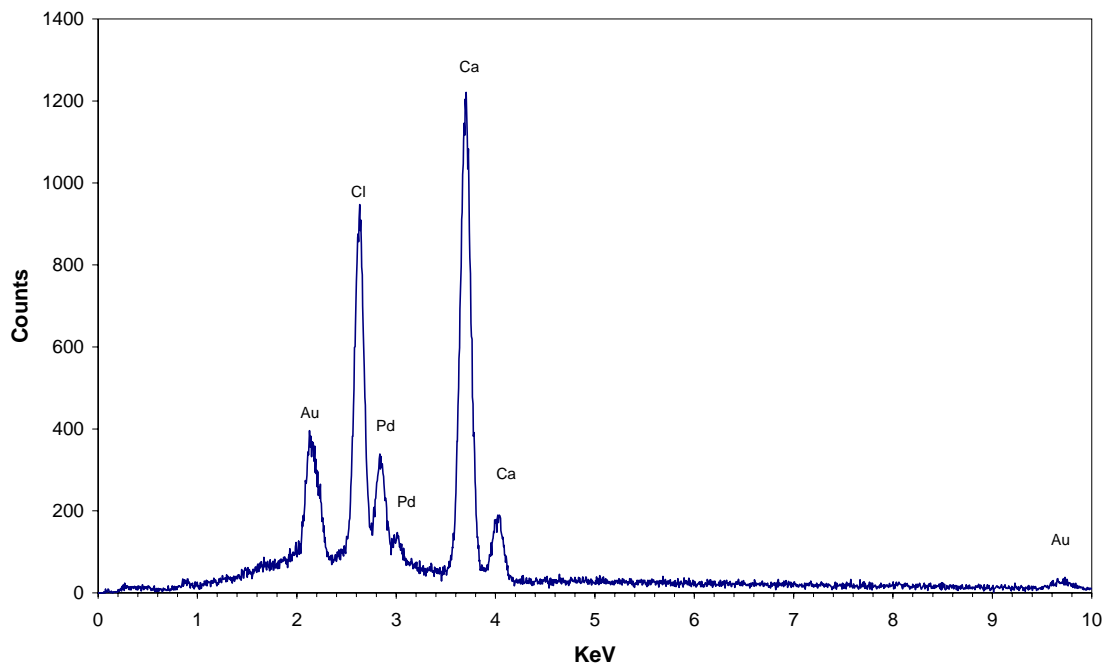


FIGURE 4-9 SEM image and EDS of Capitol cement extract without Fe(II).



Capitol Cement Extract with Fe(II):CCXFE3

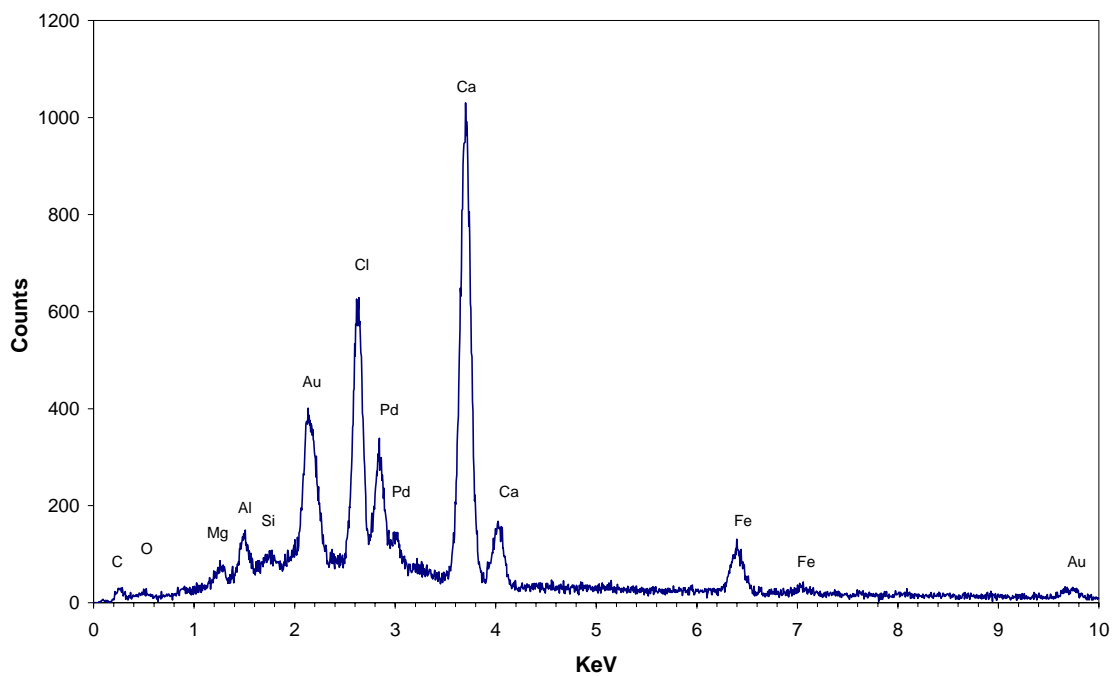


FIGURE 4-10 SEM image and EDS of Capitol cement extract with Fe(II).

4.2.3 Synthetic cement extract (SCX)

4.2.3.1 Full synthetic cement extract (FSCX)

Portlandite was identified as the major solid formed in the FSCX system. Friedel's salt was not formed. The rest of the peaks were much matched reasonably well with calcium silicate hydrates (JCPDS 23-125), except for the peak of 8.03 Å. If this peak were considered to come from GR_Cl, it and a peak of 3.95 Å would match well, but the third most intense peak of GR_Cl (2.7 Å) would be missing. Therefore, it is not clear to which solid the 8.03 Å peak should be assigned. The other peaks could be GR_Cl or/and calcium silicate hydrates.

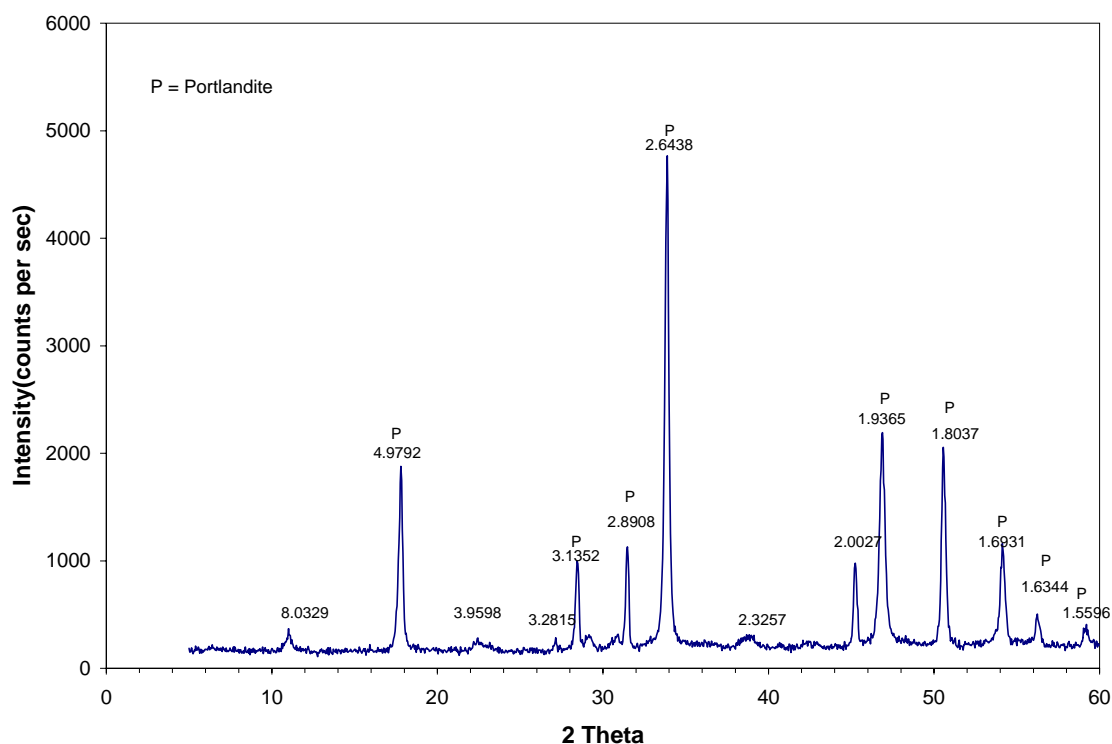
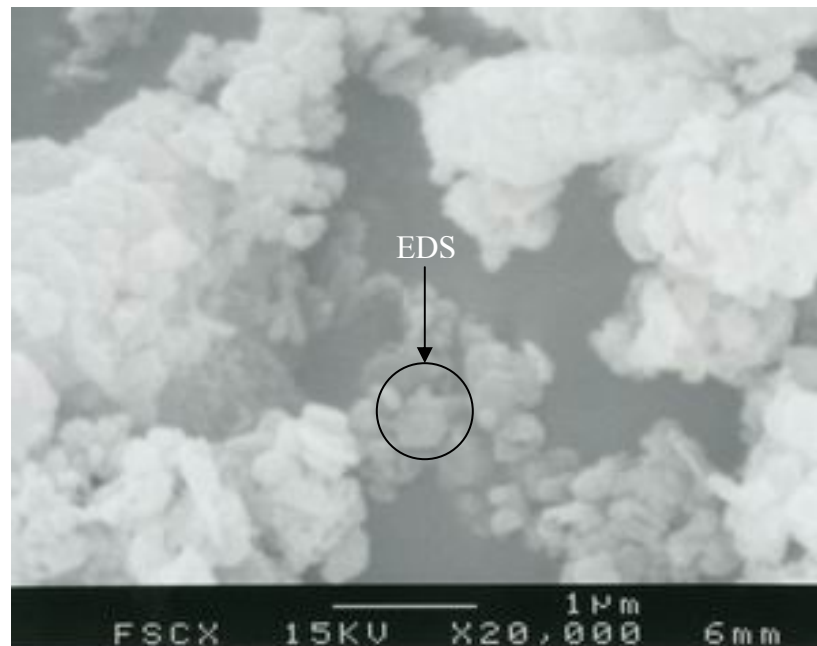


FIGURE 4-11 XRD patterns of FSCXFe solids. Unit of d-spacing is Å; FSCXFe = Full element synthetic cement extract with Fe(II).



Full Synthetic Cement Extract with Fe(II):FSCX

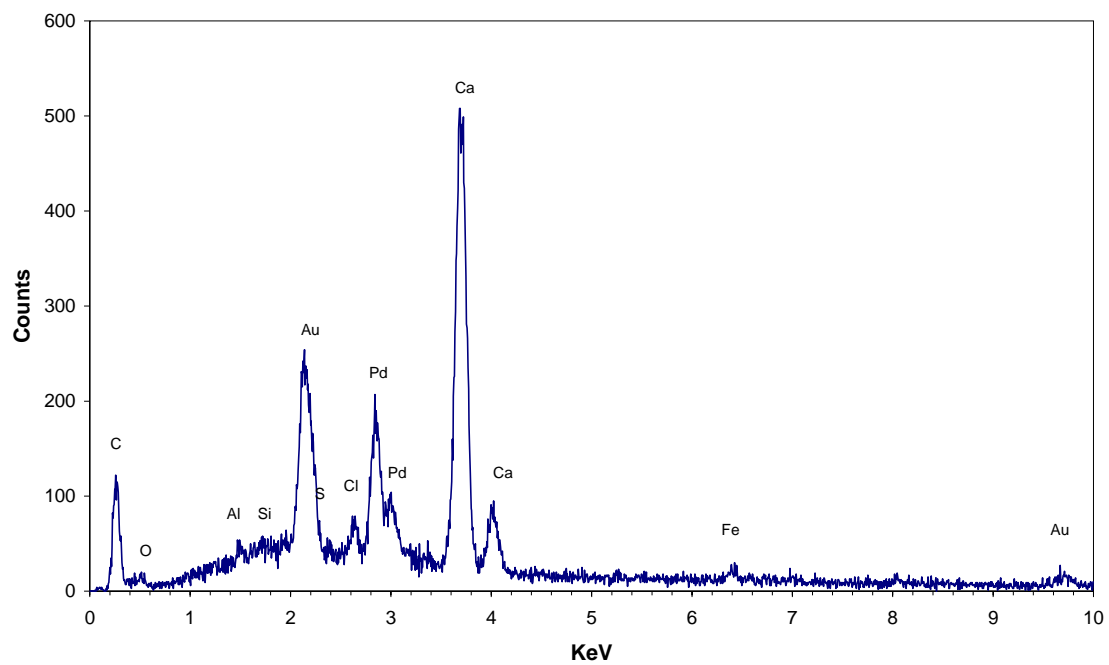


FIGURE 4-12 SEM image and EDS of full synthetic cement extract with Fe(II).

Figure 4-12 shows the SEM image and EDS spectra of full synthetic cement extract with Fe(II) addition (FSCXFe). EDS spectra were taken from single hexagonal particle. Like the cement slurry and cement extract systems, hexagonal plates were observed in FSCXFe solids. However, particle sizes of these solid were much smaller, less than 0.5 μm , than observed in the PCS and PCX system. Based on XRD and EDS spectra, these hexagonal plates might be Portlandite. Mostly Ca and a small amount of Al, Si, Cl, S, and Fe comprised the FSCXFe solids. Fe concentration in FSCXFe was lower than that in PCSFe and PCXFe solids. Even though FSCX contained the same concentrations of elements as the cement extract, all instrument analyses, as well as a PCE degradation test, indicated that solids formed in FSCX were different from ones formed in the cement slurry or the cement extract.

4.2.3.2 Minor synthetic cement extract (MSCX)

Halite and ferrous hydroxide were identified through XRD analysis as being present in solids formed in MSCX, as shown in figure 4-13. Halite came from addition of NaCl to keep the same Cl concentration as cement Cl. The MSCX produced different kinds of solids than were produced in the cement slurry, cement extract and full synthetic cement extract. This might be caused by the absence of major elements, especially Ca and Al, which are major components of the solids formed in the cement slurry and the cement extract.

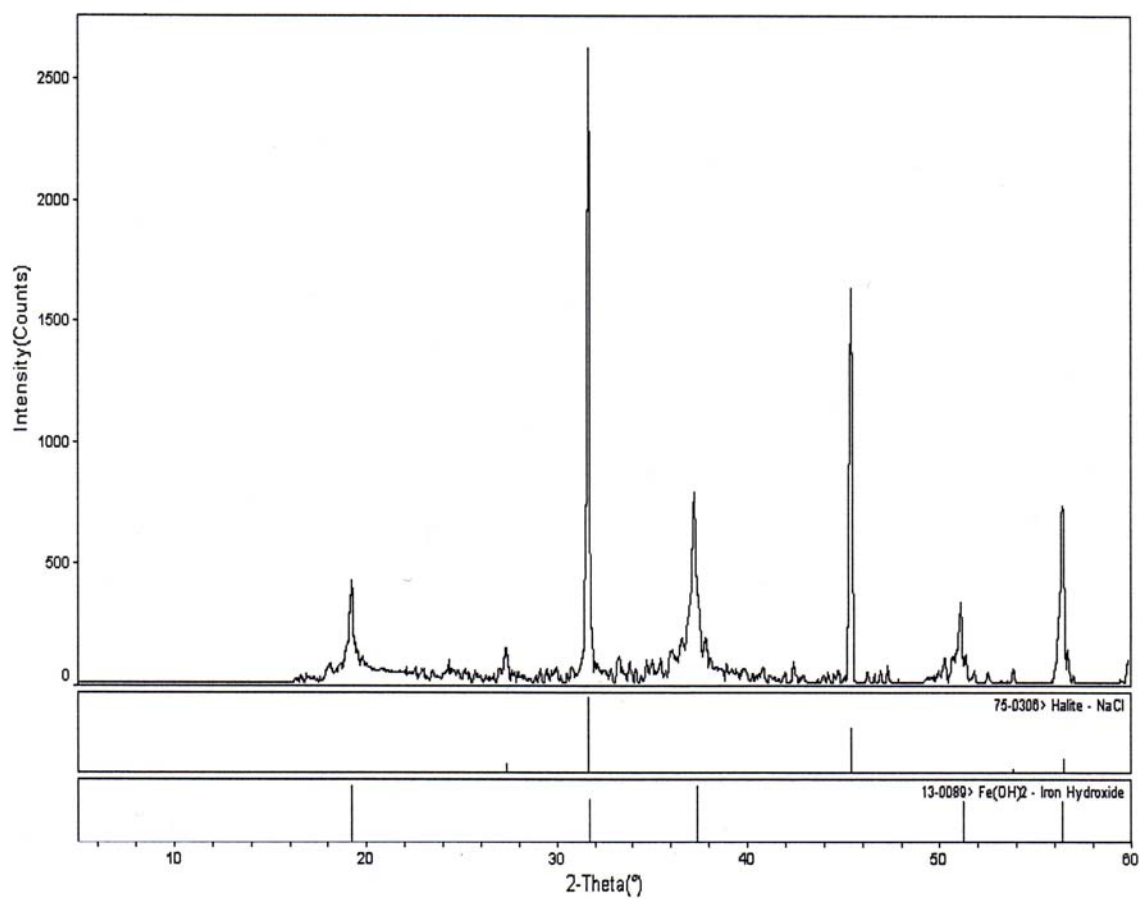
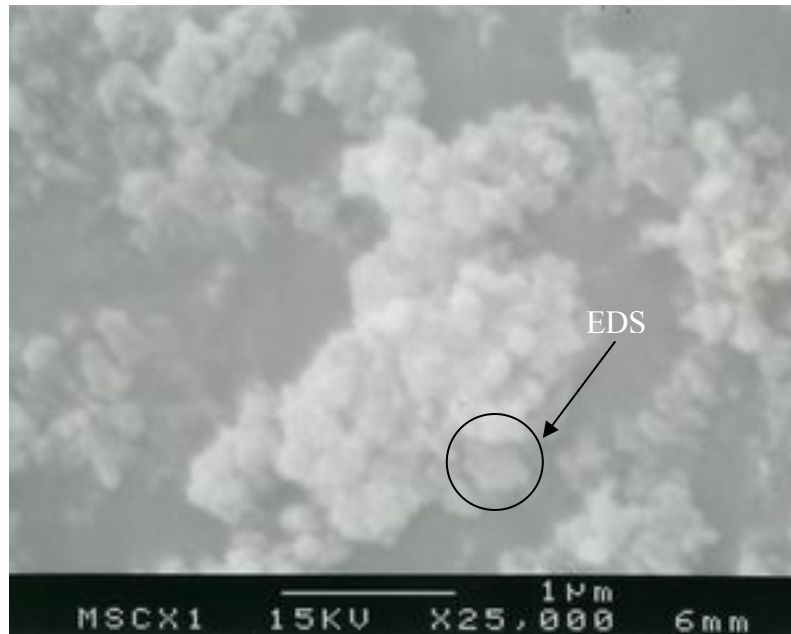


FIGURE 4-13 XRD pattern and mineral identification using software program, JADE, of MSCXFe solids. MSCXFe = Minor element synthetic cement extract with Fe(II). Note: Backgrounds of figure was adjusted by JADE. Thanks to the Texas Transportation Institute for the use of the Rigü automatic diffract.



Minor element Synthetic Cement Extract with Fe(II):MSCX1

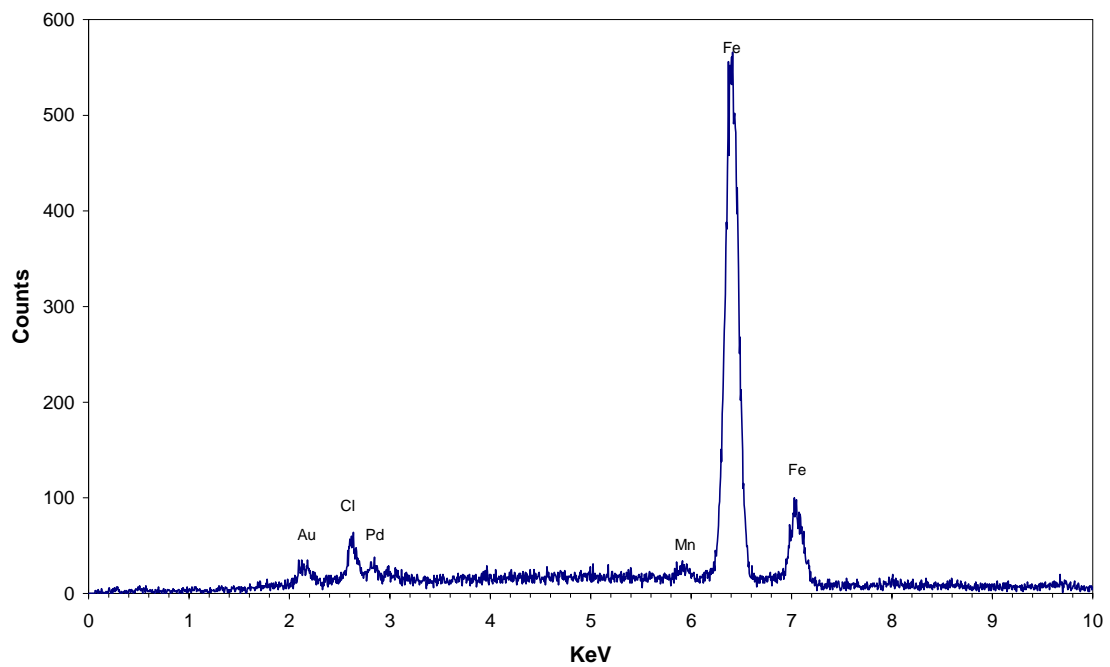


FIGURE 4-14 SEM image and EDS of minor elements synthetic cement extract with Fe(II).

Figure 4-14 shows the SEM image and EDS spectra of MSCXFe solids. EDS spectra were taken from single hexagonal particle. Even though many cement elements were added, solids in figure 4-14 were composed mainly of Fe and Cl and small amounts of Mn. This might confirm the hypothesis that iron and chloride are important in forming active agents for PCE degradation. Particle sizes of MSCXFe solids were very small, about 0.3 μ m, compared to those formed in the cement slurry and the cement extract. Small particles were too aggregated to allow an image to be taken of an individual particle. The particle shapes were also hexagonal even though MSCXFe solids were different from solids formed in cement systems, based on XRD analysis.

4.2.3.3 Fe(II)(III)Cl

Figure 4-14 shows the XRD patterns of solids formed in the mixture of FeCl₂, FeCl₃ and NaCl (Fe(II)(III)Cl) with simple mixing at pH 12 (Fe(II)(III)Cl_Simple Mixing). It also shows the patterns of solids formed using methods similar to those that are used to synthesize green rust (GR) at neutral pH (Fe(II)(III)Cl_GRN) and at pH 12 (Fe(II)(III)Cl_GR12). Ferrous hydroxide and halite were found, regardless of the synthesis method and pH. A large amount (2.2 M) of NaCl was added to keep the same concentration of chloride as in the cement extract. Extra NaCl might be left after reactions. During drying, white solids were observed along with colored solids, which could have been halite formed from excess NaCl.

Green rust chloride (GR_Cl) was not formed in the neutral pH system. This might be due to low concentration (0.4 mM) of ferric iron. GR_Cl has a ratio of Fe(II) to

Fe(III) of 3, but the ratio in this system was around 10. The color of solids produced by Fe(II)(III)Cl_GRN was dark green, the same color as GR_Cl. However, XRD peaks of GR_Cl were not observed. Their gray color also indicates the lack of GR.

Solid phases identified here were the same as in MSCXFe. In the absence of major elements of cement, only iron could participate in the formation of solids. It was not clear whether Cl was included in the solid structure or adsorbed onto the surface of solids, due to the high concentration of NaCl. Theoretically, 0.4mM of Cl could compensate the charge deficit produced if all the Fe(III) that was added formed the mixed iron hydroxide ($\text{Fe(II)}_3\text{Fe(III)(OH)}_8^+$) that is typical of Green Rust. It might be possible that the amount of GR_Cl formed in Fe(II)(III)Cl system is too small to be detected by XRD.

The backgrounds of the diffractograms of solids from MSCXFe, Fe(II)(III)Cl_Simple Mixing and Fe(II)(III)Cl_GR12 were gradually increasing, even though backgrounds were adjusted to zero by the JADE software. This phenomenon occurred due to fluorescent x-radiation of high amount of Fe in Cu radiation. However, these high backgrounds were not observed in the Fe(II)(III)Cl_GRN system, which was analyzed by Cu radiation with a monochromator between the sample and detector (118)

(a) Fe(II)(III)Cl_Simple Mixing

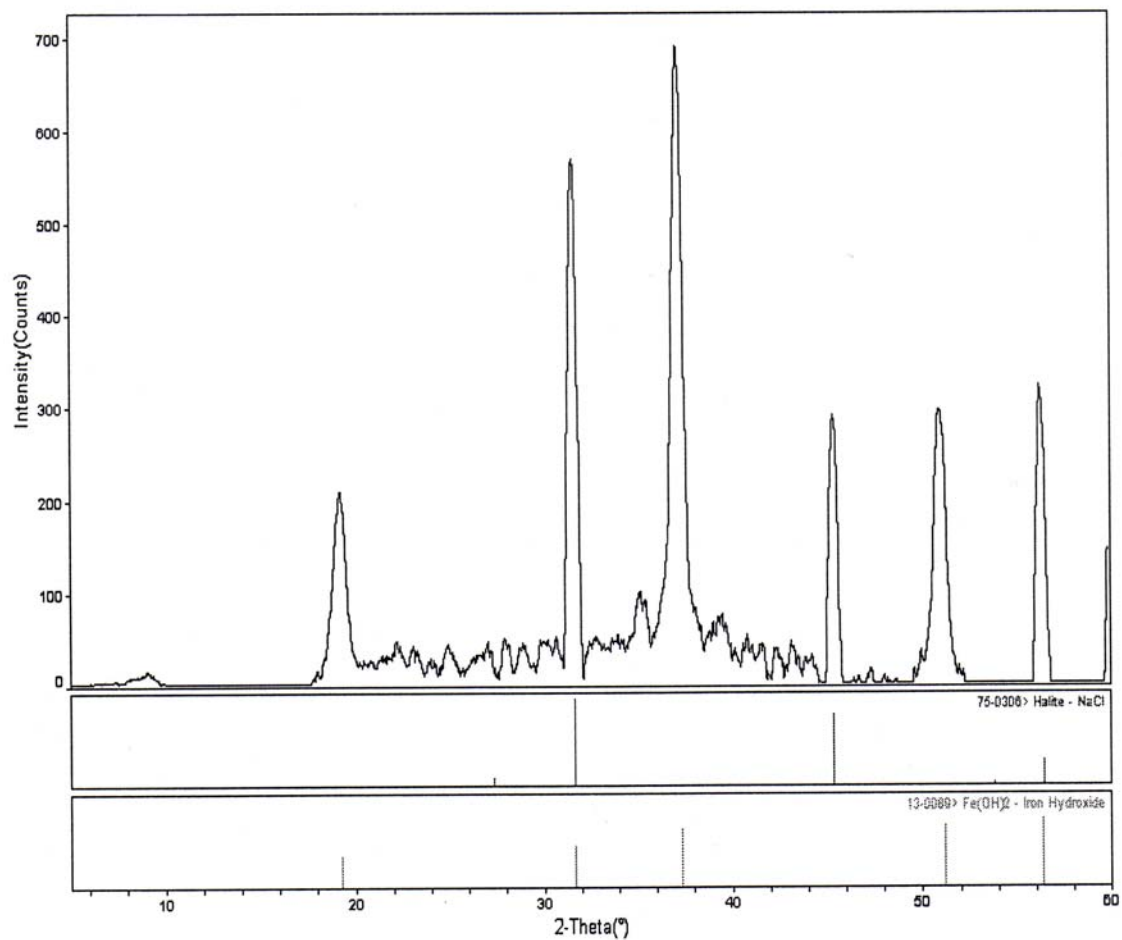


FIGURE 4-15 XRD pattern and mineral identification using software program, JADE, of Fe(II)(III)Cl solids. The background of (a) and (b) were adjusted by JADE; Capital H stands for Halite and capital F stands for Ferrous Hydroxide in (c). Thanks to the Texas Transportation Institute for the use of the Rigü automatic diffract of (a) and (b).

(b)Fe(II)(III)Cl_GR12

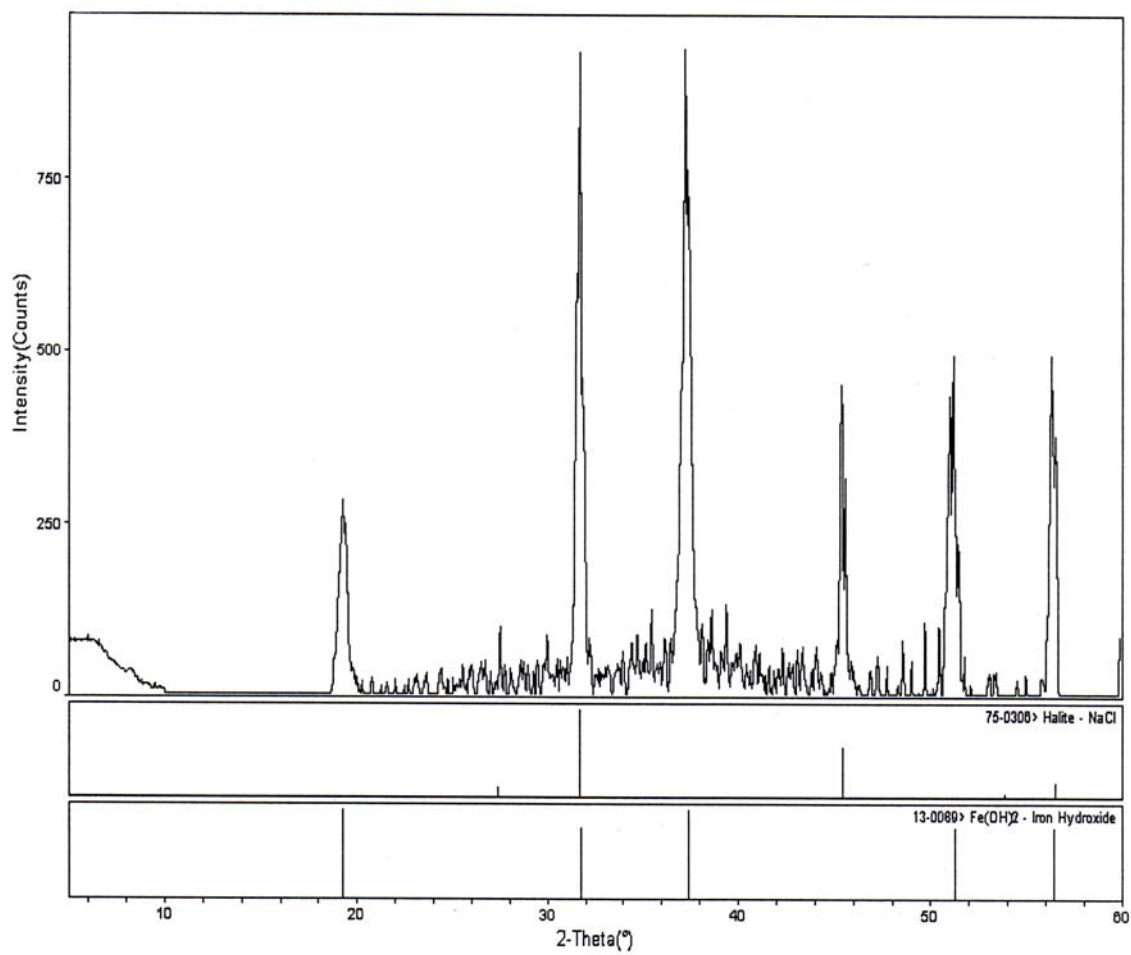


FIGURE 4-15 Continued

(c)Fe(II)(III)Cl_GRN

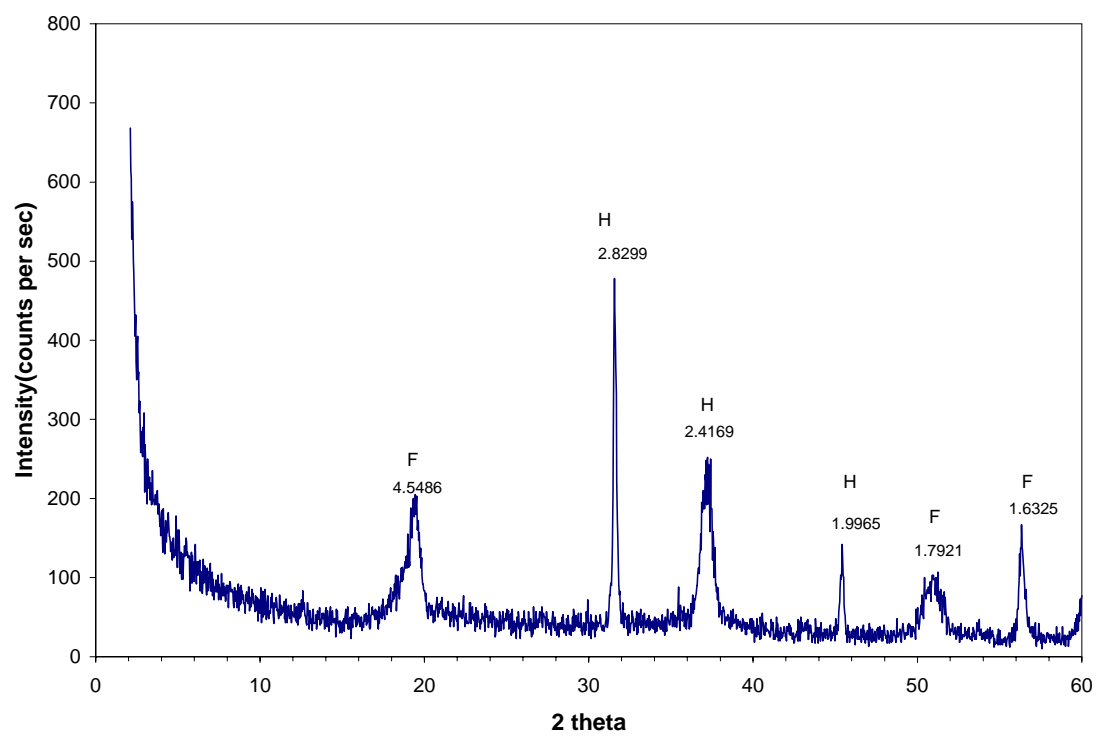
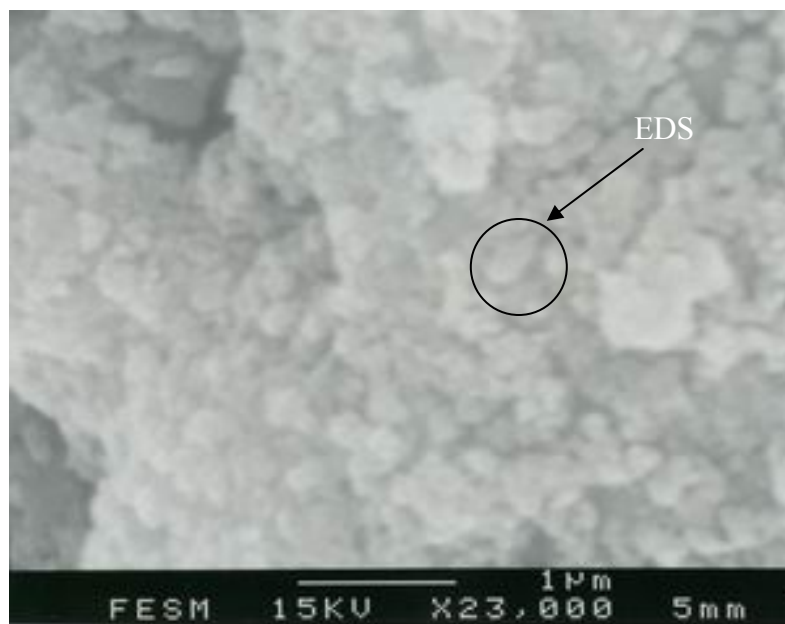


FIGURE 4-15 Continued

Figures 4-16 through 4-18 show the SEM images and EDS spectra of Fe(II)(III)Cl solids synthesized by different methods and at different pH. EDS spectra were taken from single hexagonal particle. Solids in all three systems had hexagonal shapes. However, their sizes were much smaller when they had been formed at pH 12, (Fe(II)(III)Cl_simple mixing and Fe(II)(III)Cl_GR12) than at neutral pH (Fe(II)(III)Cl_GRN). The particle sizes of Fe(II)(III)Cl_GR12, Fe(II)(III)_Simple Mixing and Fe(II)(III)Cl_GRN were about 0.5 μm , 0.2 μm , and 4 to 5 μm , respectively. The method of mixing the solids during formation did not have much of an effect on the types of solids formed. The coprecipitation method and simply mixing all of the elements at once formed the same kind of solids. The pH during solid formation showed much more of an affect that the synthesis method, particularly on the size of the solids formed.

Actually, it was not clearly shown in figure 4-18 that solids formed at neutral pH-(Fe(II)(III)Cl_GRN)-were aggregated particles or single particles. They had similar shapes as reported for GR_Cl (69), but they could be an intermediate stage between ferrous hydroxide and GR_Cl.

Particle sizes of green rust have been reported to vary from 0.02 to about 1 μm (70) to larger than 2 μm (69), probably due to the variation of crystal growth rates. The smaller particles are the larger surface area they have. Thus, the smaller particles might be more preferable for PCE degradation because they would have more active surface sites.



Fe(II)(III)Cl_simple mixing:FESM

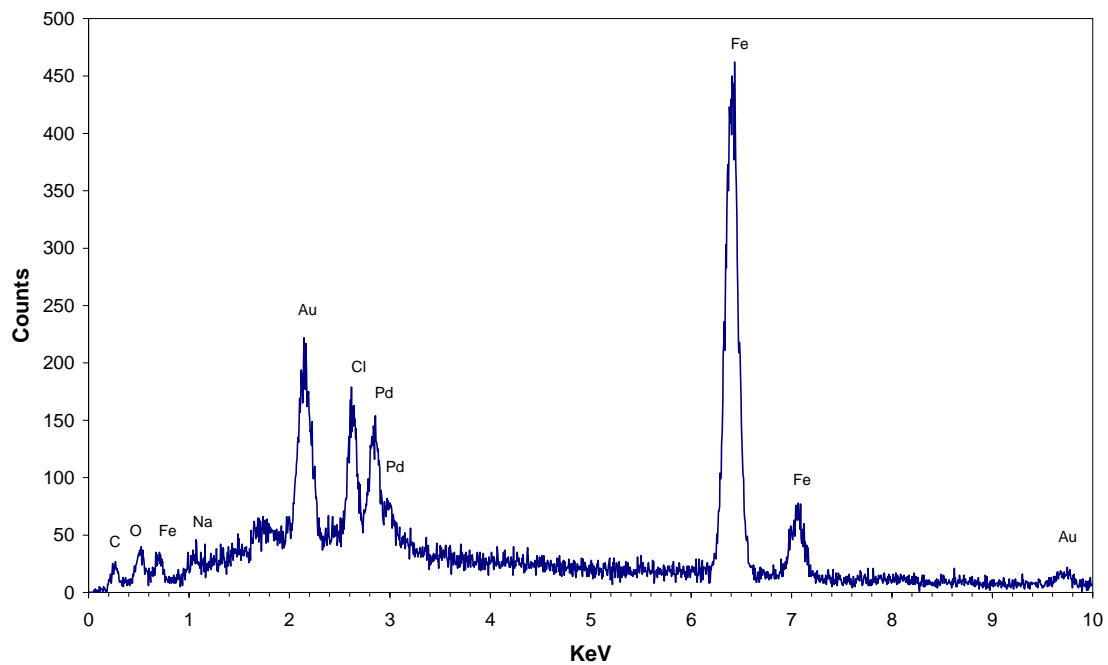
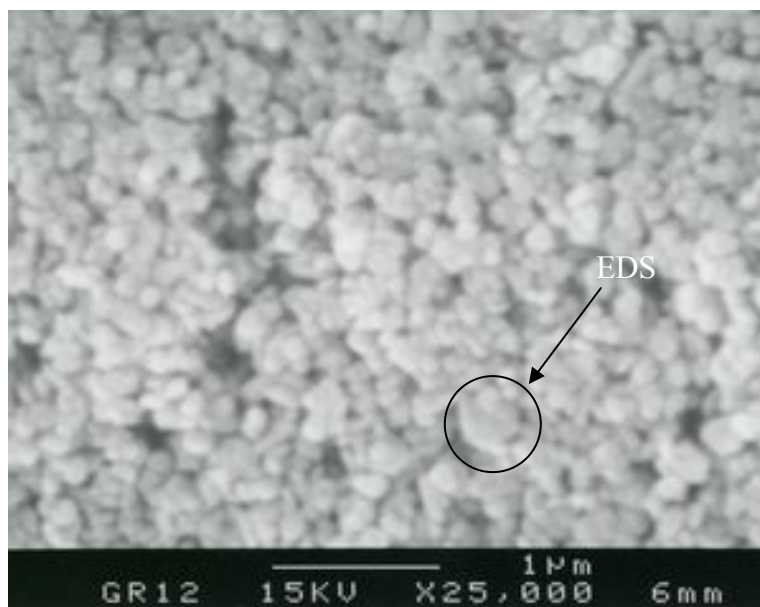


FIGURE 4-16 SEM image and EDS of Fe(II)(III)Cl_Simple Mixing.



Fe(II)(III)Cl_GR12:GR12

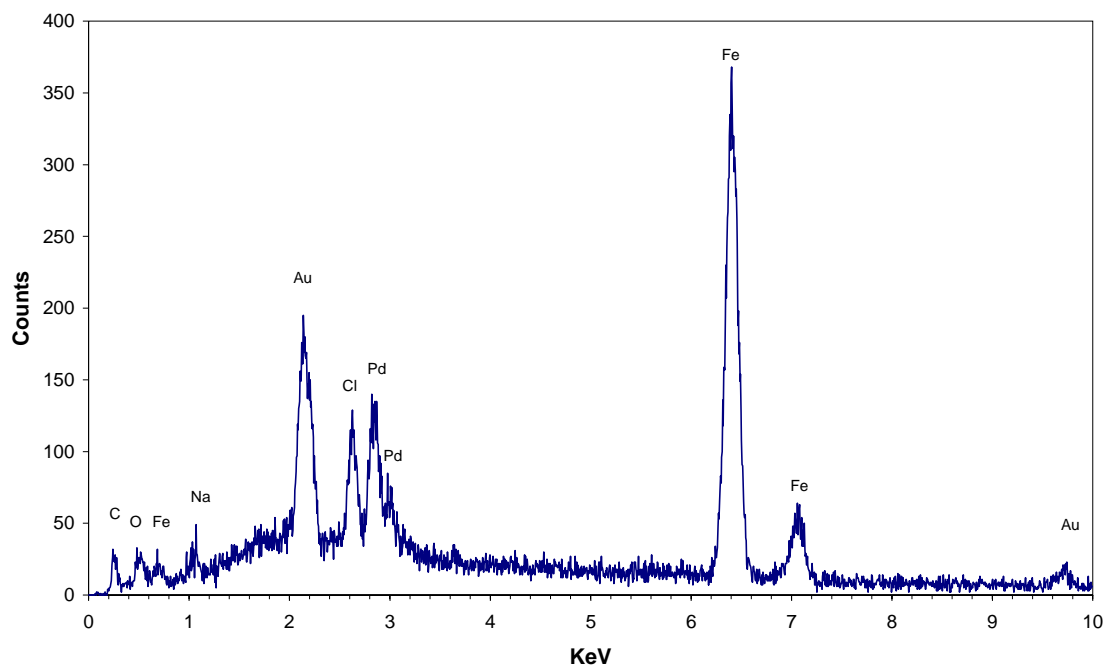
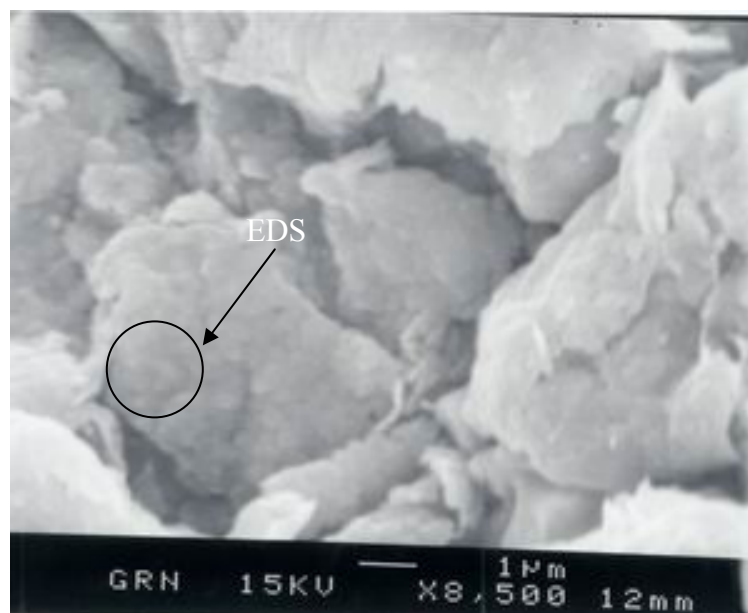


FIGURE 4-17 SEM image and EDS of Fe(II)(III)Cl_GR12.



Fe(II)(III)Cl_GRN:GRN

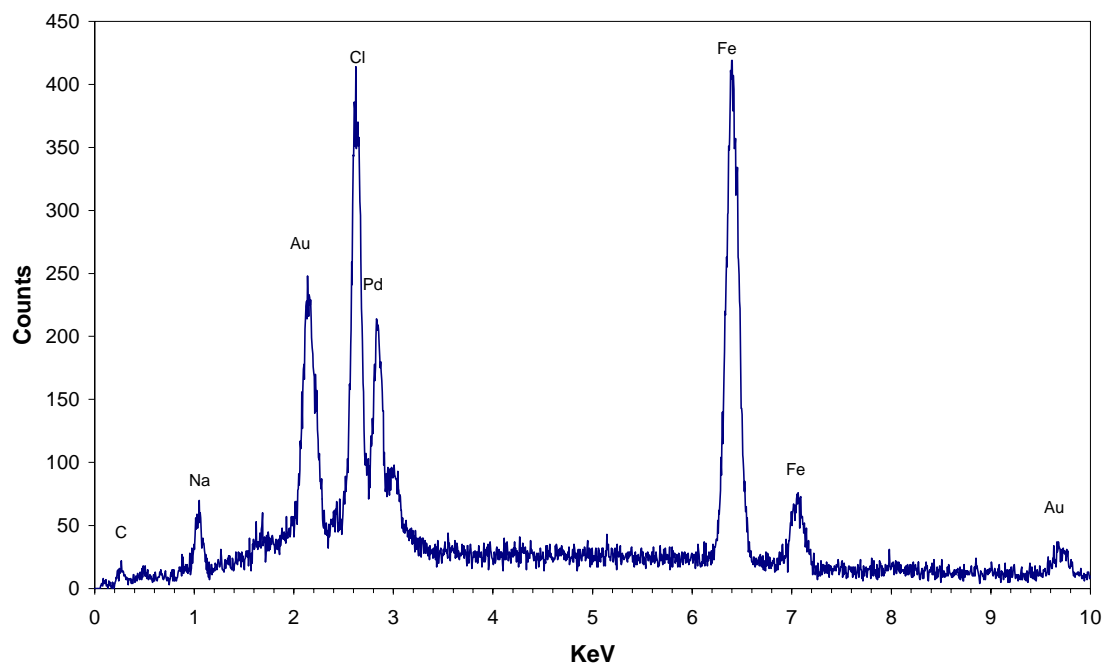


FIGURE 4-18 SEM image and EDS of Fe(II)(III)Cl_GRN.

4.3 Examination of variability of ordinary Portland cement (OPC)

4.3.1 PCE degradation kinetic tests

4.3.1.1 10% cement slurry solids with Fe(II)

Table 4-13 and figure 4-19 and 4-20 shows the results of PCE degradation experiments using 10% cement slurries from four different cement manufacturers (Txi, Quikrete, Lehigh, Capitol). They were type I Portland cements, except Txi, which was type II Portland cement. The first and second order rate constants were obtained by nonlinear regressions using Matlab. PCE degradation experiments were conducted at an average pH of 12.6 with variation of ± 0.05 .

Both first and second order kinetic models were fitted to the data for PCE degradation by the Txi cement slurry (TPCSFe, exp. 145) and these models fitted the data equally well. The pseudo first order rate constant for TPCSFe was 2 times higher than that for experiments conducted by Huang with Capitol Portland cement slurries with Fe(II) (CPCSFe) (23). The first order kinetic model fitted data from the experiment with Lehigh cement (LPCSFe, exp 147) better than the second order model. The pseudo first order rate constant for LPCSFe was 2.5 times higher than CPCSFe and 1.5 times higher than TPCSFe. About 50% of PCE was degraded in both TPCSFe and LPCSFe after 3 days. Experiments with 10% Quikrete cement slurry and Fe(II) (QPCSFe, exp. 146) showed unique PCE degradation behavior (Figure 4-19). The kinetic data fit a second-order model better than a first-order model, in contrast to data from experiments with other cement slurries. The second order kinetic model fit the initial and final data points well, but did not fit points in the middle very well. Values predicted by the kinetic

model were much below the measured values for data from days 4 to 11. Although it was the same type of cement as Capitol, it showed a different kinetic behavior of PCE degradation. About 50% of PCE was degraded within 10 hours and then the rate of PCE degradation slowed. Approximately 75% of PCE was removed within 7 days. Uncertainties in the calculated rate constants for these three cement slurry systems were significantly higher than those for CPCSFe. This is especially true for coefficients obtained with QPCSFe.

Another behavior that was different for Capitol cement was the detection of TCE. TPCSFe did not show accumulation of any TCE during the experimental period. However, some TCE was detected during PCE degradation experiments by LPCSFe and QPCSFe. TCE concentrations equal to about 20% of the PCE concentration in controls were measured in experiments with QPCSFe after 2 days. Then, TCE concentrations decreased to below 0.6% of the PCE concentration in the control after 10 days. TCE concentrations slowly increased in LPCSFe and reached a maximum of 20% of the control at 5 days. TCE concentration in LPCSFe also decreased to below 0.1% of the control after 10 days.

The PCE degradation by CPCSFe followed a reductive elimination pathway, where TCE was not detected (23). Although byproducts of PCE degradation other than TCE were not investigated in this experiment, detection of TCE indicates that PCE degradation by LPCS and QPCS might follow a hydrogenolysis pathway.

Solid phases formed in different cement slurry systems might be similar due to similar chemical compositions of Portland cements and the same experiment conditions,

such as pH and initial Fe(II) and PCE concentrations. It was not clear why four cement slurry systems showed the different behavior when degrading PCE.

TABLE 4-13 The Fe(II) concentration normalized first and second order rate constants for PCE degradation in various slurries made with Fe(II) and 10% cement

Exp	10% cement slurry	pH	$k_{1\text{Fe(II)}}^a$	SS_1^b	$k_{2\text{Fe(II)}}^c$	SS_2^d
145	TPCSFe ^e	12.6	4.1E-03 (±22%)	1.0E-03	4.5E-02 (±26%)	1.1E-03
146	QPCSFe ^f	12.6	2.5E-02 (±97%)	1.0E-02	1.7E-01 (±67%)	4.0E-03
147	LPCSFe ^g	12.6	7.0E-03 (±14%)	3.9E-04	5.9E-02 (±48%)	4.6E-03
	CPCSFe ^h	12.6	2.6E-03 (±5.4%)			

^a k_1 was the Fe(II) concentration normalized first order rate constant; Unit = (mM Fe(II)×day)⁻¹

^b SS_1 was the sum of square of the first order rate model

^c k_2 was the Fe(II) concentration normalized second order rate constant; Unit = (mM Fe(II)×mM PCE×day)⁻¹

^d SS_2 was the sum of squares of the second order rate model

^eTPCSFe stands for Fe(II)-containing 10% Txi cement slurry

^fQPCSFe stands for Fe(II)-containing 10% Quikrete cement slurry

^gLPCSFe stands for Fe(II)-containing 10% Lehigh cement slurry

^hCPCSFe stands for Fe(II)-containing 10% Capitol cement slurry. The first order rate constant was referenced from Hwang (23)

Uncertainties represent 95% confidence limits expressed in % relative to estimate k
Initial PCE concentration was 0.242 mM

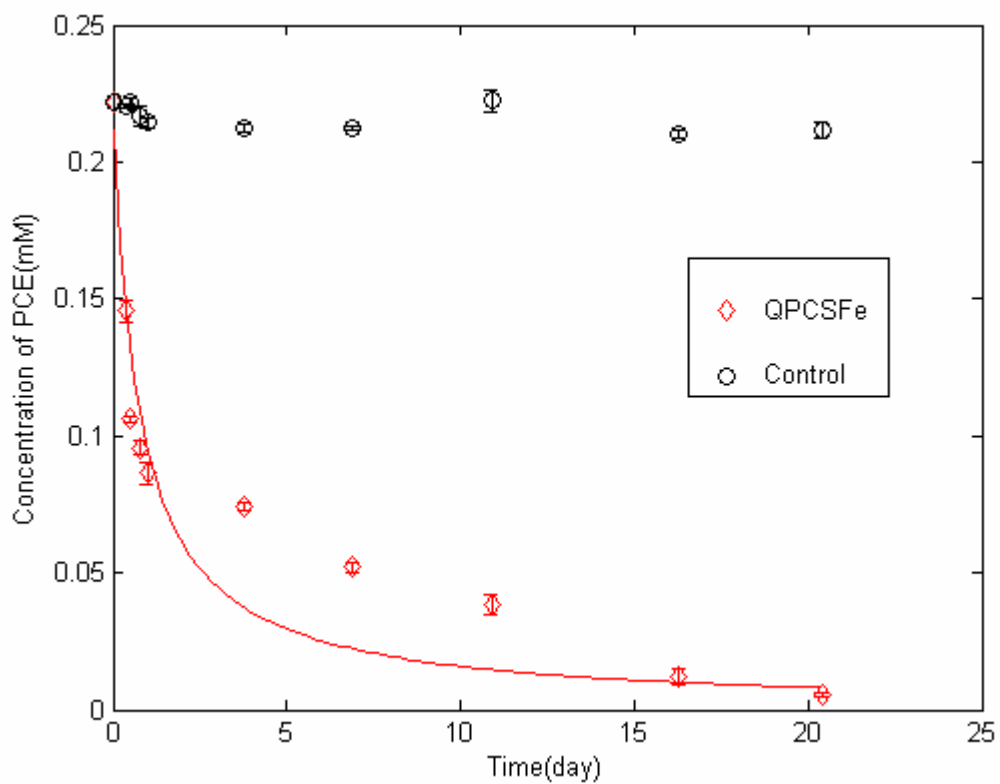


FIGURE 4-19 Kinetics of PCE reduction by slurries prepared with Fe(II) and 10% Quikrete cement, QPCSF_e. [PCE]₀ = 0.242 mM. The solid line represented the second order kinetic model fit.

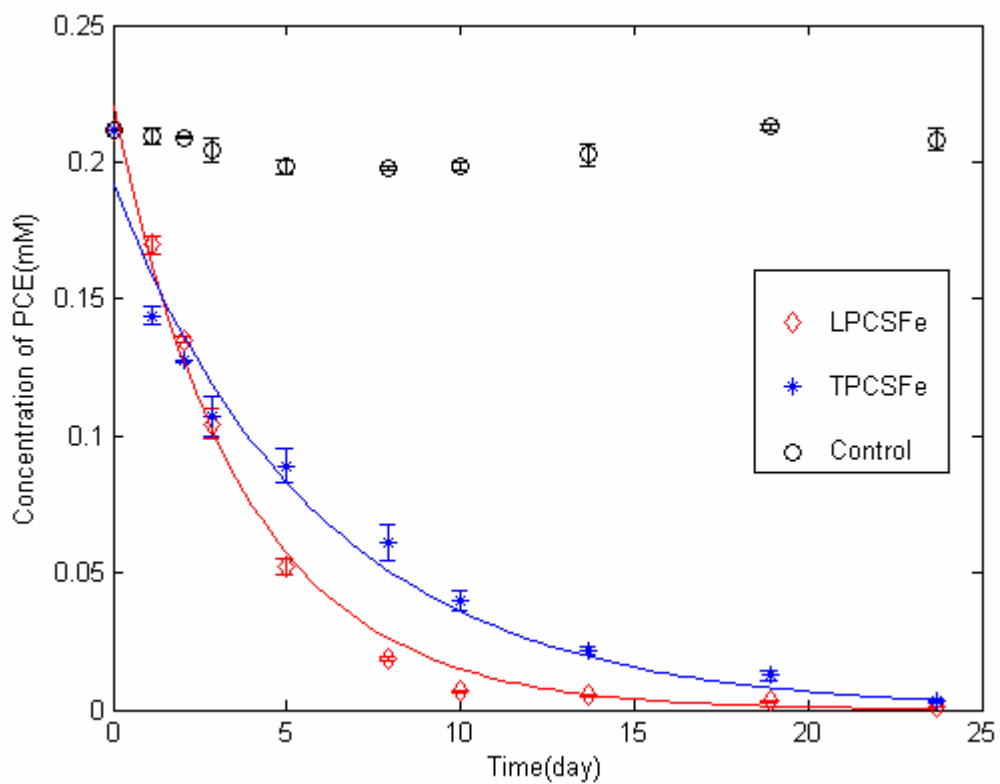


FIGURE 4-20 Kinetics of PCE reduction by slurries prepared with Fe(II) and 10% Lehigh and Txi cements, LPCSFe and TPCSFe, respectively. $[PCE]_0 = 0.242$ mM. The solid lines represented the first order kinetic model fit.

4.3.1.2 10% cement extract solids with Fe(II)

Table 4-14 and Figure 4-21 and 4-22 show results of the PCE degradation experiments conducted with 10% cement extract from four different cement manufacturers (Txi, Quikrete, Lehigh, Capitol). The first- and second-order rate constants were obtained by nonlinear regressions using Matlab. PCE degradation experiments were conducted at an average pH of 11.6 with variation of ± 0.05 for experiments with extracts made from Txi (TPCXFe), Lehigh (LPCXFe) and Quikrete (QPCXFe) cements. Although the same concentration of Ca(OH)_2 (1.25 M) was used in all experiments, pH values in experiments with TPCXFe, LPCXFe, and QPCXFe were lower than those with CPCXFe. This might result from lower initial pH of the cement extracts after acid digestion. The pH of CPCX was about 4 and others were about 3, even though the same HCl concentration (2.2 N) was used to dissolve the four different cements.

The first kinetic model fitted well to TPCXFe (exp. 148) and the second order kinetic model fitted well to QPCXFe (exp. 149) and LPCXFe (exp. 150). The pseudo first-order rate constant normalized by Fe(II) for TPCXFe was one order of magnitude lower than that for CPCXFe. About 50% of PCE was removed within 7 days and 95% was removed at the last sampling time (37 days). TPCXFe showed a $k_{\text{Fe(II)}}$ that was about 40% lower than that for TPCXFe. This contrasts with CPXFe, which had a $k_{\text{Fe(II)}}$ that was one order of magnitude higher than that for CPCXFe.

Results from experiments with QPCXFe and LPCXFe can be compared to those from experiments with CPCXFe by calculating an approximate first-order rate constant

by multiplying the second order rate constant by the average concentration observed during the experiment, i.e., the approximate first order rate constant = the second order rate constant \times average concentration ($k_1 = k_2 \times C_{\text{avg}}$). Calculated first order rate constants normalized by Fe(II) concentration ($k_{\text{Fe(II)}}$) for QPCXFe and LPCXFe were $2.3 \times 10^{-3} \text{ (mMFe(II) \times day)}^{-1}$ and $4.8 \times 10^{-3} \text{ (mMFe(II) \times day)}^{-1}$, respectively. These are one order of magnitude lower than $k_{\text{Fe(II)}}$ of CPCXFe, which was $1.1 \times 10^{-2} \text{ (mMFe(II) \times day)}^{-1}$. The experiments with QPCXFe and LPCXFe showed lower solid activities than CPCX, when measured as the time required for removal of specific percentages of the initial PCE. About 50% of initial PCE was removed by QPCXFe within 9 days and approximately 92% of PCE was removed after 37 days, which was the last sampling time. Experiments with LPCXFe showed 50% removal of PCE within 3 days, which is a similar half-life as that observed for CPCXFe. The PCE degradation rate slowed after that and it took 37 days to remove 93% of the initial PCE. This compares to reaching 98% PCE removal in 21 days with CPCXFe. Moreover, TCE was consistently detected in the range of 5 to 10% of PCE concentration in the control for QPCXFe. After 20 days, TCE concentration increased to 15% and was steady until the last sampling time. TCE was also detected in LPCXFe after one day and reached at maximum of 14% of the PCE concentration in the control after 7 days. TCE was not detected after 10 days.

Although the second-order kinetic model gave a little bit better fit to QPCXFe than the first-order kinetic model, it did not fit data points well. It underestimates in the middle of three data points and overestimates the last four data points, although it estimates well the first three data points. Data from experiments with QPCXFe and

QPCXFe did not fit well to any kinetic model. Solids from the experiment with QPCXFe showed the one order of magnitude lower solid activity than those from experiments with QPCSF_e. The second order kinetic model fitted well to data from experiments with LPCXFe, while the first-order kinetic model provided a better fit to data from experiments with LPCSF_e.

Different PCE degradation behavior was observed in experiments with cement extract and cement slurry even though they used the same brand of cement. The fact that TPCXFe, LPCXFe, and QPCXFe had lower solid activities than CPCXFe might be caused by either formation of lower amounts of the active solids or similar amounts that have lower activity, due to larger particle size or different chemical composition. After centrifugation of the mixture of PCX and Fe(II), the concentration of Fe(II) recovered in the blue solids at the top of the pellet was about 30 mM and concentration of solids was about 45 g/L. The concentration of Fe(II) recovered from CPCXFe solids was 20 mM and concentration of solids was 31 g/L. The ratio of Fe(II) to solids was about 0.67 for TPCXFe, LPCXFe, and QPCXFe and about 0.97 with CPCXFe. This supports the observation that less active solids were formed in TPCXFe, LPCXFe, and QPCXFe because they contained less Fe(II). It might also indicate that formation of active solids was very sensitive to pH, because pH values of experiments with those three PCXs were 0.2 lower than pH of CPCX. Another possible reason might be the different Fe(II) to Fe(III) ratio in the solids. The Fe(II) to Fe(III) ratio in CPCXFe solid suspensions was 3, 12 in TPCXFe, and 19 in QPCXFe and LPCXFe. The high degree of Fe(II) oxidation to Fe(III) might produce more active solids. Another possible reason might be the

formation of different kinds of active solid phases. They might have slightly different chemical compositions so that they might not produce the same solids

Formation of TCE indicates that PCX solids might follow a hydrogenolysis pathway for PCE degradation such as observed for experiments with cement slurries. PCE degradation rates of PCX solids were slower than observed for experiments with PCS solids.

TABLE 4-14 The Fe(II) concentration normalized first and second order rate constants for PCE degradation in various Fe(II) containing 10% cement extracts

Exp	10% cement slurry	pH	$k_{1\text{Fe(II)}}^a$	SS_1^b	$k_{2\text{Fe(II)}}^c$	SS_2^d
148	TPCXFe ^e	11.6	2.9E-03 (±16%)	7.6E-04	2.7E-02 (±22%)	2.4E-03
149	QPCXFe ^f	11.6	2.2E-03 (±21%)	1.5E-03	2.0E-02 (±26%)	1.3E-03
150	LPCXFe ^g	11.6	5.1E-03 (±38%)	3.3E-03	6.3E-02 (±14%)	3.3E-04
45	CPCXFe ^h	11.8	1.1E-02 (±4.9%)			

^a k_1 was the Fe(II) concentration normalized first order rate constant; Unit = (mM Fe(II)×day)⁻¹

^b SS_1 was the sum of square of the first order rate model

^c k_2 was the Fe(II) concentration normalized second order rate constant; Unit = (mM Fe(II) ×mM PCE ×day)⁻¹

^d SS_2 was the sum of squares of the second order rate model

^eTPCXFe stands for Fe(II)-containing 10% Txi cement extract

^fQPCXFe stands for Fe(II)-containing 10% Quikrete cement extract

^gLPCXFe stands for Fe(II)-containing 10% Lehigh cement extract

^hCPCXFe stands for Fe(II)-containing 10% Capitol cement extract; The Fe(II) concentration normalized first order rate constant was referenced from Ko(127)

Uncertainties represent 95% confidence limits expressed in % relative to estimate k
Initial PCE concentration was 0.242 mM

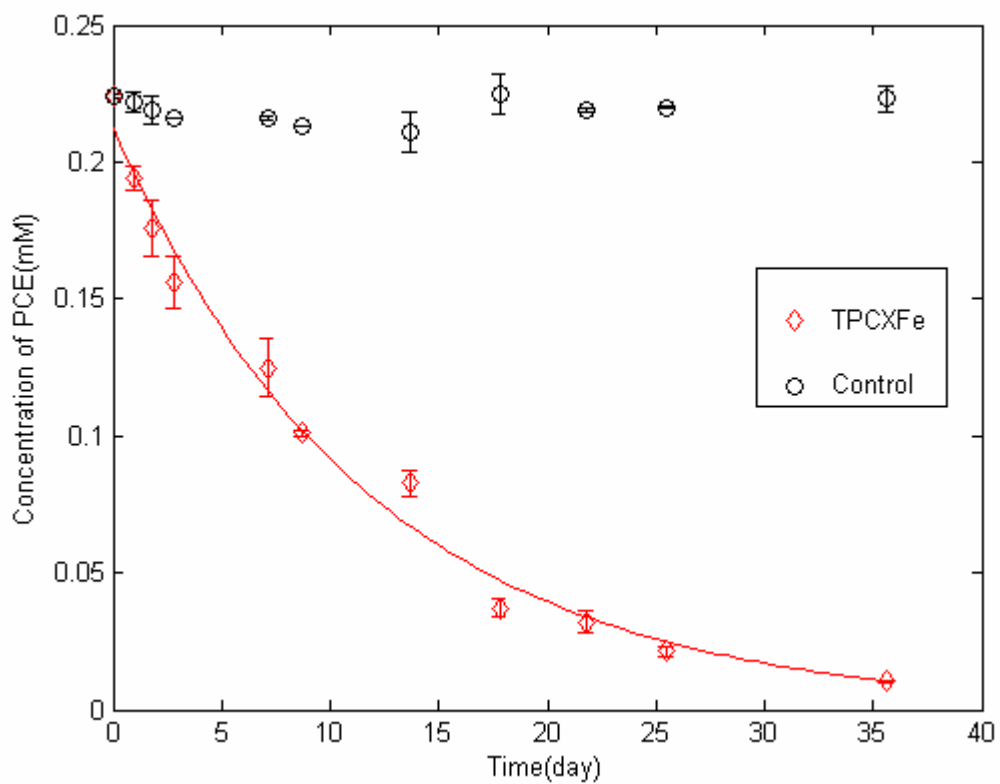


FIGURE 4-21 Kinetics of PCE reduction by extracts prepared with Fe(II) and 10% Txi cement, TPCXFe. $[PCE]_0 = 0.242$ mM. The solid line represented the first order kinetic model fit.

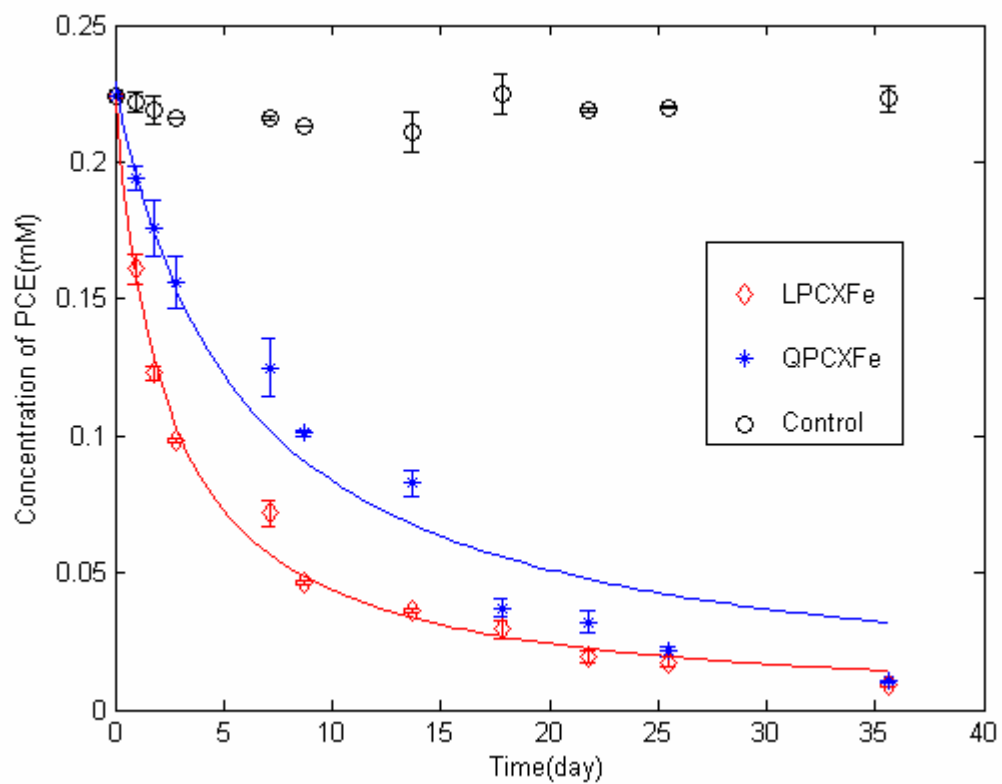


FIGURE 4-22 Kinetics of PCE reduction by extracts prepared with Fe(II) and 10% Lehigh and Quikrete cement, LPCXFe and QPCXFe, respectively. $[PCE]_0 = 0.242$ mM. The solid lines represented the second order kinetic model fit.

4.3.2 Instrumental analyses: XRD, SEM and EDS

4.3.2.1 10% cement slurry solids

Figure 4-23 shows the x-ray diffractograms for TPCSF_e, QPCSF_e, LPCSF_e and Table 4-15 presents a comparison of d-spacings for them with CPCS and CPCSF_e. Peaks at 9.50 Å, 5.54 Å and 2.75 Å in TPCSF_e solids represent Ettringite. Peaks at 7.7 Å and 3.78 Å represent Friedel's salt. The peak at 3.85 Å might come from either Ettringite or Friedel's salt. Peaks at 3.03 Å, 3.20 Å, and 2.87 Å represent calcium aluminum silicate hydrate. Other minor peaks could be considered as either Friedel's salt or calcium aluminum silicate hydrates. The presence of Ettringite in TPCSF_e was different from CPCSF_e where Ettringite was not observed.

LPCSF_e, QPCSF_e and CPCSF_e had similar XRD patterns. Friedel's salts were the most positively identified in QPCSF_e, with peaks at 8.01 Å, 3.95 Å, and 3.84 Å and in LPCSF_e with peaks at 8.02 Å, 3.97 Å, and 3.86 Å. Calcium aluminum silicate hydrates were identified with peaks at 3.07 Å in QPCSF_e and LPCSF_e. Peaks at 4.35 Å in both solids also could represent calcium aluminum silicate hydrates. Ettringite peaks were not observed in either solid. Peaks from Friedel's salt in QPCSF_e showed a higher intensity than in LPCSF_e, maybe because they were more highly crystalline. Peaks at 2.34 and 2.31 Å would be Friedel's salts. They were recognized as high intensity peaks in reference solids (7th and 8th), but they showed higher intensity in LPCSF_e and QPCSF_e than peaks at 3.96 and 3.85 Å, which were the second, and third high intense ones in reference solids.

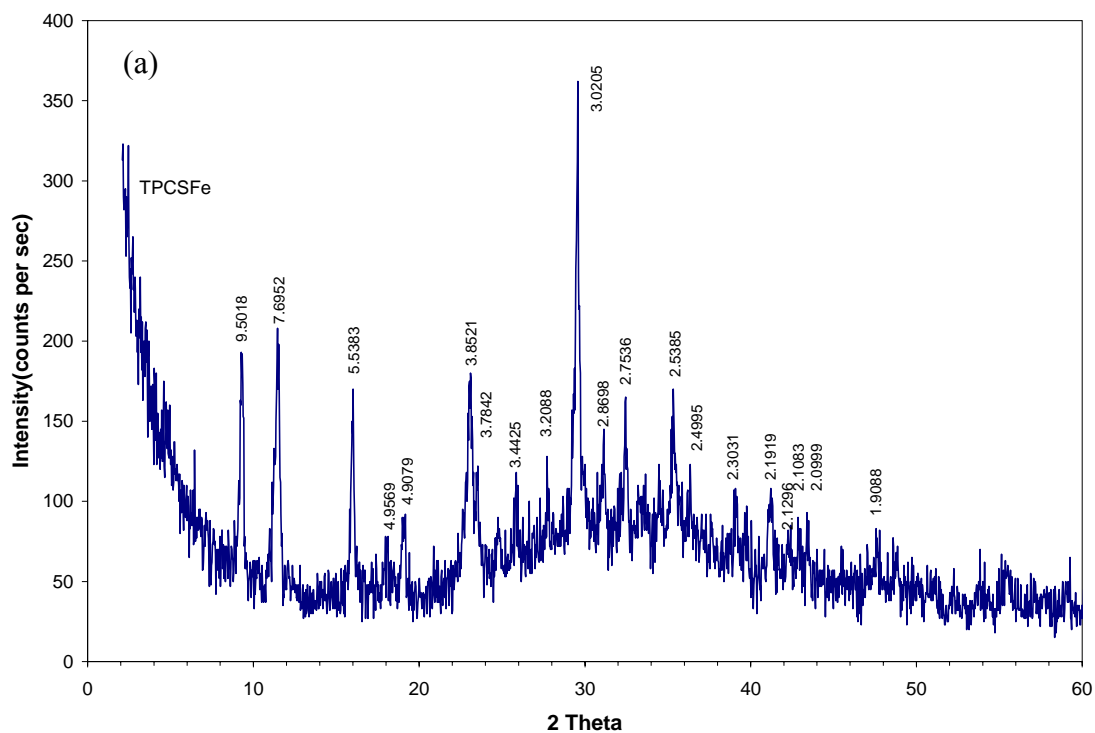


FIGURE 4-23 XRD patterns of solids prepared with Fe(II) and 10% Portland cement.

The unit of d-spacing is Å. (a) solids prepared with Fe(II) and 10% Txi Portland cement (TPCSFe); (b) solids prepared with Fe(II) and 10% Quikrete Portland cement (QPCSF_e); (c) solids prepared with Fe(II) and 10% Lehigh Portland cement (LPCSF_e).

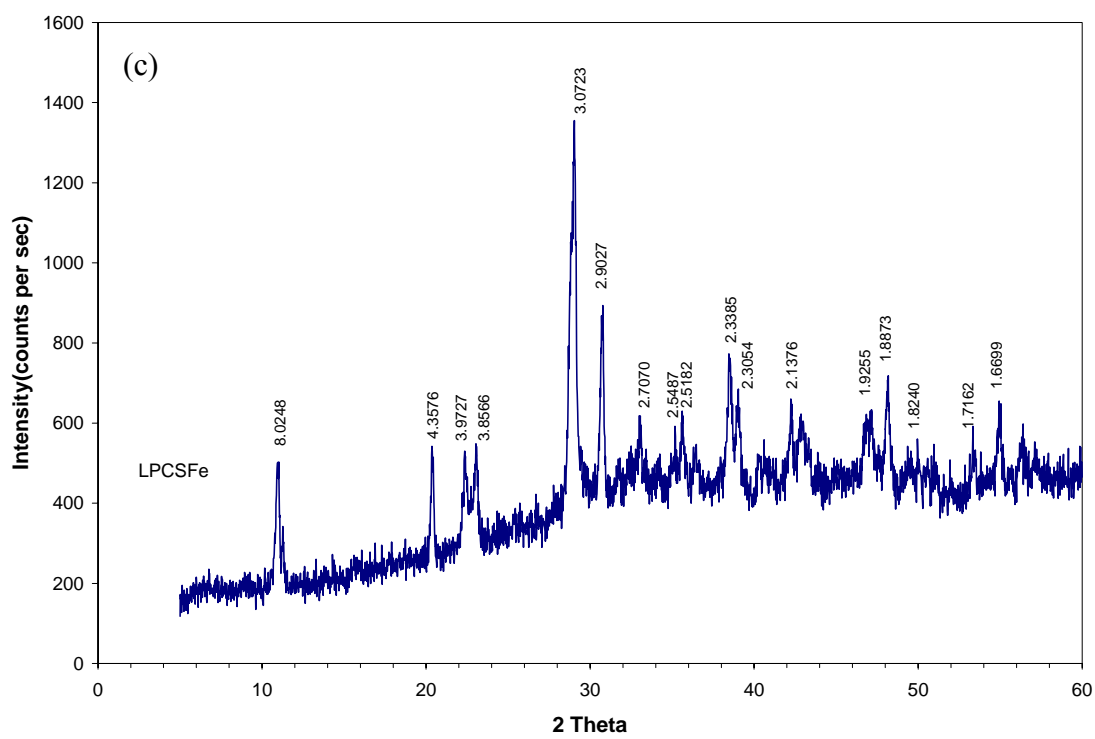
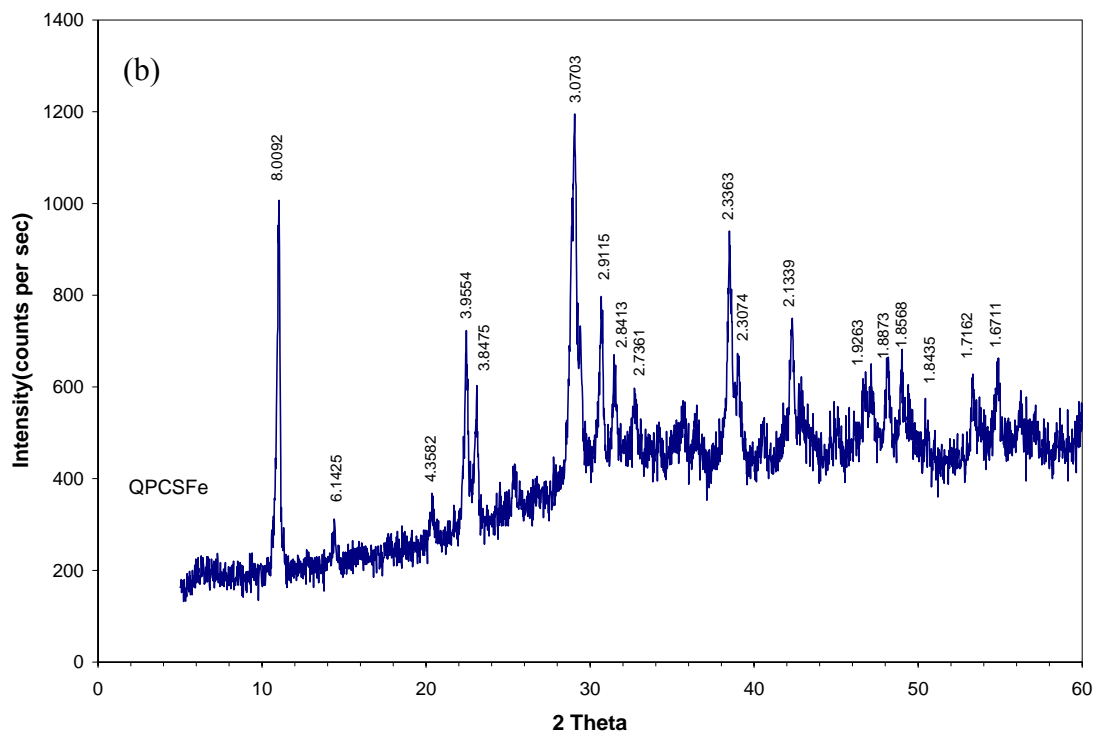


FIGURE 4-23 Continued

TABLE 4-15 The comparison of d-spacing values of 10% cement slurry solids, unit = Å

Highest intensity	CPCS	CPCSF _e	TPCSF _e	QPCSF _e	LPCSF _e
1 st	7.78 ^a	7.80 ^a	3.02 ^c	8.01 ^a	3.07 ^c
2 nd	3.03 ^c	2.89 ^c	9.50 ^b	3.07 ^c	2.90 ^c
3 rd	9.63 ^b	2.32	7.70 ^a	2.34	8.02 ^a
4 th	2.56	3.07 ^c	5.54 ^b	3.96 ^a	2.34
5 th	2.20	3.90 ^a	3.85 ^{a,b}	2.91 ^c	4.36
6 th	3.90 ^a	3.80 ^a	3.78 ^a	3.85 ^a	1.89
7 th	2.54	2.12	2.54	2.13	3.86 ^a
8 th	3.86 ^{a,b}	1.88	2.75	2.31	2.31
9 th	2.31	1.93	2.87 ^c	2.84	3.97 ^a
10 th	2.12	2.81	3.21	1.86	1.67

^aThe first three most intense peaks of Friedel's salts

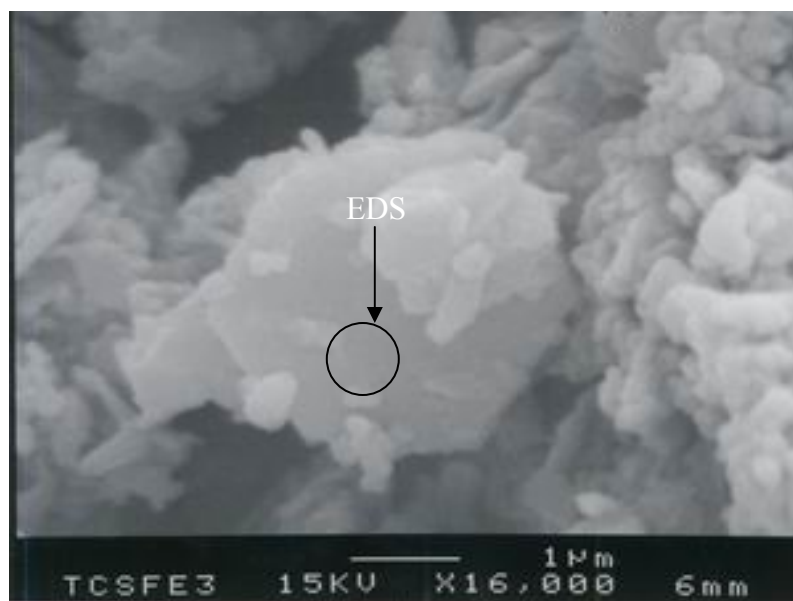
^bThe first three most intense peaks of Ettringite

^cThe first three most intense peaks of calcium aluminum silicate hydrates

The different degree of crystallization and different amounts of solids might cause intensities to differ from standards and from one another. However, four Fe(II) containing cement slurry solids had very similar XRD patterns. Friedel's salts and calcium aluminum silicate hydrates were identified in all four solids. Ettringite was only identified in TPCSF_e. d-spacing values and the order of high intensity peaks were a little bit different from reference solids. This might be caused by different chemical compositions of reference solids compared to solids formed in cement slurries with Fe(II).

Figures 4-24 to 4-26 show the SEM images and EDS spectra of TPCSF_e, QPCSF_e, and LPCSF_e solids. EDS spectra of three PCSF_e solids were taken from a certain region within single hexagonal particle. Hexagonal thin plates were the dominant solid phases in mixtures containing Fe(II). Hexagonal shapes were the most clearly observed in QPCSF_e. Particle sizes of three sets of solids were around 3 to 7 μm, which were similar to those for CPCSF_e solids. EDS spectra showed that the same elements as CPCSF_e (Ca, Cl, Al, Si, and Fe) are present in all three solids. Small amounts of Mg were detected in LPCSF_e solids.

Apparently, the results of XRD, SEM images and EDS spectra showed that Fe(II) containing cement slurry solids from four different cement had the same element presence, similar particle sizes, and similar kinds of solid phases. These instrumental analyses results supported the hypothesis that solids formed in Portland cement system are similar as long as they are formed from the same types of ordinary Portland cement. However, the results of PCE degradation kinetic experiment showed variations among the four different Fe(II)-containing cement slurry solids. One possible reason might be different chemical composition, for instance, the ratio of Fe(II) to Fe(III) might be different among the different Fe(II)-containing cement slurry solids. A quantitative elemental analysis was not conducted so that this hypothesis could not be thoroughly investigated.



Txi Cement Slurry with Fe(II):TCSFE3

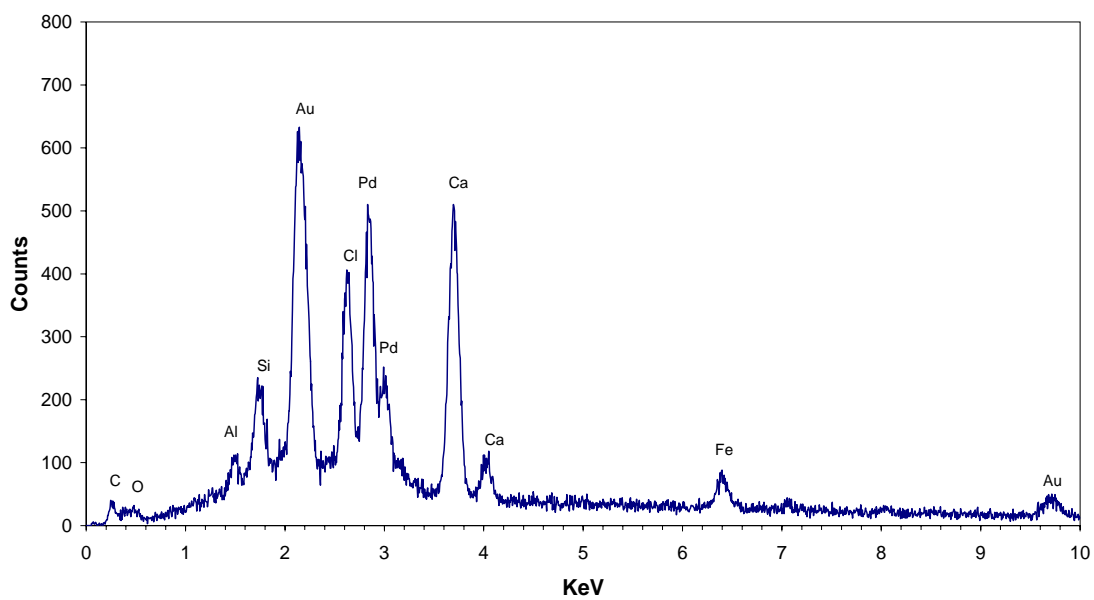
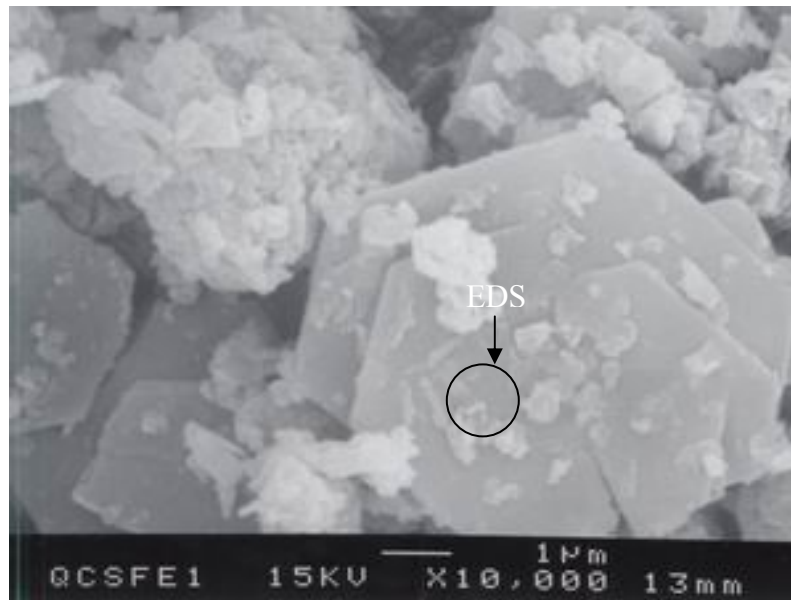


FIGURE 4-24 SEM image and EDS of solids prepared with Fe(II) and 10% Txi cement.



Quikrete Cement Slurry with Fe(II):QCSFE1

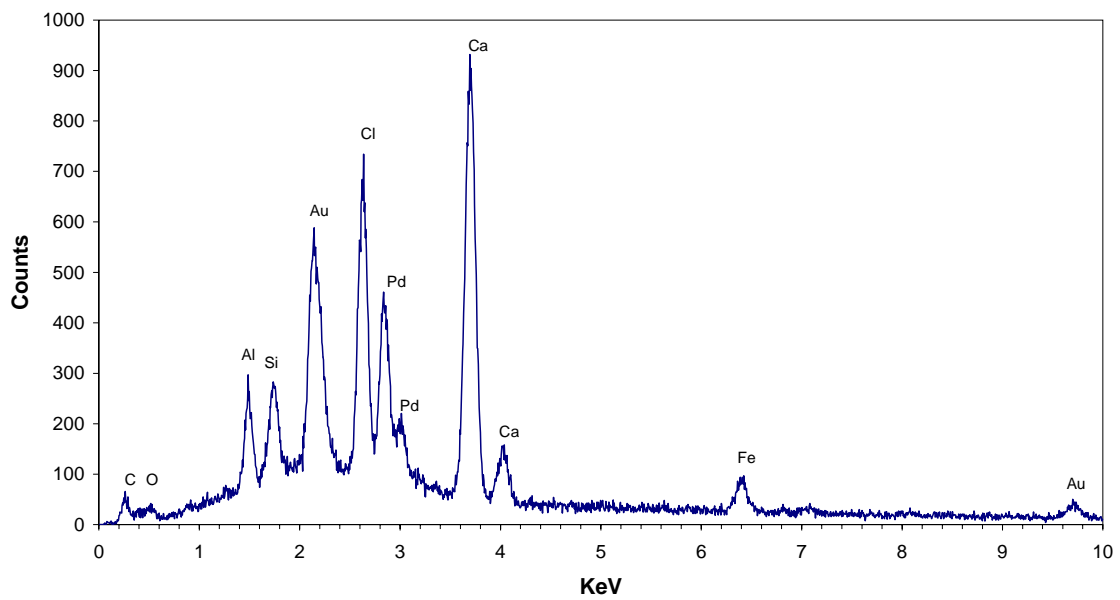


FIGURE 4-25 SEM image and EDS of solids prepared with Fe(II) and 10% Quikrete cement.



Lehigh Cement Slurry with Fe(II):LCSFE2

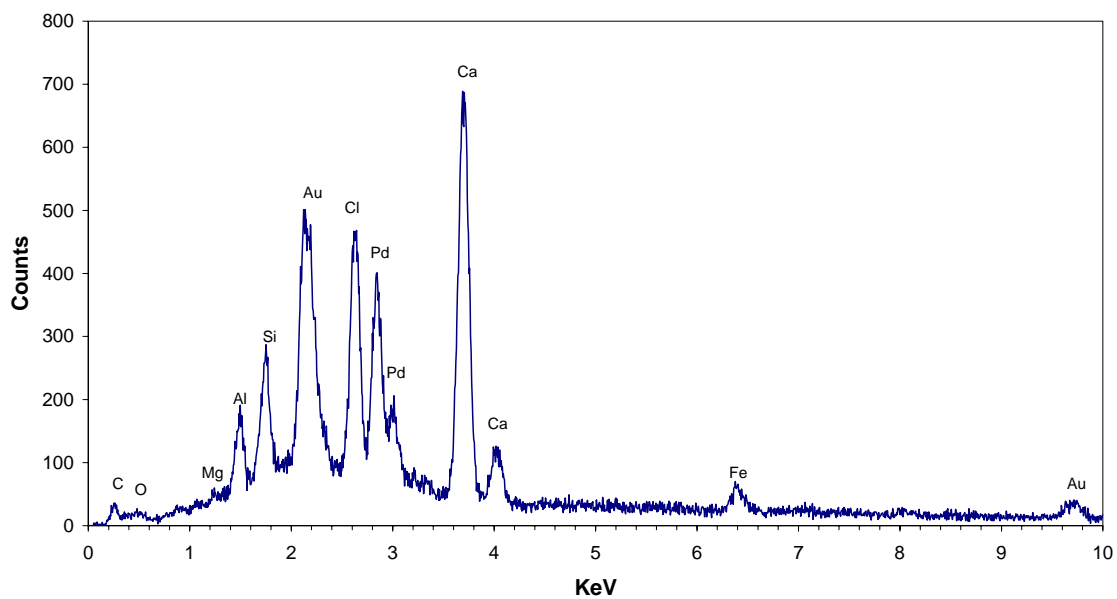


FIGURE 4-26 SEM image and EDS of solids prepared with Fe(II) and 10% Lehigh cement.

4.3.2.2 10% cement extract solids

Figures 4-27 and 4-28 and Tables 4-16 and 4-17 show the XRD patterns of solids prepared with three 10% Portland cement extract solids with and without Fe(II). Extracts were prepared using Portland cements from Txi (TPCX, TPCXFe), Quikrete (QPCX, QPCXFe), and Lehigh (LPCX, LPCXFe). Solids in these slurries contained the same solid phases, because their d-spacing values and intensities were very similar with one another.

The solid phases identified in 10% Portland cement extract solids were the same: Portlandite, calcium aluminum hydroxide hydrate, and calcium aluminum silicate hydrate. Friedel's salts were not identified in PCX solids without Fe(II) addition. Peak no.1 in TPCX, QPCX, and LPCX had a d-spacing of 8.1 Å and it was the most intense peak. On the other hand, a peak at the number 1 position in CPCX had a d-spacing 0.4 Å larger and an intensity that was not as high as those in TPCX, QPCX, and LPCX. Peaks from Portlandite showed the highest intensity in CPCX and peaks from calcium aluminum hydroxide hydrates showed a higher intensity than the other three.

The same kinds of solid phases were identified in Fe(II)-containing 10% Portland cement extract solids: Portlandite, Friedel's salt, calcium aluminum silicate hydrate and calcium aluminum hydroxide hydrate. Significant amounts of Portlandite were detected due to pH adjustment of PCXFe solids. Like CPCXFe, peaks from Friedel's salts in three PCXFe solids were clearly observed with peaks at 3.9 and 3.8 Å. Addition of Fe(II) might facilitate the formation of Friedel's salts. Several peaks from Friedel's salt and calcium aluminum hydroxide hydrate were very close to each other

due to their similar crystal structures. Thus, it was difficult to say whether Fe(II) was associated with Friedel's salt alone or with both solids, based on the sole observation of the appearance of Friedel's salt in PCXFe solids based on XRD analysis.

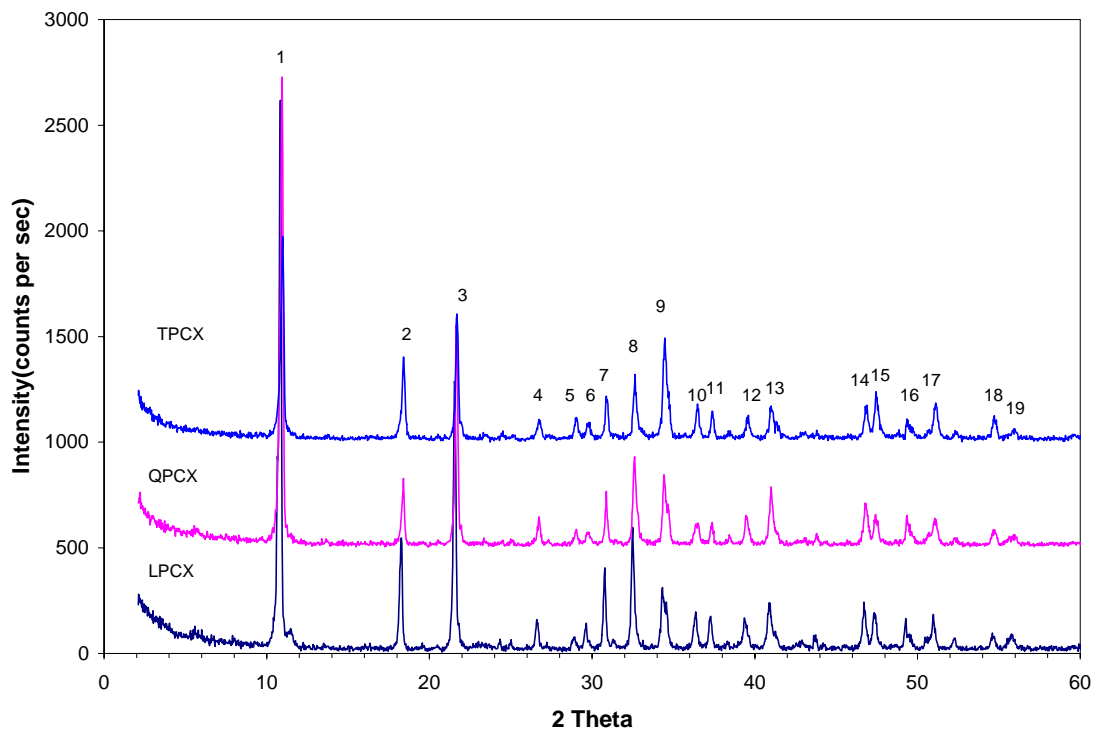


FIGURE 4-27 X-ray diffractograms of solids prepared with 10% Portland cement extracts without Fe(II). Extracts were made from cements prepared by Txi (TPCX), Quikrete (QPCX), and Lehigh (LPCX).

TABLE 4-16 Corresponding d-spacing values of peaks in Figure 4-27 and comparison to CPCX, unit = Å

Peak no	LPCX	QPCX	TPCX	CPCX	Possible solid
1	8.1626	8.0900	8.0734	8.5180	CAH ^a
2	4.8598	4.8205	4.8205	5.0067	P ^b
3	4.1222	4.0996	4.0940	4.2186	CAH
4	3.3472	3.3324	3.3251	3.4139	P
				3.1997	CASH ^c
				3.1443	P, CASH
5		3.0755	3.0755	3.0662	CASH
6	3.0175	3.0026	2.9997		CASH
				2.9530	
7	2.9053	2.8943	2.8915	2.8955	CASH
8	2.7536	2.7462	2.7437	2.7962	P
9	2.6108	2.6042	2.6020	2.6483	P
10	2.4709	2.4571	2.4630	2.5075	CAH
11	2.4113	2.4057	2.4038	2.4442	CAH
				2.3650	
12	2.2857	2.2807	2.2757	2.3099	CAH
13	2.2052	2.1990	2.1990	2.2317	CAH
14	1.9431	1.9384	1.9384	1.9396	CAH
15	1.9176	1.9141	1.9130		P
16	1.8483	1.8452	1.8441	1.8653	CAH, CASH
17	1.7902	1.7863	1.7853	1.8051	P
18	1.6786	1.6769	1.6752	1.6933	P
19	1.6462			1.6598	

^aCAH = calcium aluminum hydroxide hydrate

^bP = Portlandite

^cCASH = calcium aluminum silicate hydrate

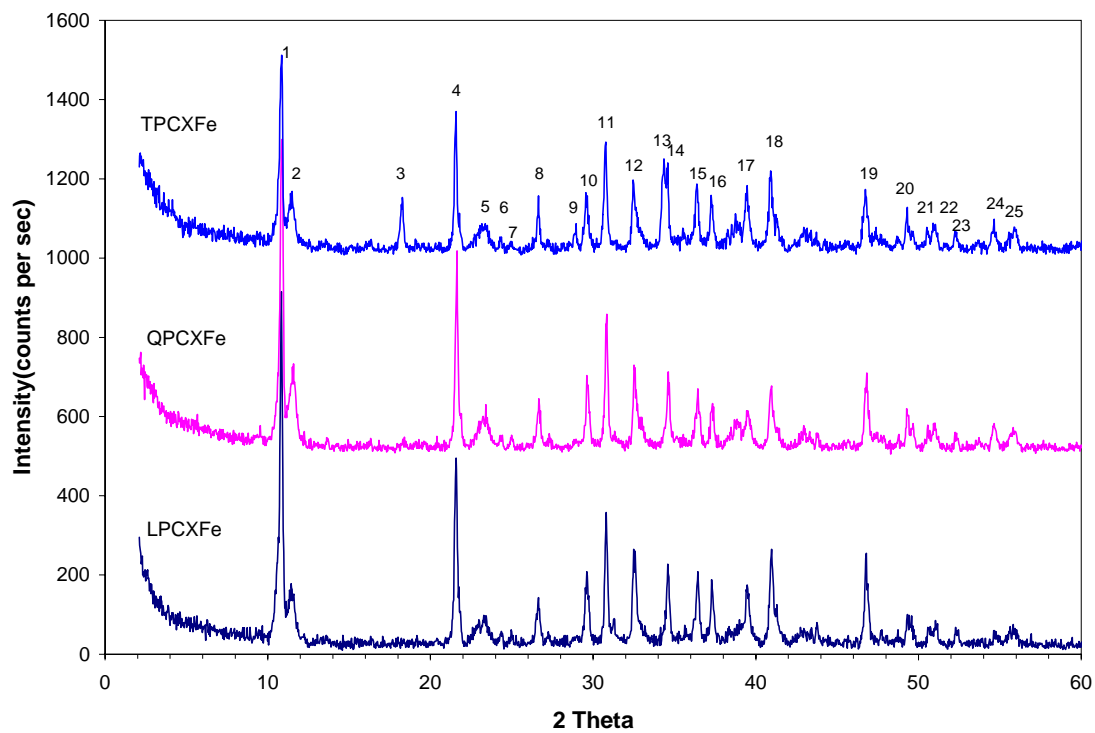


FIGURE 4-28 X-ray diffractogram of solids prepared with Fe(II) and 10% Portland cement extracts prepared from cements made by Txi (TPCXFe), Quikrete (QPCXFe), and Lehigh (LPCXFe).

TABLE 4-17 Corresponding d-spacing values of peaks in Figure 4-28 and comparison to those in CPCXFe, unit = Å

Peak no.	LPCXFe	QPCXFe	TPCXFe	CPCXFe	Possible solid
1	8.1626	8.1402	8.1852		CAH ^a
2	7.7557	7.6356	7.7557	7.8653	FS ^b
3			4.8598	4.9567	P ^c
4	4.1222	4.1109	4.1222		CAH
5	4.0662	4.0552	4.0772		CAH
6	3.8920	3.8325	3.8423	3.9047	FS
7	3.8082	3.7938	3.7986	3.8179	FS
8	3.3435	3.3398	3.3435	3.3358	P
9			3.0880	3.1534	P
10	3.0115	3.0115	3.0175		CASH ^d
11	2.9025	2.8998	2.9053	2.9187	CASH
12	2.7511	2.7511	2.7560	2.7662	CASH
13			2.6130	2.6226	P
14	2.5911	2.5885	2.5932		
15	2.4656	2.4617	2.4676	2.4781	CAH
16	2.4082	2.4082	2.4100	2.3481	FS, CAH
17	2.2812	2.2796	2.2829		FS
18	2.2011	2.2042	2.2042		FS, CAH
19	1.9411	1.9411	1.9423	1.9256	P
20	1.8466	1.8466	1.8476		CAH, CASH
21	1.8005	1.8035	1.8045		CAH
22	1.7867	1.7896	1.7906	1.7925	P
23	1.7484	1.7468	1.7484		FS
24	1.6772	1.6781	1.6789		FS, CAH
25	1.6448	1.6416	1.6432		FS

^aCAH = calcium aluminum hydroxide hydrate

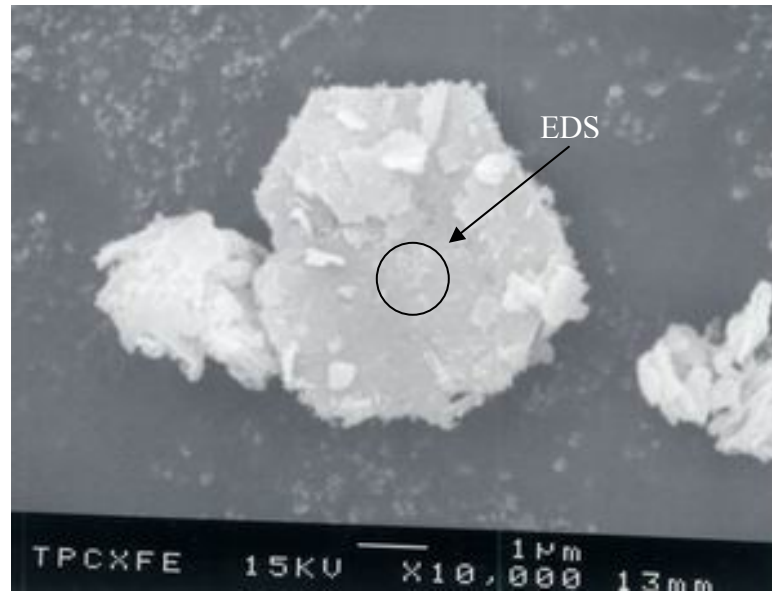
^bFS = Friedel's salt

^cP = Portlandite

^dCASH = calcium aluminum silicate hydrate

Figures 4-29 through 4-33 show SEM images and EDS spectra for TPCXFe, QPCXFe, and LPCXFe solids. EDS spectra of three PCXFe solids were taken from a certain region within a single hexagonal particle. Solids with hexagonal shapes were observed in all three Fe(II)-containing 10% cement extract solids, like CPCXFe. Although individual particle shape was not clearly observed in QPCXFe and LPCXFe, particle sizes of QPCXFe and LPCXFe solids were around 0.5 to 1 μm and TPCXFe solids were around 5 μm . Aggregated small hexagonal particles were observed next to a large hexagonal particle in Figure 4-29. The size of small particles was much smaller than in PCSFe solids (3 to 7 μm) and it was similar to sizes observed in PCXFe solids (0.3 to 1 μm).

EDS spectra results showed that the major elements in Fe(II)-containing cement extract solids were Ca, Cl, Al, and Fe. Low amounts of Si and Mg were also detected. High amounts of Cl in all solids came from a high concentration of HCl used to digest the cement to produce the extract. The particle shown in Figure 4-29 was probably Portlandite based on EDS spectra and a bigger particle size. In general, the particle size of Friedel's salts was around 2 to 3 μm and the size of tetra-calcium aluminum hydrates was around 1 μm or less than 1 μm . Portlandite was a bigger particle, with sizes up to 100 μm (42, 65). Calcium aluminum hydroxide hydrates probably were shown as aggregates of smaller particles. Based on the particle size comparison, the major solid phases in TPCXFe, QPCXFe, and LPCXFe were calcium aluminum hydroxide hydrates rather than Friedel's salt, which was the dominant solid, phase in CPCXFe.



Txi Cement Extract with Fe(II):TPCXFE

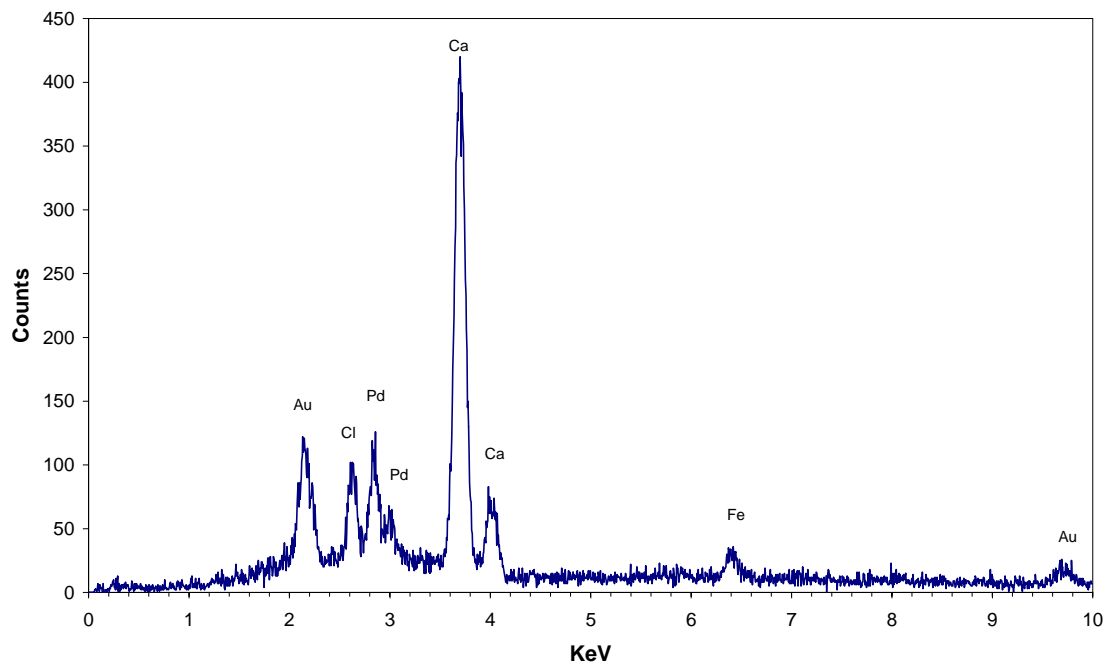


FIGURE 4-29 SEM image and EDS of solids prepared with Fe(II) and 10% Txi cement extract.



Quikrete Cement Extract with Fe(II):QCXFE2

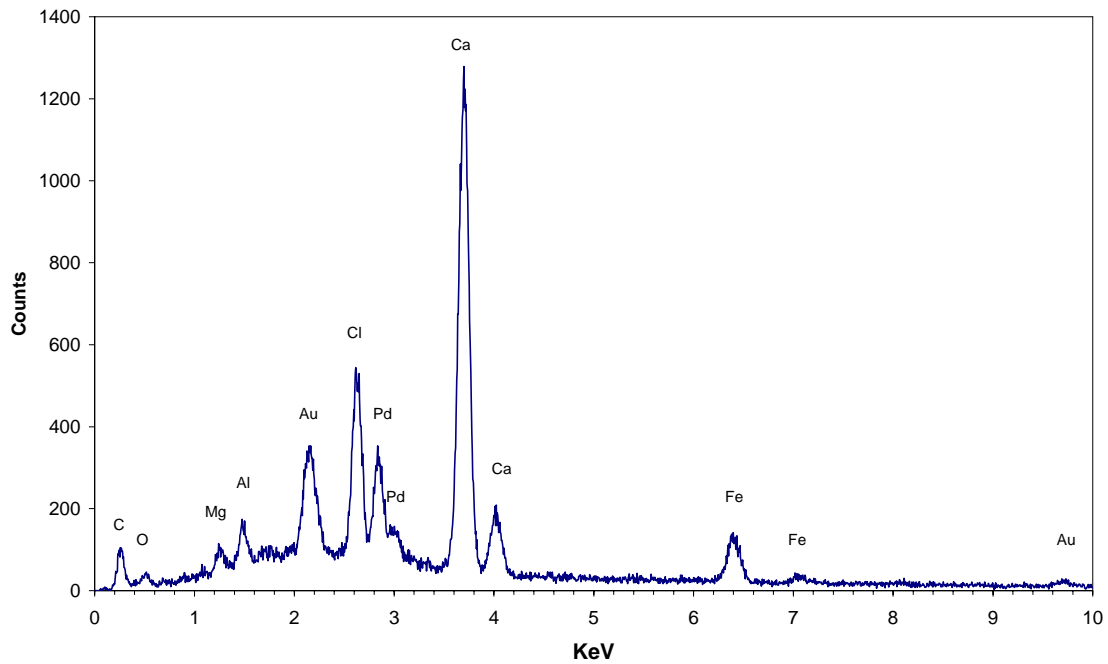


FIGURE 4-30 The first SEM image and EDS of solids prepared with Fe(II) and 10% Quikrete cement extract.



Quikrete Cement Extract with Fe(II):QCXFE

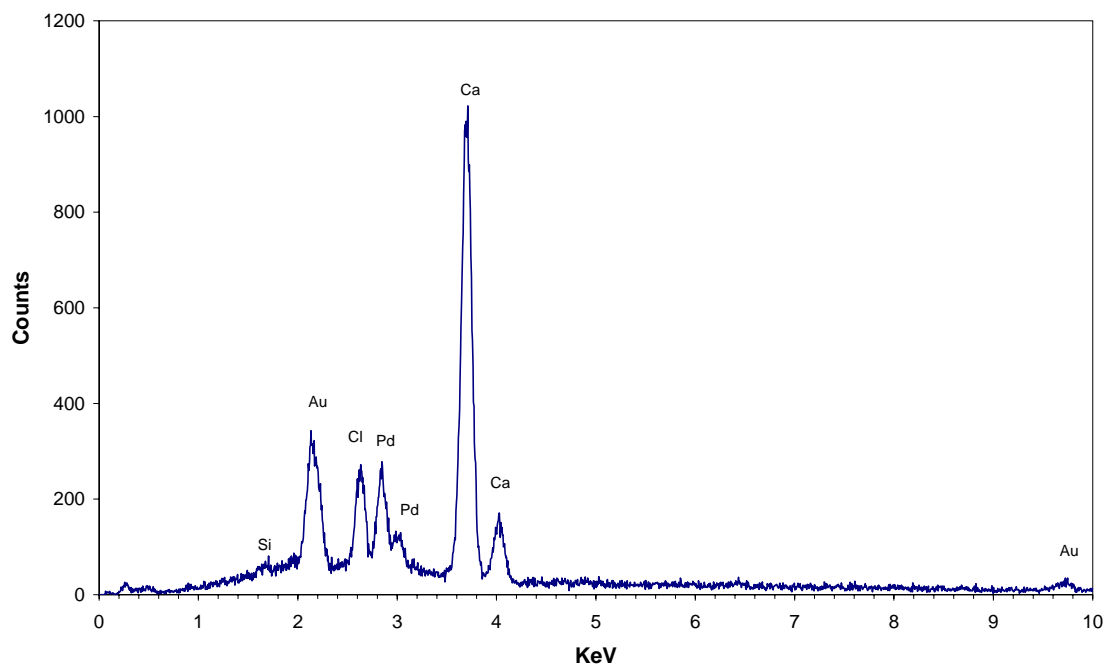


FIGURE 4-31 The second SEM image and EDS of solids prepared with Fe(II) and 10% Quikrete cement extract.



Lehigh Cement Extract with Fe(II):LCXFE2

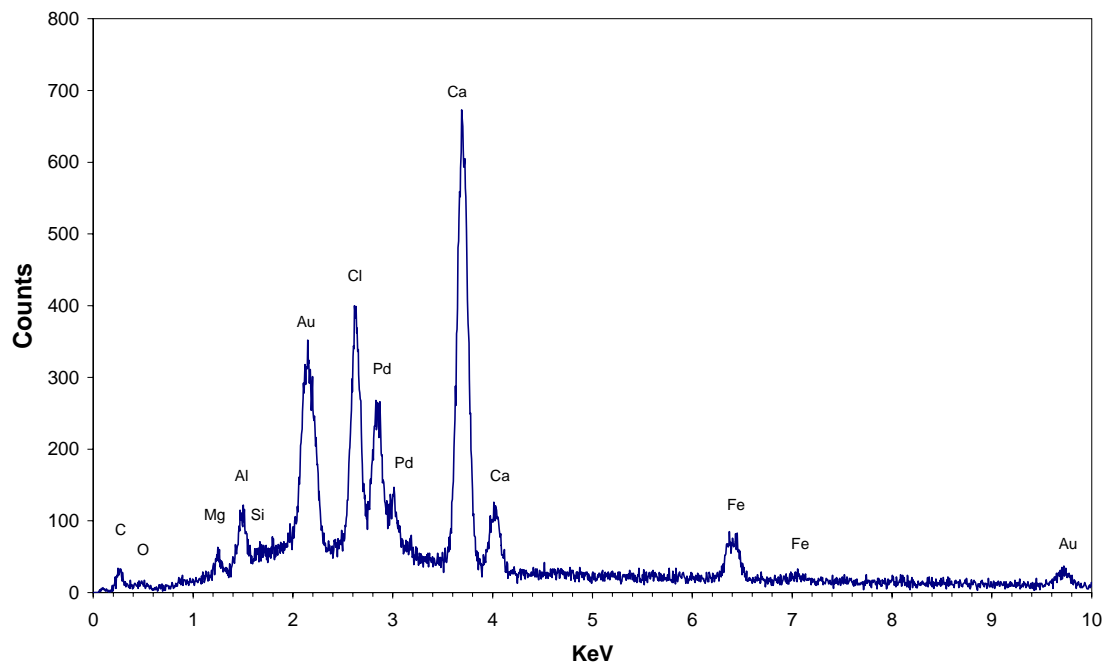


FIGURE 4-32 The first SEM image and EDS of solids prepared with Fe(II) and 10% Lehigh cement extract.



Lehigh Cement Extract with Fe(II):LCXFE3

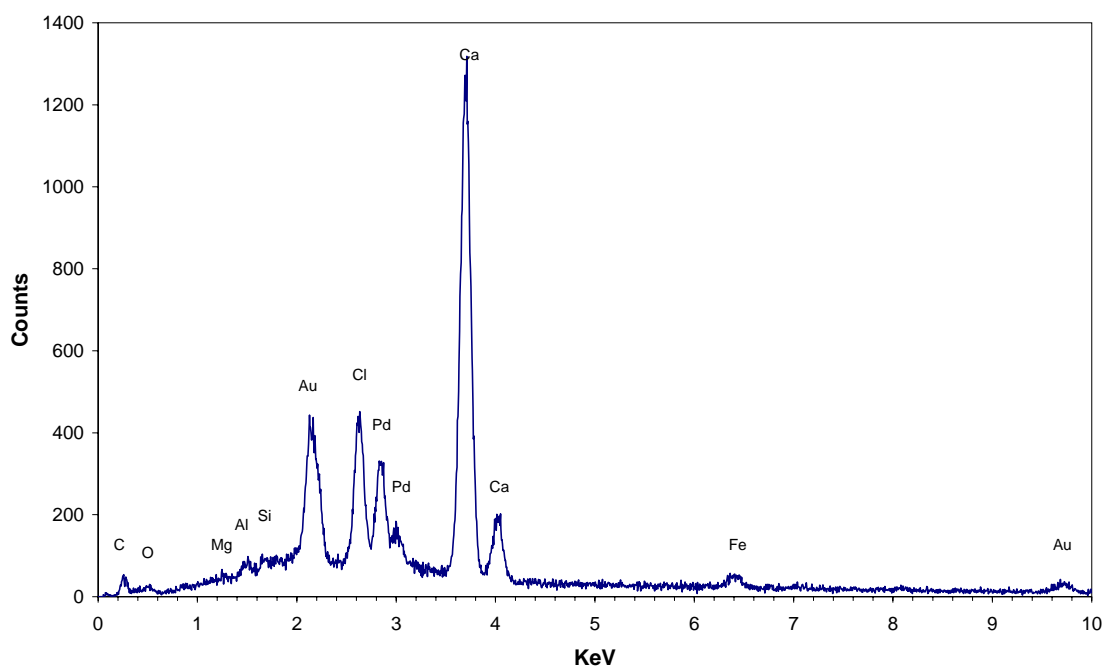


FIGURE 4-33 The second SEM image and EDS of solids prepared with Fe(II) and 10% Lehigh cement extract.

Interestingly, a much smaller amount of Fe was found in EDS spectra for solids prepared from Lehigh extract (Figure 4-33) and no Fe was detected for solids prepared from Quikrete extracts (Figure 4-31), where hexagonal shape particles were not observed. These pictures probably showed type II calcium silicate hydrate (C-S-H) (41). Figure 4-31 and 4-33 supported the supposition that Fe is preferably associated with hexagonal particles. Although it could not be known if Fe was adsorbed or substituted, it was clearly shown that hexagonal solids are associated with Fe.

CHAPTER V

SUMMARY AND CONCLUSION

Fe(II)-based degradative solidification/stabilization (Fe(II)-DS/S) technology has been developed as a modification of conventional S/S treatment. While inorganic contaminants are contained, organic contaminants, such as chlorinated aliphatic compounds, are degraded by Fe(II)-DS/S. The goal of this research was to identify the active agents for PCE degradation during Fe(II)-DS/S and to determine the conditions that promote the formation of this active agents.

Experiments designed to identify the preferable conditions for the formation of active agents showed that the most essential elements in active agents were Fe(II), Fe(III), and Cl. Pseudo first-order rate constants normalized by Fe(II) ($k_{\text{Fe(II)}}$) and solid concentrations (k_{solid}) for solids synthesized with a mixture of Fe(II), Fe(III), and Cl (identified as Fe(II)(III)Cl) were $1.3 \times 10^{-3} \text{ (mM Fe(II) \cdot day)}^{-1}$ and $3.8 \times 10^{-3} \text{ L \cdot (day \cdot g of solid)}^{-1}$, respectively. The value of $k_{\text{Fe(II)}}$ for solids produced with full cement extract elements (FSCX) was the same order of magnitude, ($6.1 \times 10^{-3} \text{ (mM Fe(II) \cdot day)}^{-1}$) as that for Fe(II)(II)Cl. The value of k_{solid} was one order magnitude lower ($9.7 \times 10^{-4} \text{ L \cdot (day \cdot g of solid)}^{-1}$) than that for Fe(II)(III)Cl. The lower value of k_{solid} for FSCX might be caused by higher amounts NaOH added to increase pH. Solids formed in synthetic cement extract had one order magnitude less activity in terms of $k_{\text{Fe(II)}}$ than solids formed in Fe(II) containing Portland cement extract (Fe(II)-PCX) solids. Solids produced in the mixture of Fe(II) and/or Fe(III) and cement hydration products; especially AFm phases,

such as Friedel's salts, monosulfates, and tetracalcium aluminates; also showed about one to two orders of magnitude lower $k_{\text{Fe(II)}}$ values than Fe(II)-PCX.

Although Fe(II)-PCX solids might be a mixture of active and inactive solids, they had higher activity than FSCX and Fe(II)-cement hydration product solids that should have been more pure than Fe(II)-PCX solids. Those experiments showed that the conditions of the mixture of Fe(II) and either FSCX or cement hydration product might not produce the same active agents as Fe(II)-PCX solids for PCE degradation. XRD analyses of Fe(II)-PCS and Fe(II)-PCX solids showed that Fe(II) facilitated the formation of Friedel's salts in those system. The effect of Friedel's salt on PCE degradation was evaluated in experiments where Fe(II) was mixed with Friedel's salt that had been formed in advance. These conditions might be different from those used when Fe(II) was added to PCS and PCX. In addition, SEM images and XRD analyses showed that solids formed in FSCX were different from those formed from PCX and PCS. Furthermore, EDS spectra indicate that FSCX solids were mainly composed of Ca and a little bit of Fe, Cl, Al, and Si. Although many other elements were added to synthesize active solids, these elements were not involved to form FSCX solids. Simply mixing all components might not be the best condition for formation of active solids. Elemental compositions of the mixtures and the conditions affecting solid formation might be the most important factors in determining how active solids are formed.

In addition, Ca might be also an important element in affecting formation an active agent in addition to Fe(II), Fe(III), and Cl. PCE degradation kinetics using solids formed from PCX after Ca was removed were different from experiments using

untreated PCX and Fe(II)-DS/S. The effects of pH and cement extract content of Ca treated PCX (CPCX) were different behaviors from Fe(II)-DS/S (23) and less activity than untreated PCX. $k_{\text{Fe(II)}}$ values of CPCX increased with pH up to 11.5, sharply decreased and then continued to increase up to pH 13 while the effect of pH on rate constants for PCE degradation of Fe(II)-DS/S fitted well with a normal distribution function with optimal pH of 12.1 (23). PCE degradation rates of CPCX were less affected by cement extract contents than those of PCX. Even though PCE degradation did not occur without Fe(II), Ca might be another element of an active agent so that solids formed in the absence of Ca would have different activities compared to those formed in the presence of Ca. Instrumental analyses showed that Fe(II)(III)Cl and MSCX solids, where Ca was not included, were different from Fe(II)-PCX and Fe(II)-PCS solids. Ferrous hydroxides were identified in Fe(II)(III)Cl and MSCX systems by XRD analysis. Fe(II)-PCX and Fe(II)-PCS solids were mainly composed of calcium aluminum hydroxide hydrate, calcium aluminum silicate hydrate, and Friedel's salt. They were composed of Ca, Fe, Cl, Al and Si while Fe and Cl were main elements of Fe(II)(III)Cl and MSCX solids. Particle sizes were also different. Fe(II)(III)Cl and MSCX solids were much smaller (less than a micron) than Fe(II)-PCX and Fe(II)-PCS solids (a few microns).

An interesting phenomenon found by analysis of SEM images and EDS spectra was that Fe tended to be associated with hexagonal thin plate particles, which were supposed to be a LDH. Fe contents in particles with different shapes were low or below detection limits. This supports the hypothesis that active agents in Fe(II)-DS/S system is

a LDH, which includes AFm phases. It cannot be determined whether Fe was structural or adsorbed onto the surface of the AFm phases. However, it does limit number of possible active agents in Fe(II)-DS/S system. Moreover, solid particle sizes of Fe(II)(III)Cl solids synthesized at pH 12 were 10 to 20 times smaller than those at neutral pH. This might indicate that the high surface area of solids were responsible for the high solid activity at high pH in Fe(II)-DS/S system.

Finally, kinetic experiments designed to examine the variation of ordinary Portland cement (OPC) showed different PCE degradation behaviors with each OPC. Solids from cement slurries containing Fe(II) and made with Capitol, Txi and Lehigh cements (CPCSF_e, TPCSF_e, and LPCSF_e) followed pseudo first-order kinetics while those made from Quikrete cement (QPCSF_e) followed second-order kinetics. Solids made by adding Fe(II) to extracts of Capitol and Txi (CPCXFe and TPCXFe) followed pseudo first-order kinetics, while those made from Lehigh and Quikrete cement extract solids (LPCXFe and QPCXFe) followed the second-order kinetics. TCE was detected in LPCSF_e, QPCSF_e, LPCXFe, and QPCXFe. Slurries with Fe(II) made from four different cements formed the same kind of solids, although their kinetic behaviors were different. This might be caused by different compositions of the cements, such as different Fe(II) to Fe(III) ratios. In the case of solids made from extracts, the main solid phases might be different because of their different particle sizes. Calcium aluminum hydroxide hydrates dominated solids made with Txi, Quikrete, and Lehigh cements and their particle sizes were 1 μm or less. However, Friedel's salt was the major phase found in solids made with Capitol cements and had particle sizes in the range of 2 to 3 μm.

The experimental studies presented here indicate that possible active agents in Fe(II)-DS/S system are a type of AFm phases, either tetracalcium aluminate or Friedel's salt. This is based on the observation that Fe(II) added to cement slurries or extracts is likely to be associated with particles that are thin hexagonal plates. However, it has not been determined if the Fe(II) is structural or adsorbed.

Although instrumental analyses indicate that AFm phases might be the possible active agents in Fe(II)-DS/S, solid activity tests were unable to confirm this. This might result from differences between simulated and real conditions for the formation of active agents. Therefore, the first step of future research should be concentrated on the identification of desired conditions of the formation of active agents without cement. The second step should concentrate on developing both qualitative and quantitative solid analysis techniques that could be used to identify active agents more precisely. Finally, characterization of active agents and elucidation of dechlorination mechanism in Fe(II)-DS/S system will be necessary to apply identified active agents to various contaminated systems, such as soil, groundwater, or wastewater.

LITERATURE CITED

1. LaGrega, M. D.; Buckingham, P. L.; Evans, J. C. *Hazardous Waste Management*; McGraw-Hill: New York, 1994
2. U.S. EPA *Common Chemicals Found at Superfund Sites*; EPA 540/R-94/044; Office of Emergency and Remedial Response: Washington, DC, 1994.
3. U.S. Department of Health and Human Services, Public Health Service. *Agency for Toxic Substances and Disease Registry (ASTDR) Toxicological Profile for Tetrachloroethylene*; Atlanta, GA, September, 1997, retrieved at URL <http://www.atsdr.cdc.gov/toxprofiles/phsl8.html>
4. Federal Remediation Technologies Roundtable. *Remediation Technologies Screening Matrix and Reference Guide, Version 4.0*, retrieved at URL <http://www.frtr.gov>
5. Birnbaum, L.; Burke, T.; Carberry, J. B.; Clark, E.; Daisey, J. et al. *Environ. Sci. Technol.* **1996**, *30*, 24A-44A
6. Cudahay, J. Thermal Destruction. *Seminar/Workshop on Innovative Site Remediation Technologies*; American Academy of Environmental Engineers: Annapolis, MD, 1994
7. Vogel, R. M.; Craddle, C. S.; McCarty, P. L. *Environ. Sci. Technol.* **1987**, *21*, 722-736
8. Macalady, D. L. *J. Contam. Hydrol.* **1986**, *1*, 1-28
9. Tsukano Y. *J. Contam. Hydrol.* **1986**, *1*, 47-63

10. Kriegman-King, M. R.; Reinhard, M. *Environ. Sci. Technol.* **1994**, *28*, 692-700
11. Kriegman-King, M. R.; Reinhard, M. *Environ. Sci. Technol.* **1992**, *26*, 2198-2206
12. Amonette, J. E.; Szecsody, J. E.; Schaef, H. T.; Templeton, J. C.; Gorby, Y. A.; Fruchter, J. S. Abiotic Reduction of Aquifer Materials by Dithionite: A Promising In-situ Remediation Technology. 33rd *Hanford Symposium on Health and the Environment*, November 7-11, 1994, Pasco, WA; Battelle Press: Columbus, OH, 1994; pp851-881
13. Arnold, W. A.; Roberts, A. L. *Environ. Sci. Technol.* **2000**, *34*, 1794-1805
14. Johnson, T. J.; Scherer, M. M.; Tratnyek, P. G. *Environ. Sci. Technol.* **1996**, *30*, 2634-2640
15. Zhang, W-X.; Wang, C-B.; Lien, H-L. *Catal. Today*, **1998**, *40*, 387-395
16. Fennelly, J. P.; Roberts, A. L. *Environ. Sci. Technol.* **1998**, *32*, 1980-1988
17. Kim, Y-H.; Carraway, E. R. *Environ. Sci. Technol.* **2000**, *34*, 2014-2017
18. Doong, R-A.; Chen, K-T.; Tsai, H-C. *Environ. Sci. Technol.* **2003**, *37*, 2575-2581
19. Roberts, A. L.; Totten, L. A.; Arnold, W. A.; Burris, D. R.; Campbell, T. J. *Environ. Sci. Technol.* **1996**, *30*, 2654-2659
20. Scherer, M. M.; Balko, B. A.; Gallagher, D. A.; Tratnyek, P. G. *Environ. Sci. Technol.* **1998**, *32*, 3026-3033
21. Arnold, W. A.; Roberts, A. L. *Environ. Sci. Technol.* **1998**, *32*, 3017-3025
22. Arnold, W. A.; Ball, W. P.; Roberts, A. L. *J. Contam. Hydrol.* **1999**, *40*, 183-200
23. Hwang, I.; Batchelor, B. *Environ. Sci. Technol.* **2000**, *34*, 5017-5022
24. Hwang, I.; Batchelor, B. *Chemosphere*, **2002**, *48*, 1019-1027

25. Jung, B.; Batchelor, B. Transformation of 1,1,1,-trichloroethane by Fe(II) in Cement Slurries. In *The 4th Proceedings of the International Conference on Remediation of Chlorinated and Recalcitrant Compounds*, May 24-27, 2004, Monterey, CA; in press
26. Erbs, M.; Hansen, H. C. B.; Olsen, C. E. *Environ. Sci. Technol.* **1999**, *33*, 307-311
27. Lee, W.; Batchelor, B. *Environ. Sci. Technol.* **2002**, *36*, 5348-5354
28. O'Loughin, E. J.; Kemner, K. M.; Burris, D. R. *Environ. Sci. Technol.* **2003**, *37*, 2905-2912
29. Choi, J.; Batchelor, B. Methods for Producing High-Activity Modified Green Rusts. In *The 4th Proceedings of the International Conference on Remediation of Chlorinated and Recalcitrant Compounds*, May 24-27, 2004, Monterey, CA; in press
30. Butler, E. C.; Hayes, K. F. *Environ. Sci. Technol.* **2000**, *34*, 422-429
31. Butler, E. C.; Hayes, K. F. *Environ. Sci. Technol.* **1998**, *32*, 1276-1284
32. Butler, E. C.; Hayes, K. F. *Environ. Sci. Technol.* **1999**, *33*, 2021-2027
33. Jeong, H. Y.; Hayes, K. F. *Environ. Sci. Technol.* **2003**, *37*, 4650-4655
34. Gander, J. W.; Parkin, G. F.; Scherer, M. M. *Environ. Sci. Technol.* **2002**, *36*, 4540-4546
35. Weerasooriya, R.; Dharmasena, B. *Chemosphere*, **2001**, *42*, 389-396
36. Lee, W.; Batchelor, B. *Environ. Sci. Technol.* **2002**, *36*, 5147-5154
37. McCormick, M. L.; Adrianens, P. *Environ. Sci. Technol.* **2004**, *38*, 1045-1053
38. Maithreepala, R. A.; Doong, R-A. *Environ. Sci. Technol.* **2004**, *38*, 260-268
39. Reinhard, M.; Curtis, G. P.; Kriegman, M. R. *Abiotic Reductive Dechlorination of Carbon Tetrachloride and Hexachloroethane by Environmental Reductans*;

EPA/600/S2-90/040; United States Environmental Protection Agency: Ada, OK, September, 1990

40. Kriegman-King, M. R.; Reinhard, M. *Environ. Sci. Technol.* **1992**, *26*, 2198-2206
41. Talyor, H. F. W. *Cement Chemistry*, 2nd ed; Thomas Telford: London, England, 1997
42. St John, D. A.; Poole, A.W.; Sims, I. *Concrete Petrography*, Arnold: London, England, 1998
43. Stutzman, P. Chemistry and Structure of Hydration Products. In *Cements Research Progress*; American Ceramic Society: Columbus, OH, 1998; pp 29-65
44. Glasser, F. P. Chemistry of Cement-Solidified Waste Forms. In *Chemistry and Microstructure of Solidified Waste Forms*; Spence, R. D., Ed; Lewis Publishers: Boca Raton, FL, 1993
45. Csizmadia, J.; Balazs, G.; Tamas, F. D. *Cem. Concr. Res.* **2001**, *31*, 577-588
46. Suryavanshi, A. K.; Scantlebury, J. D.; Lyon, S. B. *Cem. Concr. Res.* **1995**, *25*, 581-592
47. Birnin-Yauri, U. A.; Glasser, F. P. *Cem. Concr. Res.* **1998**, *28*, 1713-1723
48. Czernin, W. *Cement Chemistry and Physics for Civil Engineers*, 2nd English ed ; George Godwin Ltd: London, England, 1980
49. Copeland, L. E.; Kantro, D. L. Chemistry of Hydration of Portland Cement at Ordinary Temperature. In *The Chemistry of Cements*, Academy Press: London, England, 1964; *Vol. 1*, pp313-370
50. Rapin, J-P.; Walcarius, A.; Lefevre, G.; Francois, M. *Acta Cryst.* **1999**, *C55*, 1957-1959

51. Renaudin, G.; Kubel, F.; Rivera, J.-P.; Francois, M. *Cem. Concr. Res.* **1999**, *29*, 1937-1942
52. Zhouiri, E.; Hajbi, A. E. *Ann. Chim. Sci. Mat.* **1999**, *24*, 57-62
53. Roy, A. D.; Forano, C.; Malki, K. E.; Bess, J-P. Anionic Clays: Trends in Pillaring Chemistry. In *Expanded Clays and Other Microporous Solids*; Ocelli, M. L., Robson, H. E. Eds; Van Nostrand Reinhold: New York, 1992; pp108-169
54. You, Y.; Vance, G. F.; Zhao, H. *Colloids Surf. A.* **2002**, *205*, 161-172
55. You, Y.; Vance, G. F.; Zhao, H. *App. Clay Sci.* **2001**, *20*, 13-25
56. Refait, P.; Simon, L.; Genin, J. M. R. *Environ. Sci. Technol.* **2000**, *34*, 819-825
57. Miyata, S. *Clays Clay Miner.* **1983**, *31*, 305-311
58. Seida, Y.; Nakano, Y. *Wat. Res.* **2000**, *34*, 1487-1494
59. Goswamee, R. L.; Sengupta, P.; Bhattacharyya, K. G.; Dutta, D. K. *Appl. Clay Sci.* **1998**, *13*, 21-34
60. Simon, L.; Genin, J. M. R. *Corros. Sci.* **1997**, *39*, 1673-1685
61. Sagoe-Crentsil, K. K.; Glasser, F. P. *Corrosion*, **1993**, *49*, 457-463
62. Refait, Ph.; Drissi, S. H.; Pykiewicz, J.; Genin, J. M. R. *Corros. Sci.* **1997**, *39*, 1699-1710
63. Goldstein, J. I.; Newbury, D. E.; Echlin, P.; Joy, D. C.; Roming, A. D.; Lyman, C. E.; Fiori, C.; Lifshin, E. *Scanning Electron Microscopy and X-ray Microanalysis : A Text for Biologists, Materials Scientists, and Geologists*, 2nd ed ; Plenum Press: New York, 1981

64. Stutzman, P. E. Scanning Electron Microscopy in Concrete Petrography, In *Materials Science of Concrete Special Volume: Calcium Hydroxide in Concrete*; Skalny, J. P., Gebauer, J., Odler, I. Eds; The American Ceramic Society: Columbus, OH, 2001; pp59-72
65. Luo, R.; Cai, Y.; Wang, C.; Huang, X. *Cem. Concr. Res.* **2003**, *33*, 1-7
66. Tronto, J.; Reis, M. J.; Silverio, F.; Balbo, V. R.; Marchetti, J. M.; Valim, J. B. *J. Phys. Chem. Solids*, **2004**, *65*, 475-480
67. Beres, A.; Palinko, I.; Kiricsi, I.; Mizukami, F. *Solid State Ionics*, **2001**, *141-142*, 259-263
68. Peulon, S.; Antony, H.; Legrand, L.; Chausse, A. *Electrochim. Acta*, **2004**, *49*, 2891-2899
69. Peulon, S.; Legrand, L.; Antony, H.; Chausse, A. *Electrochem. Commun.*, **2003**, *5*, 208-213
70. Gehin, A.; Ruby, C.; Abdelmoula, O.; Benali, O.; Ghanbaja, J.; Refait, P.; Genin, J-M. R. *Solid State Sci.* **2002**, *4*, 61-66
71. Carja, G.; Nakamura, R.; Niiyama, H. *Appl. Catal. A.* **2002**, *236*, 91-102
72. Middeldorp, P. J. M.; Luijten, M. L. G.C.; van de Pas, B. A.; van Eekert, M. H. A.; Kengen, S. W. M.; Schraa, G.; Stams, A. J. M. *Biorem. J.* **1999**, *3*, 151-169
73. Vogel, T. M.; McCarty, P. L. *Environ. Sci. Technol.* **1987**, *21*, 1208-1213
74. Adrain, L.; Gorisch, H. *Res. Microbiol.* **2002**, *153*, 131-137
75. Freedman, D. L.; Grossett, J. M. *Appl. Environ. Microbiol.* **1989**, *55*, 2144-2151

76. deBruin, W. P.; Kotterman, M. J.; Posthusmsu, M. A.; Schraa, G.; Zehnder, A. J. B. *Appl. Environ. Microbiol.* **1992**, *58*, 1996-2000
77. Gao, J.; Skeen, R. S.; Hooker, B. S.; Quesenberry, R. D. *Wat. Res.* **1997**, *31*, 2479-2486
78. He, J.; Sung, Y.; Dollhopf, M. E.; Fathepure, B. Z.; Tiedje, J. M.; Loffler, F. E. *Environ. Sci. Technol.* **2002**, *36*, 3945-3952
79. Gatell-Maymo, X.; Chien, Y-T.; Gossett, J. M.; Zinder, S. H. *Science*, **1997**, *276*, 1568-1571
80. Bradley, P. M.; Chapelle, F. H. *Environ. Sci. Technol.* **1997**, *31*, 2692-2696
81. Chen, C.; Puhakka, J. A. ; Ferguson, J. F. *Environ. Sci. Technol.* **1996**, *30*, 542-547
82. Skubal, K. L.; Haack, S. K.; Forney, L. J.; Adriaens, P. *Phys, Chem. Earth B.* **1999**, *24*, 517-527
83. Doong, R-A.; Wu, S-C.; Chen, T-F. *Chemosphere*, **1996**, *32*, 377-390
84. Mohn, W. W.; Tiedje, J. M. *Microbiol. Rev.* **1992**, *56*, 482-507
85. Ferguson, J. F.; Pietari, J. M. H. *Environ. Pollut.* **2000**, *107*, 209-215
86. Krumholz, L. R.; Sharp, R.; Fishbain, S. *Appl. Environ. Microbiol.* **1996**, *62*, 4108-4113
87. Krumholz, L. R. *Int. J. Syst. Bacteriol.* **1997**, *47*, 1262-1263
88. Beurskens, J. E. M.; Dekker, C. G. C.; van den Heuvel, H.; Swart, M.; de Wolf, J.; Dolfing, J. *Environ. Sci. Technol.* **1994**, *28*, 701-706
89. Holliger, C.; Schraa, G.; Stams, A. J. M.; Zehnder, A. J. B. *Appl. Environ. Microbiol.* **1992**, *58*, 1636-1644

90. Middeldorp, P. J. M.; de Wolf, J.; Zehnder, A. J. B.; Scharr, G. *Appl. Environ. Microbiol.* **1997**, *63*, 1225-1229
91. Kengen, S. W. M.; Breidenbach, C. G.; Felske, A.; Schraa, G.; Stams, A.J. M.; de Vos, W. M. *Appl. Environ. Microbiol.* **1999**, *65*, 2312-2316
92. Skubal, K. L.; Barcelona, M. J.; Adriaens, P. J. *Contam. Hydrol.* **2001**, *49*, 151-169
93. Gerritse, J.; Kloetstra, G.; Alphenaar, A.; Spuij, F.; Urlings, L.; Gottschal, J. C. In-Situ Bioremediation of Soil Polluted with Chlorinated Ethenes by Imposing Sequential Anaerobic and Aerobic Conditions. *The 3rd International Symposium on In Situ and On-Site Bioremediation*, April, 1995, San Diego, CA; Battell Press: Columbus, OH, 1995 ; ppB5
94. Gregory, K. B.; Mason, M. G.; Picken, H. D.; Weathers, L. J.; Parkin, G. F. *Environ. Eng. Sci.* **2000**, *17*, 169-198
95. Kao, C. M.; Chen, Y. L.; Chen, S. C.; Yeh, T. Y.; Wu, W. S. *Wat. Res.* **2003**, *37*, 4885-4894
96. Kao, C. M.; Chen, S. C.; Wang, J. Y.; Chen, Y. L.; Lee, S. Z. *Wat. Res.* **2003**, *37*, 27-38
97. Kao, C. M.; Lei, S. E. *Wat. Res.* **2000**, *34*, 835-845
98. Komatsu, T.; Shinmyo, J.; Momonoi, K. *Wat. Sci. Tech.* **1997**, *36*, 125-132
99. Eisenbeis, M.; Kreisel-Bauer, P.; Scholz-Muramatsu, H. *Wat. Sci. Tech.* **1997**, *36*, 191-198
100. Matheson, L. J.; Tratnyek, P. G. *Environ. Sci. Technol.* **1994**, *28*, 2045-2053

101. Conner, J. R.; Hoeffner, S. L. *Critical Reviews in Environ. Sci. Technol.* **1998**, *28*, 325-396
102. Fanning, D. S.; Ragenhorst, M. C.; Burch, S. N.; Islam, K. R.; Tangren, S. A. Sulfides and Sulfate. In *Soil Mineralogy with Environmental Applications*, Dixon, *et al.*, Eds.; Soil Science Society of America: Madison, WI., 2002
103. Sakaguchi, T.; Burgess, J. G.; Matsunaga, T. *Nature*, **1993**, *365*, 47-49
104. Bazylinski, D. A.; Moskowitz, B. M. Microbial Biomineralization of Magnetic Iron Minerals : Microbiology, Magnetism, and Environmental Significance, In *Geomicrobiology : Interactions between Microbes and Mineals*, Banfield, *et al.*, Eds; Reviews in Mineralogy, Mineralogical Society of American: Washington, DC, 1997 ; Vol. 35
105. Glasauer, S.; Weidler, P. G.; Langley, S.; Beveridge, T. J. *Geochim. Cosmochimi. Acta*, **2003**, *67*, 1277-1288
106. Lovley, D. R.; Woodward, J. C.; Chapelle, F. H. *Nature*, **1994**, *370*, 128-131
107. Cornell, R. M.; Schwertmann, U. *The Iron Oxides : Structure, Properties, Reactions, Occurrence, and Uses*, Wiley-VCH: Weinheim, Germany, 1996
108. Segal, M. G.; Sellers, R. M. *J. Chem. Soc. Chem. Comm.* **1980**, *863*, 991-993
109. Arnold, R. G.; DiChristina, T. J.; Hoffman, M. R. *Biotechnol. Bioeng.* **1986**, *32*, 1081-1096
110. Mann, S.; Sparks, N. H. C.; Couling, S. B.; Larcombe, M. C.; Frankel, R. B. *J. Chem. Soc. Faraday Trans. 1*, **1989**, *85*, 3033-3044
111. Gillham, R. W.; O'Hannesin, S. F. *Ground Water* **1994**, *32*, 958-967

112. O'Hannesin, S. F.; Gillham, R. W. *Ground Water* **1998**, *36*, 164-170
113. Furukawa, Y.; Kim, J-W.; Watkins, J.; Wiklin, R. T. *Environ. Sci. Technol.* **2002**, *36*, 5469-5475
114. Phillips, D. H.; Watson, D. B.; Roh, Y.; Gu, B. *J. Environ. Qual.* **2003**, *32*, 2033-2045
115. Gu, B.; Phelps, T. J.; Liang, L. Dickey, M. J.; Roh, Y.; Kinsall, B. L.; Palumbo, A. V.; Jacobs, G. K. *Environ. Sci. Technol.* **1999**, *33*, 2170-2177
116. Klein, C.; Hurlbult, C. S. Jr. *Manual of Mineralogy*; 21st ed.; John Wiley & Sons, Inc.: New York, 1999
117. Schulze, D. G. An Introduction to Soil Mineralogy, In *Soil Mineralogy with Environmental Applications*, Dixon, J. B., Schulze, D. G., Eds.; Soil Science Society of America: Madison, WI., 2002
118. Zussman, J. X-ray Diffraction, In *Physical Methods in Determinative Mineralogy*, Zussman, J. Ed.; 2nd ed.; Academy Press: New York, 1977; pp391-473
119. Nesse, W. D. *Introduction to Mineralogy*, Oxford University Press: New York, 2000
120. White, G. N.; Dixon, J. B. *Soil Mineralogy Laboratory Manual*, Texas A&M University: College Station, 2003
121. Whittig, L. D.; Allardice, W. R. X-ray Diffraction Techniques, In *Methods of Soil Analysis, Part 1. Physical and Mineralogical Methods*, Klute, A. Ed.; 2nd ed.; Soil Science Society of America: Madison, WI, 1986

122. Long, J. V. P., Electron Probe Microanalysis, In *Physical Methods in Determinative Mineralogy*, Zussman, Ed; 2nd ed.; Academy Press: New York, NY 1977
123. Gibbs, C. R. *Analy. Chem.* **1976**, 48, 1197-120
124. Ghorab, H.Y.; Kishar, E. A.; Elfetouh, S. H. A. *Cem. Concr. Res.* **1998**, 28, 763-771
125. Chudek, J. A.; Hunter, G.; Jone, M. R.; Scrimgeour, S. N.; Hewlett, P. C.; Kudryavtsev, A. B. *J. Mater. Sci.* **2000**, 35, 4275-4288
126. Glasser, F. P.; Kindness, A.; Stronach, S. A. *Cem. Concr. Res.* **1999**, 29, 861-866
127. Ko, S. B. M.S. Thesis, Texas A&M University: College Station, 2001
128. Gehin, A.; Ruby, C.; Abdelmoula, M.; Benali, O.; Ghanbaja, J.; Refait, P.; Genin, J. M. R. *Solid State Sci.* **2002**, 4, 61-66

APPENDIX A
TABULATED DATA

TABLE A-1 Changes in aqueous phase PCE concentration over time in the activity tests

Exp. 1		Exp. 2		Exp. 3		Exp. 4	
Time days	PCE conc. mM	Time days	PCE conc. mM	Time days	PCE conc. mM	Time days	PCE conc. mM
4	0.206	3	0.176	4	0.207	3	0.196
4	0.204	3	0.178	4	0.205	3	0.202
4	0.199	3	0.177	4	0.197	3	0.210
4	0.189	3	0.176	4	0.199	3	0.210
4	0.191	3	0.178	4	0.196	3	0.205
4	0.191	3	0.176	4	0.199	3	0.201
4	0.180	3	0.180	4	0.193	3	0.204
4	0.194	3	0.172	4	0.192	3	0.195
4	0.193			4	0.191	3	0.207

Exp. 5		Exp. 6		Exp. 7		Exp. 8	
Time days	PCE conc. mM	Time days	PCE conc. mM	Time days	PCE conc. mM	Time days	PCE conc. mM
3.5	0.196	3.5	0.165	3.5	0.130	3.5	0.0285
3.5	0.139	3.5	0.187	3.5	0.176	3.5	0.0274
3.5	0.173	3.5	0.148	3.5	0.170	3.5	0.0319

Exp. 9		Exp. 10		Exp. 11	
Time days	PCE conc. mM	Time days	PCE conc. mM	Time days	PCE conc. mM
3.5	0.196	3.5	0.165	3.5	0.130
3.5	0.139	3.5	0.187	3.5	0.176
3.5	0.173	3.5	0.148	3.5	0.170

Exp. 13		Exp. 15		Exp. 16	
Time days	PCE conc. mM	Time days	PCE conc. mM	Time days	PCE conc. mM
4	0.198	4	0.187	4	0.196
4	0.198	4	0.191	4	0.195
4	0.211			4	0.191

TABLE A-1 Continued

Exp. 18		Exp.19		Exp. 20		Exp. 21	
Time days	PCE conc. mM	Time days	PCE conc. mM	Time days	PCE conc. mM	Time days	PCE conc. mM
3	0.193	3	0.194	3	0.193	3	0.190
3	0.195	3	0.193	3	0.193	3	0.193
3	0.196	3	0.194	3	0.189	3	0.195

Exp. 22		Exp.23		Exp. 24	
Time days	PCE conc. mM	Time days	PCE conc. mM	Time days	PCE conc. mM
13	0.200	13	0.171	13	0.175
13	0.197	13	0.171	13	0.180
13	0.197	13	0.179		

Exp. 26		Exp.27		Exp. 29	
Time days	PCE conc. mM	Time days	PCE conc. mM	Time days	PCE conc. mM
3.8	0.143	3.8	0.192	3.8	0.159
3.8	0.153	3.8	0.196	3.8	0.155

Exp. 30		Exp.31		Exp. 32		Exp. 33	
Time days	PCE conc. mM	Time days	PCE conc. mM	Time days	PCE conc. mM	Time days	PCE conc. mM
4.5	0.110	4.5	0.149	4.5	0.146	4.5	0.115
4.5	0.117	4.5	0.142	4.5	0.158	4.5	0.114
		4.5	0.145	4.5	0.154	4.5	0.114

Exp. 34		Exp.35		Exp. 36		Exp. 37	
Time days	PCE conc. mM	Time days	PCE conc. mM	Time days	PCE conc. mM	Time days	PCE conc. mM
4.5	0.126	4.9	0.175	4.9	0.129	4.9	0.137
4.5	0.126	4.9	0.172	4.9	0.114	4.9	0.140
4.5	0.119	4.9	0.174			4.9	0.145

TABLE A-1 Continued

Exp. 38		Exp.39		Exp. 40		Exp. 41	
Time days	PCE conc. mM	Time days	PCE conc. mM	Time days	PCE conc. mM	Time days	PCE conc. mM
4.9	0.157	5.7	0.153	5.7	0.139	5.7	0.133
4.9	0.164	5.7	0.151	5.7	0.142	5.7	0.134
4.9	0.167			5.7	0.147	5.7	0.134

Exp. 42	
Time days	PCE conc. mM
5.7	0.149
5.7	0.152
5.7	0.150

Exp. 43		Exp. 44	
Time days	PCE conc. mM	Time days	PCE conc. mM
4	0.127	6.9	0.0793
4	0.135	6.9	0.0737
4	0.130	6.9	0.0962
4	0.139	6.9	0.0792
4	0.148	6.9	0.0857
4	0.134	6.9	0.0700
4	0.143	6.9	0.0732
4	0.130	6.9	0.0983
4	0.134	6.9	0.0714
		6.9	0.0701
		6.9	0.0698
		6.9	0.0762
		6.9	0.0834
		6.9	0.0806

TABLE A-1 Continued

Exp. 47		Exp.48		Exp. 49		Exp. 50	
Time days	PCE conc. mM	Time days	PCE conc. mM	Time days	PCE conc. mM	Time days	PCE conc. mM
8.5	0.141	7	0.146	7	0.163	7	0.160
8.5	0.166	7	0.142	7	0.164	7	0.162
8.5	0.140	7	0.154	7	0.161	7	0.151
8.5	0.154						
8.5	0.166						
8.5	0.171						
8.5	0.165						
8.5	0.166						
8.5	0.165						
8.5	0.149						
8.5	0.169						
8.5	0.147						
8.5	0.169						
8.5	0.170						
8.5	0.165						
8.5	0.166						
8.5	0.165						
8.5	0.146						

Exp. 51		Exp.52		Exp. 53		Exp. 54	
Time days	PCE conc. mM	Time days	PCE conc. mM	Time days	PCE conc. mM	Time days	PCE conc. mM
7	0.153	7	0.167	7	0.143	7	0.151
7	0.161	7	0.167	7	0.145	7	0.158
7	0.161	7	0.175	7	0.134	7	0.150

Exp. 55		Exp.56		Exp. 57		Exp. 58	
Time days	PCE conc. mM	Time days	PCE conc. mM	Time days	PCE conc. mM	Time days	PCE conc. mM
5.6	0.142	5.6	0.161	5.6	0.166	5.6	0.163
5.6	0.148	5.6	0.168	5.6	0.166	5.6	0.160
5.6	0.166	5.6	0.164	5.6	0.166	5.6	0.159

TABLE A-1 Continued

Exp. 59	
Time days	PCE conc. mM
7	0.136
7	0.167
7	0.162
7	0.139
7	0.158
7	0.164
7	0.157
7	0.152
7	0.141
7	0.135
7	0.165
7	0.155
7	0.153
7	0.152
7	0.159

Exp. 60		Exp.61		Exp. 62		Exp. 63	
Time days	PCE conc. mM	Time days	PCE conc. mM	Time days	PCE conc. mM	Time days	PCE conc. mM
7	0.158	7	0.146	7	0.152	7	0.155
7	0.159	7	0.161	7	0.162	7	0.153
7	0.164	7	0.159	7	0.157	7	0.129

Exp. 64		Exp.65		Exp. 66		Exp.67	
Time days	PCE conc. mM	Time days	PCE conc. mM	Time days	PCE conc. mM	Time days	PCE conc. mM
7	0.157	7	0.156	7.9	0.154	7.9	0.151
7	0.149	7	0.157	7.9	0.156	7.9	0.152
7	0.156	7	0.141	7.9	0.149	7.9	0.155

Exp. 68		Exp.69		Exp. 70	
Time days	PCE conc. mM	Time days	PCE conc. mM	Time days	PCE conc. mM
7.9	0.145	7.9	0.157	7.9	0.158
7.9	0.147	7.9	0.151	7.9	0.153
7.9	0.130	7.9	0.148	7.9	0.158

TABLE A-1 Continued

Exp. 71		Exp.72		Exp. 73		Exp.74	
Time days	PCE conc. mM	Time days	PCE conc. mM	Time days	PCE conc. mM	Time days	PCE conc. mM
7.7	0.154	7.7	0.168	7.7	0.149	7.7	0.159
7.7	0.158	7.7	0.157	7.7	0.144	7.7	0.157
7.7	0.136	7.7	0.158	7.7	0.159		

Exp.75		Exp. 76		Exp.77		Exp. 78	
Time days	PCE conc. mM	Time days	PCE conc. mM	Time days	PCE conc. mM	Time days	PCE conc. mM
7.7	0.110	6.9	0.160	6.9	0.159	6.9	0.136
7.7	0.120	6.9	0.159	6.9	0.157	6.9	0.153
		6.9	0.164	6.9	0.159	6.9	0.151

Exp.79		Exp. 80		Exp.81		Exp. 82	
Time days	PCE conc. mM	Time days	PCE conc. mM	Time days	PCE conc. mM	Time days	PCE conc. mM
6.9	0.161	6.9	0.151	6.9	0.130	6.9	0.140
6.9	0.154	6.9	0.150	6.9	0.152	6.9	0.151
6.9	0.155	6.9	0.135	6.9	0.155	6.9	0.145

Exp.83		Exp. 84		Exp.85		Exp. 86	
Time days	PCE conc. mM	Time days	PCE conc. mM	Time days	PCE conc. mM	Time days	PCE conc. mM
6.9	0.093	6.9	0.122	6.9	0.135	7	0.156
6.9	0.103	6.9	0.133	6.9	0.112	7	0.159
6.9	0.110	6.9	0.136	6.9	0.114	7	0.145

Exp.87		Exp. 88		Exp.89		Exp. 90	
Time days	PCE conc. mM	Time days	PCE conc. mM	Time days	PCE conc. mM	Time days	PCE conc. mM
7	0.152	7	0.126	7	0.153	7	0.141
7	0.132	7	0.106	7	0.150	7	0.133
7	0.152			7	0.155	7	0.141

TABLE A-1 Continued

Exp.91		Exp. 92		Exp.93		Exp. 94	
Time days	PCE conc. mM	Time days	PCE conc. mM	Time days	PCE conc. mM	Time days	PCE conc. mM
5.7	0.160	5.7	0.152	5.7	0.139	5.7	0.166
5.7	0.163	5.7	0.151	5.7	0.136	5.7	0.158
5.7	0.154	5.7	0.156	5.7	0.148	5.7	0.163

Exp.95		Exp. 96		Exp.97		Exp. 98	
Time days	PCE conc. mM	Time days	PCE conc. mM	Time days	PCE conc. mM	Time days	PCE conc. mM
5.7	0.154	5.7	0.123	4	0.149	4	0.155
5.7	0.159	5.7	0.122	4	0.157	4	0.164
5.7	0.151	5.7	0.140	4	0.159	4	0.160

Exp.99		Exp. 100		Exp.101		Exp. 102	
Time days	PCE conc. mM	Time days	PCE conc. mM	Time days	PCE conc. mM	Time days	PCE conc. mM
4	0.157	4	0.164	4	0.163	4	0.141
4	0.154	4	0.164	4	0.162	4	0.153
4	0.160	4	0.157	4	0.135	4	0.153

Exp.103		Exp. 104		Exp.105		Exp. 106	
Time days	PCE conc. mM	Time days	PCE conc. mM	Time days	PCE conc. mM	Time days	PCE conc. mM
4.6	0.129	4.6	0.136	4.6	0.144	4.6	0.167
4.6	0.134	4.6	0.152	4.6	0.141	4.6	0.158
		4.6	0.154	4.6	0.138	4.6	0.165

TABLE A-1 Continued

Exp.107		Exp. 108	
Time days	PCE conc. mM	Time days	PCE conc. mM
4.6	0.143	4.2	0.145
4.6	0.142	4.2	0.143
4.6	0.140	4.2	0.139
		4.2	0.126
		4.2	0.130
		4.2	0.138
		4.2	0.124
		4.2	0.127
		4.2	0.118
		4.2	0.136
		4.2	0.126
		4.2	0.135
		4.2	0.139
		4.2	0.143
		4.2	0.147

Exp.109		Exp. 110		Exp. 111		Exp. 112	
Time days	PCE conc. mM	Time days	PCE conc. mM	Time days	PCE conc. mM	Time days	PCE conc. mM
7	0.108	7	0.163	7	0.153	7	0.161
7	0.145	7	0.157	7	0.151	7	0.157
7	0.140	7	0.159	7	0.148	7	0.163

Exp.113		Exp. 114		Exp.115		Exp. 116	
Time days	PCE conc. mM	Time days	PCE conc. mM	Time days	PCE conc. mM	Time days	PCE conc. mM
7	0.152	7	0.127	4.9	0.167	4.9	0.163
7	0.160	7	0.129	4.9	0.164	4.9	0.165
7	0.160	7	0.142	4.9	0.165	4.9	0.164

Exp.117		Exp. 118		Exp.119		Exp. 120	
Time days	PCE conc. mM	Time days	PCE conc. mM	Time days	PCE conc. mM	Time days	PCE conc. mM
4.9	0.160	4.9	0.154	4.9	0.163	4.9	0.155
4.9	0.164	4.9	0.151	4.9	0.137	4.9	0.159
		4.9	0.162			4.9	0.161

TABLE A-1 Continued

Exp.121		Exp. 122		Exp.123		Exp. 124	
Time days	PCE conc. mM	Time days	PCE conc. mM	Time days	PCE conc. mM	Time days	PCE conc. mM
5.6	0.138	5.6	0.140	5.6	0.142	5.6	0.127
5.6	0.144	5.6	0.133	5.6	0.143	5.6	0.117
5.6	0.142	5.6	0.144	5.6	0.150	5.6	0.128

Exp.125		Exp. 126	
Time days	PCE conc. mM	Time days	PCE conc. mM
5.6	0.116	5.6	0.145
5.6	0.118	5.6	0.137
5.6	0.131		

Exp.127		Exp. 128		Exp. 129		Exp. 130	
Time days	PCE conc. mM	Time days	PCE conc. mM	Time days	PCE conc. mM	Time days	PCE conc. mM
5.8	0.158	5.8	0.163	5.8	0.139	5.8	0.157
5.8	0.158	5.8	0.162	5.8	0.128	5.8	0.160
5.8	0.156	5.8	0.157	5.8	0.141	5.8	0.156

Exp.131		Exp. 132		Exp.133		Exp. 134	
Time days	PCE conc. mM	Time days	PCE conc. mM	Time days	PCE conc. mM	Time days	PCE conc. mM
5.8	0.152	5.8	0.134	4.9	0.147	4.9	0.154
5.8	0.144	5.8	0.136	4.9	0.160	4.9	0.120
5.8	0.145	5.8	0.115	4.9	0.152	4.9	0.142

Exp.135		Exp. 136		Exp.137		Exp. 138	
Time days	PCE conc. mM	Time days	PCE conc. mM	Time days	PCE conc. mM	Time days	PCE conc. mM
4.9	0.144	4.9	0.138	4.9	0.118	4.9	0.129
4.9	0.146	4.9	0.113	4.9	0.136	4.9	0.133
4.9	0.160	4.9	0.147	4.9	0.157	4.9	0.129

TABLE A-1 Continued

Exp.139		Exp. 140		Exp.141		Exp. 142	
Time days	PCE conc. mM	Time days	PCE conc. mM	Time days	PCE conc. mM	Time days	PCE conc. mM
4.5	0.153	4.5	0.161	4.5	0.135	4.5	0.161
4.5	0.145	4.5	0.158	4.5	0.138	4.5	0.165
4.5	0.139	4.5	0.164	4.5	0.135	4.5	0.163

Exp.143		Exp. 144	
Time days	PCE conc. mM	Time days	PCE conc. mM
4.5	0.139	4.5	0.135
4.5	0.133	4.5	0.150

Exp.145		Exp. 146		Exp.147	
Time days	PCE conc. mM	Time days	PCE conc. mM	Time days	PCE conc. mM
1.2	0.146	0.4	0.145	1.2	0.167
1.2	0.146	0.4	0.142	1.2	0.174
1.2	0.140	0.4	0.150	1.2	0.169
2	0.128	0.5	0.0863	2	0.137
2	0.127	0.5	0.0850	2	0.134
2	0.128	0.5	0.0867	2	0.135
2.9	0.106	0.8	0.0752	2.9	0.109
2.9	0.115	0.8	0.0783	2.9	0.105
2.9	0.100	0.8	0.0735	2.9	0.0986
5	0.0963	1	0.0920	5	0.0559
5	0.0852	1	0.0987	5	0.0505
5	0.0856	1	0.0986	5	0.0506
7.9	0.0595	3.8	0.0743	7.9	0.0190
7.9	0.0686	3.8	0.0724	7.9	0.0178
7.9	0.0553	3.8	0.0753	7.9	0.0186
10	0.0366	6.9	0.0517	10	0.0063
10	0.0436	6.9	0.0504	10	0.0064
10	0.0388	6.9	0.0539	10	0.0071
13.7	0.0206	10.9	0.0425	13.7	0.0052
13.7	0.0206	10.9	0.0349	13.7	0.0049
13.7	0.0236	10.9	0.0382	13.7	0.0054
18.9	0.0141	16.3	0.0096	18.9	0.0027
18.9	0.0108	16.3	0.0117	18.9	0.0035
18.9	0.0128	16.3	0.0148	18.9	0.0028
23.7	0.0040	20.4	0.0047	23.7	0.0009
23.7	0.0029	20.4	0.0064	23.7	0.0012
23.7	0.0031	20.4	0.0052	23.7	0.0011

TABLE A-1 Continued

Exp.148		Exp. 149		Exp.150	
Time days	PCE conc. mM	Time days	PCE conc. mM	Time days	PCE conc. mM
0.96	0.196	0.96	0.1847	0.96	0.158
0.96	0.197	0.96	0.1824	0.96	0.157
0.96	0.189	0.96	0.1894	0.96	0.167
1.8	0.181	1.8	0.1597	1.8	0.120
1.8	0.164	1.8	0.1766	1.8	0.123
1.8	0.182	1.8	0.1625	1.8	0.125
2.8	0.151	2.8	0.1700	2.8	0.098
2.8	0.167	2.8	0.1584	2.8	0.098
2.8	0.151	2.8	0.1407	2.8	0.0993
7.1	0.1244	7.1	0.1415	7.1	0.0772
7.1	0.1138	7.1	0.1263	7.1	0.0706
7.1	0.1356	7.1	0.1349	7.1	0.0673
8.7	0.1028	8.7	0.0960	8.7	0.0472
8.7	0.1006	8.7	0.0994	8.7	0.0460
8.7	0.1007	8.7	0.0901	8.7	0.0455
13.7	0.0780	13.7	0.0850	13.7	0.0354
13.7	0.0829	13.7	0.0835	13.7	0.0366
13.7	0.0876	13.7	0.0839	13.7	0.0365
17.8	0.0392	17.8	0.0751	17.8	0.0299
17.8	0.0385	17.8	0.0782	17.8	0.0260
17.8	0.0333	17.8	0.0754	17.8	0.0320
21.8	0.0329	21.8	0.0411	21.8	0.0194
21.8	0.0276	21.8	0.0409	21.8	0.0212
21.8	0.0355	21.8	0.0498	21.8	0.0173
25.5	0.0195	25.5	0.0432	25.5	0.0150
25.5	0.0209	25.5	0.0340	25.5	0.0188
25.5	0.0235	25.5	0.0403	25.5	0.0187
35.6	0.0099	35.6	0.0334	35.6	0.0094
35.6	0.0103	35.6	0.0229	35.6	0.0098
35.6	0.0109	35.6	0.0231	35.6	0.0086

TABLE A-2 Changes in aqueous phase PCE concentration over time in the activity tests with the variation of pH

pH 10		pH 10.5		pH 11		pH 11.5	
Time days	PCE conc. mM	Time days	PCE conc. mM	Time days	PCE conc. mM	Time days	PCE conc. mM
3	0.117	3	0.109	3	0.130	3	0.126
3	0.133	3	0.126	3	0.109	3	0.123
3	0.125	3	0.129	3	0.126	3	0.113

pH 12		pH 12.5		pH 13		pH 11.7	
Time days	PCE conc. mM	Time days	PCE conc. mM	Time days	PCE conc. mM	Time days	PCE conc. mM
3	0.141	3	0.144	3	0.139	3	0.134
3	0.145	3	0.146	3	0.138	3	0.133
3	0.142	3	0.140	3	0.147	3	0.137

APPENDIX B

COMPUTER PROGRAM (MATLAB) TO ESTIMATE PSEUDO FIRST-ORDER

RATE CONSTANT FOR PCE DECHLORINATION

```

data = load('data.txt'); % file name
t2=data(:,1); % measured values of time
cmeas2=data(:,2); % measured values of concentration of PCE
e2=data(:,3);
errorbar(t2,cmeas2,e2,'rd');
hold on;

[beta r,j]=nlinfit(t2,cmeas2,@Rmodel_first,[0.01, 0.02]);
disp('parameters of C0 and k in PCE degradation exp')
beta
ci=nlparci(beta,r,j);
disp('95% confidence intervals of parameters, Co and k')
ci

dt2=(max(t2)-min(t2))/100;
t2p=min(t2):dt2:max(t2);
for i=1:size(t2p,2)
ESTC2p(i)=beta(1)*exp(-(beta(2)*t2p(i)));
end

data = load('data_control.txt'); % file name
t1 = data(:,1); % measured values of time
c1 = data(:,2); % measured values of concentration of PC
e1 = data(:,3);
errorbar(t1,c1,e1,'ko');

plot(t2p,ESTC2p,'r-');
legend('data','control');

xlabel('Time(day)');
ylabel('Concentration of PCE(mM)');

-----
function ESTC=Rmodel(beta,t)
ESTC=beta(1)*exp(-(beta(2)*t));

```

APPENDIX C

COMPUTER PROGRAM (MATLAB) TO ESTIMATE SECOND-ORDER RATE

CONSTANT FOR PCE DECHLORINATION

```

data = load('data.txt'); % file name
t2=data(:,1); % measured values of time
cmeas2=data(:,2); % measured values of concentration of PCE
e2=data(:,3);
errorbar(t2,cmeas2,e2,'rd');
hold on;

[beta r,j]=nlinfit(t2,cmeas2,@Rmodel_second,[0.01, 0.02]);
disp('parameters of C0 and k in PCE degradation exp')
beta
ci=nlparci(beta,r,j);
disp('95% confidence intervals of parameters, Co and k')
ci

dt2=(max(t2)-min(t2))/100;
t2p=min(t2):dt2:max(t2);
for i=1:size(t2p,2)
ESTC2p(i)=(beta(1))./(1+beta(1)*beta(2)*t2p(i)); % dcdt=kc^2, c=C0/(1+C0kt)
end

data = load('data_control.txt'); % file name
t1 = data(:,1); % measured values of time
c1 = data(:,2); % measured values of concentration of PC
e1 = data(:,3);
errorbar(t1,c1,e1,'ko');

plot(t2p,ESTC2p,'r-');
legend('data','control');

xlabel('Time(day)');
ylabel('Concentration of PCE(mM)');

-----
function ESTC=Rmodel(beta,t)
ESTC=(beta(1))./(1+beta(1)*beta(2)*t);

```

VITA

Sae Bom Ko was born in Inchon, Korea. She grew up in Seoul, Korea. She received a Bachelor of Science degree in chemistry at Dongguk University in February, 1993 and a Master of Science degree in civil engineering at Texas A&M University in December, 2001. She started her Ph.D program at Texas A&M University in 2002. Her research has been focused on remediation of soils contaminated with chlorinated organic compounds that are degraded by reductants, such as Fe(II). Her research interested includes chlorinated organic compounds transformation kinetics and their transformation mechanism by reductive dechlorination. Her permanent address is 482 Kaebong-2-dong Hyundae Apartment #106-2201, Guro-Gu, Seoul, Korea, 152-755.